ORTA DOĞU TEKNİK ÜNİVERSİTESİ
MIDDLE EAST TECHNICAL UNIVERSITY

MECHANICAL ENGINEERING DEPARTMENT

ME 407 MECHANICAL ENGINEERING DESIGN

GROUP - K2

CONTROL SYSTEM DESIGN OF MICROPROCESSOR-CONTROLLED PROSTHETIC KNEE JOINT

23rd January 2023

Team Members		
Ali Fuat Şahin	Address- Arabacialani Mh. Dogu Sk. Yildizevler No:20 Daire No:1 Serdivan/Sakarya Phone- 0 535 037 98 42	Email- sahin.fuat@metu.edu.tr
Can Uludoğan	Address- Yeni Batı Mah. 2424.sok 11/16 Yenimahalle/ANKARA Phone-0 532 788 03 73	Email- e230847@metu.edu.tr
Egemen İlikmen	Address- İşçi blokları Mah. 1538.sok 3/24 Phone-05369737940	Email- e237824@metu.edu.tr
Faysal Turkistani	Address-9. Yurt, ODTU Kampüsü, Çankaya/ANKARA Phone- 05369389833	Email- e234953@metu.edu.tr
Hüsnü Furkan Evci	Address- Varlik Mh. Yudum Sk. 4/1 Yenimahalle/ANKARA Phone- 0543 643 6607	Email- furkan.evci@metu.edu.tr
Mehmet Furkan Doğan	Address- Peyami Safa Mah. 344. Cad. 26/10 Mamak/ANKARA Phone- 0542 524 5417	Email- e237797@metu.edu.tr
Osman Berkin İnci	Address- Ragıp Tüzün Mah. Pazar Cad. Anıl Sok. 62/4 Yenimahalle/ANKARA Phone- 0543 889 9439	Email- e237030@metu.edu.tr
Supervisor	Prof. Erhan İlhan KONUKSEVEN	
Teaching Assistant	Koray Melih Yatağan	

1. Abstract

This project is aimed to design and implement the control system of a semi active microprocessor controlled prosthetic knee joint. The purpose is to allow lower limb amputees to have a normal walking gait cycle by automatically identifying the gait phase cycles and varying the damping provided by the knee joint. The control system is designed according to the Ottobock C-leg knee to adapt to the walking characteristics of people of weights up to 130 kg and walking speeds of up to 2 m/s. Literature survey and patent research is presented. Requirements, specifications and evaluation criteria are determined. Project planning and management is explained. A morphological chart identifying sub functions and the different concepts generated for each is created. The design uses Fuzzy logic to control the valve opening angles and decision tree algorithm embedded in 2 Raspberry Pi Pico microprocessors to identify the gait phase. The relevant program codes, engineering calculations, analysis, and technical drawings are presented. Detailed discussion and project conclusions are carried out.

Özet

Bu proje, yarı aktif mikroişlemci kontrollü protez diz ekleminin kontrol sisteminin tasarımını ve uygulamasını amaçlamaktadır. Amaç, aşağı bacak amputelere normal yürüyüş döngüsüne sahip olmasını ve diz ekleminin sağladığı sönümlemeyi otomatik olarak tanımlayan yürüyüş döngüsünün varyasyonunu sağlamaktır. Kontrol sistemi, 130 kg'a kadar ağırlıkta ve 2 m/s hızda yürüyen insanların yürüyüş özelliklerine uyacak şekilde Ottobock C-Leg protez ürününe göre tasarlanmıştır. Literatür taraması ve patent araştırması sunulmaktadır. Gereksinimler, özellikler ve değerlendirme kriterleri belirlenir. Proje planlama ve yönetimi açıklanır. Fonksiyonların alt bölümleri ve her bölüm için oluşan farklı konseptleri tanımlayan bir morfolojik şema oluşturulur. Tasarım, vana açma açılarının kontrolü için Fuzzy mantığını ve 2 Rasberry Pi Pico mikroişlemcide yerleştirilmiş bir karar ağacı algoritmasını kullanır. İlgili program kodları, mühendislik hesaplamaları, analiz ve teknik çizimler sunulur. Detaylı tartışma ve proje sonuçları yapılır.

KEYWORDS:

Microprocessor controlled knee, Artificial limb, Semi-Active Prosthesis, Actuation, Control, Transfemoral, Lower-Limb, Adaptive, Biomechatronic, Bionic, Intelligent, Rehabilitation

Table of Contents

1. Abstract 2
Özet 2
KEYWORDS 3
2. Introduction 14
3. Literature Survey 16
3.1 INTRODUCTION 16
3.2 COMMERCIAL PRODUCTS 16
3.3 STATE-OF-THE ART ON RELATED TECHNOLOGIES 19
3.4 PATENT 21
3.5 SUMMARY AND CONCLUSION 24
4. PROJECT PLANNING & MANAGEMENT 25
4.1 INTRODUCTION 25
4.2 ORGANIZATION OF THE PROJECT 25
4.3 EXPLANATION OF THE TASKS AND THEIR DEFINITIONS 25
4.3.1 Literature Survey 25
4.3.2. Conceptual Design 26
4.3.4 Detailed Design 26
4.3.5 Supplying Material and Manufacturing 27
4.4 Documentation 28
4.5 Modeling 28
4.5.1 Solid modeling 28
4.5.2 Kinematic Analysis 28
4.5.3 Flow analysis 28
4.6 TIME TABLE 29
4.7 TIMELINE 30
4.8 SUMMARY AND CONCLUSION 31
5. CONCEPTUAL DESIGN 32
5.1 INTRODUCTION 32
5.2 CONCEPT DEVELOPMENT AND PRESENTATION 32
5.2.1 Functional Decomposition Chart 32
5.2.2 Functional Decomposition List 32
5.4 Identifying Gait Phase: 37
5.4.1 Decision Tree 37
5.4.2 Artificial Neural Networks 37
5.4.3 Evolutionary Algorithms 38

5.4.4 Combined System 38
5.5 Controlling Valve Angles 38
5.5.1 PD Control 38
5.5.2 PID 39
5.5.3 Fuzzy Logic 39
5.5.4 Combined System 39
5.6 Ensuring Safety for User 40
5.6.1 Predictive Confidence Level Approach 40
5.6.2 Statistical Profiling Approach 40
5.6.3 Clustering Based Unsupervised Approach 41
5.7 Managing Power Consumption 41
5.7.1 BMS Module 41
5.8 Communication with User 42
5.8.1 Buzzer 42
5.8.2 Vibration Motor 42
5.8.3 Mobile app 42
5.8.4 Combined System 43
5.9 Measuring Knee Angle 43
5.9.1 Incremental Encoder 43
5.9.2 Optical Encoder 43
5.9.3 Magnetic Encoder 44
5.10 Measuring the Ground Reaction Forces 44
5.10.1 Active Quarter Bridge 45
5.10.2 Orthogonal – Active Half Bridge System 45
5.10.3 Orthogonal – Active Full Bridge System 46
5.11 Microprocessor Selection 47
5.11.1 Raspberry Pi Pico 47
5.11.2 Raspberry Pi Pico and multiplexing 47
5.11.3 Arduino Mega 47
5.11.4 Arduino Nano 47
5.12 Filtering 48
5.13 EVALUATION OF CONCEPTS 49
5.13.1 Full List of Evaluation Criteria 49
5.13.2 Identifying gait phase and calculating valve angles 50
5.13.3 Controlling valve angles 51
5.13.4 Ensuring safety for user 52

5.13.5 Measuring Ground Reaction Forces 53
5.13.6 Microcontroller 54
5.13.7 Filtering 55
5.13.8 Measuring Knee Angle 56
5.13.9 Communication with User 57
5.14 Overall Design Concepts and Their Evaluation 58
5.15 THE BEST CONCEPT 59
5.16 SUMMARY AND CONCLUSION 60
6. DETAILED DESIGN 61
6.1. INTRODUCTION 61
6.2 PROPERTIES OF DESIGNED SYSTEM 61
6.2.1 Operating Principle 61
6.2.2 Important aspects of design 62
6.2.3 The system and subsystems 63
6.3 ENGINEERING CALCULATIONS 64
6.3.1 Healthy Walking Model 64
6.3.2 Prosthesis Walking Model 65
6.3.3 Hydraulic Model of the Piston 66
6.3.4 Control System Model 68
6.3.5 Calculation of Valve Opening for Different Motor Angles 71
6.4 ANALYSES 72
6.4.1 Strain Analysis of the Lower Leg 72
6.4.2 Stress Analysis of the Lower Leg 72
6.4.3 Flow Analysis of the Valves 73
6.5 TESTS 74
6.5.1 Spring Stiffness Measurement 74
6.5.2 Energy Storage and Return (ESAR) Foot Stiffness Measurement 74
6.5.3 Leg Center of Mass Measurement 75
6.5.4 Knee Joint Damping Measurement 75
6.5.5 Leg Moment of Inertia Measurement 75
6.5.6 Material Determination of the Strain Gauge Holder 76
6.6 Tests That Will be Conducted to Assess the System Performance 77
6.6.1 Walking Speed Test 77
6.6.2 Standing Test 77
6.6.3 Power Test 77
6.6.4 Weighing 77

6.6.5 Response Time Measurement 77
6.7 Design Decisions 78
6.8 ANALYSIS RESULTS 78
6.8.1 Healthy Walking Model 78
6.8.2 Stress Strain Analysis of the Lower Leg 79
6.8.3 Analysis of the Hydraulic System's Servovalve 81
6.8.4 Simulink Results 82
6.8.5 Calculation of Valve Openings Results 83
6.9 DISCUSSION OF CONTROL ALGORITHMS AND SOFTWARE 84
6.10 OPTIMIZATION 85
6.11 SYSTEM TO BE MANUFACTURED 87
6.12 SUSTAINABILITY ANALYSIS 88
6.13 TEST PLAN 89
6.14 STANDARDS USED FOR DESIGN PROCEDURES and PERFORMANCE EVALUATION 90
6.14.1 Design Standards 90
6.14.2 Performance and Test Standards 91
6.15 DISCUSSIONS AND CONCLUSIONS 91
7. Discussion 93
8. Conclusion 95
9. References 96
10 Appendix 98
APPENDIX A – WORKING DRAWINGS 98
APPENDIX B – ROUTE SHEETS 100
APPENDIX C – MATLAB CODES 101
APPENDIX D – COST ANALYSIS 112
APPENDIX E – SUSTANIBILITY ANALYSIS RESULTS 113

List of Tables

Table 1 Comparison between Different Prosthetic Knee ProductsTable 17
Table 2 Typical power requirements of components.....21
Table 3 Team Member Names and Initials.....25
Table 4 Time table showing the overall distribution of the workload.....29
Table 5 Morphological Chart.....34
Table 6 Decision matrix for identifying gait phase and calculating valve angles 50
Table 7: Decision matrix for controlling valve angle 51
Table 8: Decision matrix for ensuring safety for user 52
Table 9: Decision matrix for measuring ground reaction forces 53
Table 10: Decision matrix for microcontroller selection.....55
Table 11 : Decision matrix for filtering 55
Table 12: Decision matrix for measuring knee angle 56
Table 13 : Decision matrix for communication with user 57
Table 14: Overall design concepts.....58
Table 15: Overall points for each concept 58
Table 16: Overall design concepts and the selected one shown in green 59
Table 17 Table of Test Plans 89

List of Figures

Figure 1 22
Figure 2 22
Figure 3 22
Figure 4 22
Figure 5 22
Figure 6 23
Figure 7 23
Figure 8 23
Figure 9 24
Figure 10 24
Figure 11. Gantt Chart 30
Figure 12: Example Decision Tree Algorithm for determining gait phases 37
Figure 13: A Neural Network Algorithm used for controlling a microprocessor controlled prosthetic knee 37
Figure 14:Flow chart of an evolutionary algorithm 38
Figure 15: Block diagram of a feedback control system with PD controller 38
Figure 16: Block diagram of a feedback control system with PID controller 39
Figure 17: Block diagram of a feedback control system with a fuzzy logic controller 39
Figure 18: Block diagram of a feedback control system with a PID controller and a fuzzy logic controller combined 39
Figure 19: Time series graph for predictive confidence level approach 40
Figure 20: Time series graph for statistical profiling approach 40
Figure 21: Time series graph for clustering based unsupervised approach 41
Figure 22: Battery Management System (BMS) Module for a single cell Li-Ion Battery 41
Figure 23: A buzzer 42
Figure 24: A vibration motor 42
Figure 25: Mobile Phone Application 42
Figure 26: Figure explaining the functional principle of a optical incremental encode. As (4) moves shaded and lighted areas chances 43
Figure 27:Figure showing the functional principle of a absolute optical encoder 43
Figure 28: The physical composition of a magnetic encoder 44
Figure 29: Circuit diagram showing the connections of an active quarter bridge system 45
Figure 30: The physical positioning of the strain gauge used in active quarter bridge system45
Figure 31: Circuit diagram showing the connections of an orthogonal active half bridge system 45
Figure 32: The physical positioning of the strain gauges used in orthogonal active half bridge system 45
Figure 33: Circuit diagram showing the connections of an orthogonal active full bridge system, ... 46
Figure 34: The physical positioning of the strain gauges used in orthogonal active full bridge system 46
Figure 35: Block diagram explaining a band pass filter 48
Figure 36: Block diagram for a band stop filter 48
Figure 37: Hierarchical objective tree for identifying gait phase and calculating valve angles 50
Figure 38: Hierarchical objective tree for ensuring safety for user 52
Figure 39: Hierarchical objective tree for measuring ground reaction forces 53
Figure 40: Hierarchical objective tree for microcontroller selection 54

Figure 41: Hierarchical objective tree for filtering 55
Figure 42: Hierarchical objective tree for measuring knee angle 56
Figure 43: Circuit diagram of the system 63
Figure 44: : Link lengths, weight and frame rate information for the data obtained by David A. Winter 64
Figure 45: Body segment leghts as a fraction of persons height H 65
Figure 46: Hydraulic schematic of C-leg 67
Figure 47: Simulink Block Diagram for Hydraulic System 67
Figure 48 : Membership Functions for The First Fuzzy Interference System 68
Figure 49 : Output Membership Function of Gait Phase 69
Figure 50: Input Membership Function for Velocity 70
Figure 51: Precalculated System Damping Coefficient 71
Figure 52: Simulink Block Diagram for Calculating Motor Angles 72
Figure 53: Simplified Valve Geometry and Section View 73
Figure 54: Fluid Body Volume 73
Figure 55: Foot Stiffness Test Mechanism 74
Figure 56: Angle for free swing of the leg showing raw and filtered data as well as local extrema 75
Figure 57: Angle for free swing of the leg showing raw and filtered data as well as mathematical model created 76
Figure 58: Spectrochemical Analysis Results 76
Figure 59: Knee angle in one gait cycle 78
Figure 60: Ankle angle in one gait cycle 78
Figure 61: Piston length in one gait cycle 79
Figure 62: Ankle angle in one gait cycle 79
Figure 63: Ground reaction force parallel to the ground for one gait cycle 79
Figure 64: Ground reaction force perpendicular to the ground for one gait cycle 79
Figure 65: Strains on strain gauges in one gait cycle 80
Figure 66: Factor of Safety of the leg based on strain gauge distance from the below 80
Figure 67: Maximum strain on strain gauges based on strain gauge distance from the below 80
Figure 68: Factor of safety plot on the tube located at the lower leg 81
Figure 69: Factor of safety plot of the strain gauge holder part 81
Figure 70: Velocity Contour Plot 81
Figure 71 : Streamlines Plot 82
Figure 72: Pressure Contour Plot 82
Figure 73:Variation of Damping Coefficient with Given Ramp Velocity Input 83
Figure 74: Curve Fitting for Valve Opening 83
Figure 75: Block Diagram of the Control System 84
Figure 76: Incremental Fuzzy Tree 85
Figure 77: Strains on strain gauges in one gait cycle 86
Figure 78: Factor of Safety of the leg based on strain gauge distance from the below 86
Figure 79: Maximum strain on strain gauges based on strain gauge distance from the below 86
Figure 80: Rigid Models of Strain Gage Holder and Outer Pipe 87
Figure 81: Strain Gage Amplifier Circuit 87

List of Equations

$$R = \rho \cdot \frac{L}{A} \tag{1}$$

$$e_0 = \frac{E}{4} \cdot \kappa_s \cdot \varepsilon_0 \tag{2}$$

$$e_0 = \frac{(1+\nu) \cdot E}{4} \cdot \kappa_s \cdot \varepsilon_0 \tag{3}$$

$$e_0 = \frac{(1+\nu) \cdot E}{2} \cdot \kappa_s \cdot \varepsilon_0 \tag{4}$$

$$a_k = \frac{1}{T} \cdot \int_0^T F \cdot e^{-i \cdot k \cdot \omega_0 \cdot t} \cdot dt \tag{5}$$

$$F_f(t) = \sum_{k=-n}^{n} |a_k| \cdot \cos\left(k \cdot 2\pi \cdot t + \varphi_k\right) \tag{6}$$

$$I\left(\ddot{\theta}_{hip} - \ddot{\theta}_{knee}\right) + mgL_{cm} \sin\left(\theta_{hip} - \theta_{knee}\right) + c_{knee}\left(\dot{\theta}_{hip} - \dot{\theta}_{knee}\right) + c_{piston} b\left(\dot{\theta}_{hip} - \dot{\theta}_{knee}\right) \sin(\alpha) + k_{piston} b \cdot \theta \cdot \sin(\alpha) = 0 \tag{7}$$

$$\sin(\alpha) = \frac{a \cdot \sin\left(\frac{\pi}{2} - \theta_{knee}\right)}{\sqrt{a^2 + b^2 - 2 \cdot a \cdot b \cdot \cos\left(\frac{\pi}{2} - \theta_{knee}\right)}} \tag{8}$$

$$F = c \cdot V \tag{9}$$

$$\delta = \frac{1}{n} \ln \frac{\theta(t)}{\theta(t + nT)} = 0.807 \tag{10}$$

$$\xi = \frac{1}{\sqrt{1 + \left(\frac{2\pi}{\delta}\right)^2}} = 0.127 \tag{11}$$

$$c = \xi \cdot c_c = \xi \cdot 2 \cdot \sqrt{m \cdot g \cdot L_{cm} \cdot I} \tag{12}$$

$$I \cdot \ddot{\theta} + c \cdot \dot{\theta} + mgL_{cm} \cdot \sin(\theta) = 0 \tag{13}$$

$$I_i = \frac{T^2}{4\pi^2} \cdot mg \cdot L_{cm} \tag{14}$$

List of Engineering Drawings

Technical Drawing of Strain Gage Holder 98
Technical Drawing of Outer Pipe 99

Nomenclature

L: resistor length
A: resistor area
ρ: specific resistance
e_0: output voltage
E: input voltage
κ_s: gauge factor
ε_0: strain
e_0: output voltage
E: input voltage
κ_s: gauge factor
ε_0: strain
ν: Poisson's ratio
a_k: k^{th} Fourier series coefficient
F: kinematic or kinetic data
T: Gait period
ω_0: Angular frequency
$F_f(t)$: Function fitted to kinematic or kinetic data
φ_k: Phase shift ($\angle a_k$)
θ_{hip}: Hip angle
θ_{knee}: Knee angle
m: Total mass of the prosthesis
L_{cm}: Distance between the center of mass of the prosthsis and the knee axis
c_{knee}: Damping coefficient of the knee joint
c_{piston}: Damping coefficient of the piston
a: Distance between piston upper joint and the knee axis
b: Distance between piston lower joint and the knee axis
α: The angle between piston and the leg
ξ: Damping ratio
δ: Logarithmic decrement

2. Introduction

A generic passive prosthetic knee does not have any sensors or control system which makes it a simpler design that uses mechanical or hydraulic components to provide support for an amputee person. Due to the complex nature of walking pace, a passive prosthetic knee cannot be proficient to ensure the ergonomic needs of the user. Therefore, a need for a smarter design arises. Sensors and a control system can be used to adjust the walking pace of the user. This type of prosthetic knee can respond to changes in user's gait cycle and provide more natural and adaptive movement. In this microprocessor controlled prosthetic knee project the main variable to respond to changes is damping coefficient created by the piston.

In this particular project, we are required to design a microprocessor-controlled prosthetic knee that adjusts its parameter according to the gait cycle. This design should provide specified requirements. The goal of the finalized project is to fulfil the requirements as follows:

Project Requirements

• The control system design should be developed based on the kinematic, cylinder and valve structures of Ottobock C-Leg prosthetic knee.

• The control system of the prosthetic knee should identify the phase in the gait cycle and should be adjustable for different walking speeds.

• The control system should work with effective energy consumption.

• The simulation of the prosthetic knee should be executed, including all phases of the gait cycle, on a control system design tool software.

• Safety precautions for mechanism from unexpected user behaviours; interruption of the operating process.

• The prosthetic knee should be adaptable to different user sizes and characteristics.

Project Specifications

• It should allow patients to walk at a self-selected speed of up to 2 m/s.

• It should allow patients to stand without moving.

• It should allow patients to rotate their knees at different angles, which are between 0 and 130 degrees.

• It should allow patients to walk approximately 15,000 steps with a velocity of 1.6 m/s with a full charge.

• The delay of the response of the control system must be less than 5ms.

• The total weight of the control system should be less than 300 grams.

• The total cost of the system shouldn't surpass the cost of C-leg by 350$

Design Criteria

• Adjustable damping according to the gait cycle for different walking speeds. (30%)

• Adjustable damping according to the gait cycle for various person weights. (20%)

• The control system provides a smooth gait cycle with smooth damping values. (15%)

• Energy consumption. (15%)

• Cost (10%)

- Safety precautions for mechanism from unexpected user behaviors; interruption of the operating process. (10%)
- IoT. (5% Bonus)
- Wi-Fi or Bluetooth connection. (%5 Bonus)
- User interface. (%5 Bonus)

3. Literature Survey

3.1 INTRODUCTION

To begin with, lower limb amputation becomes a significant issue for excessive amounts of people. For example, the worldwide incidence of lower-limb amputations is high and varies from 3.6 to 68.4/100,000 people, and about 30% of lower-limb amputations are at the transfemoral level. Transfemoral amputations lead to restricted mobility, reduced societal participation, and increased risk of falling [1]. In addition, transfemoral amputees have the possibility of musculoskeletal problems caused by loading asymmetry during activities, such as prolonged standing, particularly on uneven or sloped ground [11].

Professionals must select a specific prosthetic knee joint that allows the patient to function optimally with the prosthesis daily. This selection is a complicated and challenging task because each patient is unique. Today, multiple examples of prosthetic knee joints exist that, established on how these joints are controlled, can be separated into two groups, such as prosthetic knee joints with entirely mechanical control properties, and microprocessor-controlled prosthetic knee joints (MPKs). MPKs, however, controls the dynamic parameters of the leg after detecting the gait phase based on the sensory inputs.[5]. The aim is to detect potential hazardous situations and to activate stumble and fall protection [1].

According to relevant research, one of the advantageous examples of MPKs is semi-active prostheses, the type of specific product for K3 and K4 transfemoral amputees C-leg (Ottobock) that we selected. The following parts will explain the reasons and the sense behind our selection. Furthermore, semi-active prostheses are able to alter their behavior immediately due to microprocessor technology; therefore, they can react to situations instantaneously. As opposed to the fact that they offer greater flexibility, they have some limitations in generating resisting forces [2]. Moreover, the benefits of utilizing an MPK are related to the possibility of walking with self-selected speed due to the adaptive control. Moreover, due to the adaptive nature of the system, MPK's can perform similar to the healthy walking pattern. It causes to decrease the metabolic energy consumption and gait asymmetry. [5].

We are focusing on the control system design of an MPK, specifically C-leg. The improvements of the above-mentioned benefits of MPK's are results of the successful control algorithms. [3]. We aim to design a control system for C-Leg to reach a smooth movement and adapt to different walking speeds.

3.2 COMMERCIAL PRODUCTS

There are various commercial products related to the project. There are couple of widely used microprocessor controlled prosthetic knee joints (MPKs). Since they can be adjusted based on the sensor data and user inputs, different modes to accommodate different uses of the prosthesis. It is especially important for patients to perform their activities of daily livings (ADL's) without help.

The first and most important product (the one that we will control) is C-Leg that is produced by Ottobock a German company. C-Leg is a widely used MPK. It relies entirely on hydraulic pistons to adjust the damping coefficient depending on the gait phase. Patients using C-leg experiences less falls compared to other MPK's.[13] The other important product in the market is Orion (Blatchford Group, Basingstoke, Hampshire, United Kingdom). Different than C-leg, Orion uses hydraulics alongside with

pneumatics. Genium is another MPK produced by Ottobock in 2011. Like C-leg, Genium uses a hydraulics to control swing and extension phases.

Table 1 Comparison between Different Prosthetic Knee ProductsTable

	C-Leg (Ottobock, Germany)	**Orion (Blatchford, UK)**	**Rheo (Ossur, Iceland)**	**Genium (Ottobock, Germany)**
Mechanism, Sensors and Actuators	Linear hydraulic system that generates resistance in direction of flexion/extension. 2 Microprocessor controlled servo valves adjust the resistance. Spring and hydraulic channel produce extension resistance. IMU to measure position, rotation, and acceleration of the knee joint. Knee angle sensor to detect flexion angle and angular velocity	Mechanism contains one hydraulic servo valve, and one pneumatic needle valve. Flexion resistances by microprocessor control, a hydraulic servo valve and a pneumatic needle valve.	Magnetorheological fluid chamber to control knee flexion/extension. Knee angle sensor and strain gauges deployed to measure axial load and bending moment of the shank. Operating frequency – 1 kHz	Increased gait cycle symmetry, stance flexion, shock absorption, and improved reciprocal ramp and stair descent compared to C-Leg.
Mobility	When comparing non-amputees with amputees: In 20% of criteria C-Leg dominates significantly better for non-amputees compared to Genium users			When comparing non-amputees with amputees: In 80% of criteria Genium dominates significantly better for non-amputees compared to C-Leg users (Endurance, lower and upper body strength, balance and coordination)
Extension/ flexion	Better loading bearing capacity and flexion resistance compared to Rheo. Greater maximum knee flexion angle compared to Rheo. C-Leg: 46.2 ± 7.9 °. Rheo: 44.8 ± 4.7 °		Slower extension speed compared to C-Leg	
Stance Phase	Shorter stance phase duration compared to Rheo. C-Leg 68.9 ± 2.8%; Rheo 72.3 ± 2.1%		Slight buckling during the first half of stance	

Swing Phase	Initiated easily at all walking velocities. Hip moment: -82.1 ± 14.1 Nm	Hip moment: -88.0 ± 16.3 Nm		
Knee angular velocity, flexion moment and angular acceleration	323.4 ± 33.8°/s 1.14 ± 0.13 Nm/kg -2565±1431°/s²	-3149±1014°/s²	188.5 ± 40.7°/s 0.90 ± 0.08 Nm/kg	
Quality of Life	C-Leg was advantageous compared to Genium In fields of feeling off balance, and satisfaction.			It is observed that Genium had improvement in 7/10 items compared to C-Leg. (Comfortable standing, walking in tight spaces, going down stairs, walking up hill, walking on slippery surface, satisfaction during walking.)
Cost and Market availability	40,000 - 50,000 USD (Available in Market)	30,000 – 40,000 USD (Available in Market)	40,000 – 50,000 USD (Not Available in Market)	70,000 USD (Available in Market)

C-Leg's Working Principle

Two separate hydraulic valves control the flexion and extension characteristics of C-leg. It causes the joint resistance to change depending on the gait phase. Those valves can be controlled continuously by the microcontroller depending on the inputs. [4]

Orion's Working Principle

Hydraulic and pneumatic systems are used together to control the knee joint resistance. Two independent circuits on one piston are used. Microprocessor is controlling the hydraulic servo valve and pneumatic needle valve to control flexion resistance. [4]

Rheo Knee's Working Principle

A magnetorheological damper is used in Rheo Knee for changing joint resistance. A knee angle sensor and strain gauges are used the determine the position of the knee and the forces applied to the shank. At swing phase, low resistance is used to allow a smooth swing phase. Stance phase is detected using the stain gauge inputs and knee resistance is increase compared to swing phase.[3]

3.3 STATE-OF-THE ART ON RELATED TECHNOLOGIES

Prosthetic knee technologies are concentrated on non-microprocessor-controlled prosthetic knees (NMPKs) and microprocessor-controlled prosthetic knees (MPKs). Furthermore, the MPKs can be divided into semi-active MPKs and active MPKs. In this subsection of the report, semi-active MPKs and active MPKs will be considered.

The benefits of Medicare Functional Classification Level [MFCL]-3 have been well established in community ambulators with transfemoral amputation (TFA). MPK leads to clinical improvements, such as improved walking speed, gait symmetry, and obstacle assessment. These clinical improvements, in turn, are associated with sizeable reductions in injurious falls and incident osteoarthritis and, as a result, lower mortality rates. MPK is related to improved mobility, safety, user confidence, activities of daily living, the ability to live independently, satisfaction, and thus a substantially better quality of life for amputees [9].

Mechanical control elements:

Regarding semi-active controlled prostheses, ankle and knee function loss of above-knee amputees are made up for by controlling the energy transferred through the residual limb. This regulation is accepted for most horizontal level walking and going down the stairs, since the useful energy needed by the knee is negative and must be absorbed. But the prosthetics are not able to supply positive energy to do certain tasks or walking periods as for quick push on horizontal ground walking and going up the stairs.[8]

In the semi-active MPKs, damping is usually modulated by fluid control. Hydraulic, pneumatic, and magnetorheological dampers are the most common choice. Dampers limit knee angular velocity in the early (flexion), and the late (extension) swing phases; semi-active devices can provide this functionality. Sensors are used to detect speed and gait phases during the gait cycle. [7] Hydraulic actuation systems can generate substantial forces considering that liquids are effectively incompressible. These systems generally contain pressurized reservoirs, gear pumps, DC machines, valves, and hydraulic cylinders with piston rods.[12]

On the other hand, active (powered) prosthetic knees have actuators that can provide extra energy to fulfill knee joint function during gait. Brushless DC motors actuated the joints. Three-stage transmissions consisting of a primary multi-V belt stage, a secondary roller chain stage, and a tertiary double-roller chain stage were adopted to drive the joints [7]. The actuation systems of robotic transfemoral prostheses include;

- electromagnetic actuators (i.e., occasionally featuring series elastic elements),
- pneumatic actuators (i.e., pneumatic cylinders and artificial muscles), and
- hydraulic actuators.

A significant design challenge for engineers involves computing the optimal actuator mechanical power [12].

Above mentioned various control strategies and high-tech controllers control above mentioned mechanical control elements. A high-level supervisory controller monitors the movements and inputs of the amputee and generates commands related to the amputee's intent, such as the motion that the prosthesis should perform. These commands are then forwarded to an underlying low-level controller responsible for controlling the prosthesis. Depending on the chosen high-level control strategies (see below), the controlled variables are angle/ position for echo control or force/torque for gait recognition and direct EMG control.

Control strategies:

- Echo control.
- Gait recognition
- Direct EMG control
- Other/Extra

Concerning echo control, the movement of a fit let is captured using sensors and replayed on the artificial side with a half-gait cycle delay. Different sensors such as gyroscopes, magnetometers, strain gauges, pressure sensors micro-electromechanical system (MEMS) accelerometers are used to record measurements which are used to evaluate surface electromyography (sEMG) signals, angular positions, ground reaction forces and amputee exerted forces. These measurements help to recognize the phase of the gate during the gate cycle.[2]

The gait cycle is divided into individual phases, and parameters for the spring and damper are defined to match the impedance of the prosthesis with the one of the physiological joint. This approach gives the user more intuitive control than rigid position control[2].
Echo control is a somewhat limited framework that does not facilitate arbitrary motions and thus appears less appropriate for dynamic locomotion. Currently, gait mode recognition, which adapts to the impedance of the prostheses, is applied more frequently due to its higher flexibility and stability [2].
Direct EMG control or myoelectric control enables deliberate control over the prosthesis based on surface EMG signals obtained from electrodes in the prosthesis socket. The amputee is then capable of altering the torque by his muscle contractions. Technical challenges are signal noise and high latency. In addition, the amputee requires extensive training to visually check his leg's position because of the lack of proprioceptive feedback [2].

Different high-level control strategies are applied to enable different locomotion modes; therefore, enabling the amputee a high degree of voluntary control over the prosthesis. High-level approaches are echo control, gait mode recognition, and direct EMG control. Widely used control strategies are gait mode recognition in combination with low-level impedance control and direct EMG control [2].

Innovative Technologies:

Innovative technologies are discussed related to energy recovery. The advent and adoption of energy storage and return (ESR) prosthetics, containing a mechanical spring or pneumatic restoring force mechanism, can help to minimize users' energy expenditure compared to traditional solid prosthetics. To prevent over-burdening the user with unnecessary parasitic effects careful power control and damping switching are required. The idea is to recover kinetic energy, which would otherwise be dissipated to the ambiance, and not draw extra energy from the user. [6]

Practically, onboard batteries should be minimal in size and weight to not overburden the user: transtibial amputees. While the user sleeps at night, the battery itself can be recharged in a charging hub at night and the battery is trickle-charged by the energy recovered through regenerative gait motion. The presence of regenerative gait can help minimize the size and weight of the onboard battery. It is predicted that nearly 0.4 W of average electrical power can be recovered for a running gait (9 km/h) and 45 mW for a walking gait (3 km/h). This amount of power satisfies power requirement of intelligent microsystems, including wireless systems, microprocessing units, and MEMS sensors.

Required nominal power input of various sensors, controllers, wireless systems, motors, and actuators are presented in Table 2. [6]

Table 2 Typical power requirements of components

Device/Operation Mode	*P* (mW)	Notes
Microproccessing unit (MPU)	0.36	active mode [39]
32-bit ARM Cortex	0.002	standby mode [39]
Bluetooth 5 + RF chip	27	transceiver mode [40]
	0.045	sleep mode, clock [40]
MEMS 9 DOF motion sensor + MPU	0.05	InvenSense [41]
MEMS strain gauge + ASIC	0.01	Uni. Cambridge [35]
MEMS pressure sensor + ASIC	0.2	Omron [42]
DC Motor at 0.85 kg f.cm torque	4,500	3 units of 1.5 W motor
Servo actuator with 5 N starting force	9,000	3 units of 3 W motor
Power conditioning circuit	0.1	switch mode type [33]
Other electrical components + leakage	0.5	estimate

It is easy to observe that meeting the power requirements of sensors, microprocessors and wireless systems is possible with power recoverable from gait motion. Hence, regenerative energy can sustain all sensing and smart computation capabilities. Motors and actuators would be most power consuming elements as duty-cycled by adaptive control to help arrange gait motion and pattern as required. The second most power consuming element would be considered wireless communication which is also can be duty-cycled. Moreover, improving regenerative prosthetics to assist sustaining the power requirement for supplement the battery drain by motors and functionalities as sensors. As more sensors and motors are added to develop prosthetics' comfort and gait patterns, the proposed regenerative energy harvesting capability is crucial to enable these functions without overburdening the user with a heavy battery pack.

3.4 PATENT

There are various patents about both mechanical construction and the control strategies for microprocessor controlled prosthetic knees.

Various sensors are needed for detecting the gait and controlling the system according to it.

A magnetic knee positioning sensor is designed at [14]. It has a similar system to what we have in C-leg. Understanding the sensor system can help us to get the knee angle data correctly. Getting the correct data is critical for a successful control algorithm.

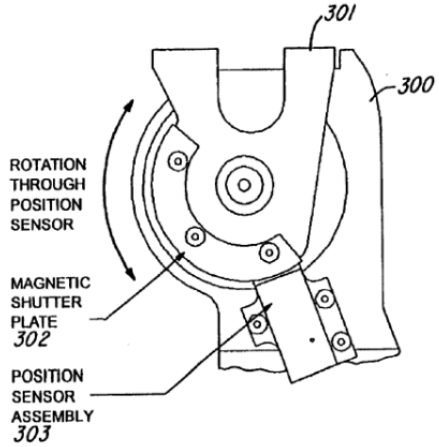

Figure 1

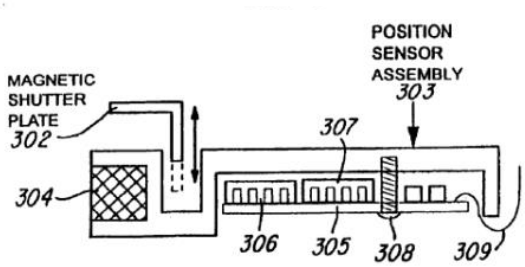

Figure 2

The measured angles and the flow chart of the control algorithm for changing the joint resistance is shown below. [15] From that we can see that the angle measurements are critical while controlling the parameters of the prosthetic knee.

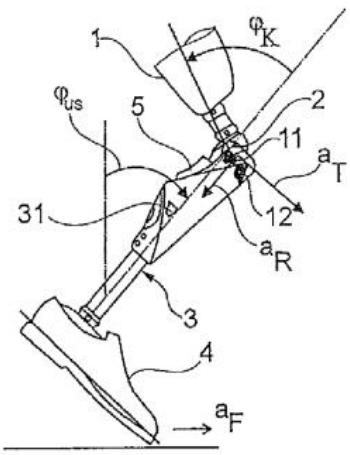

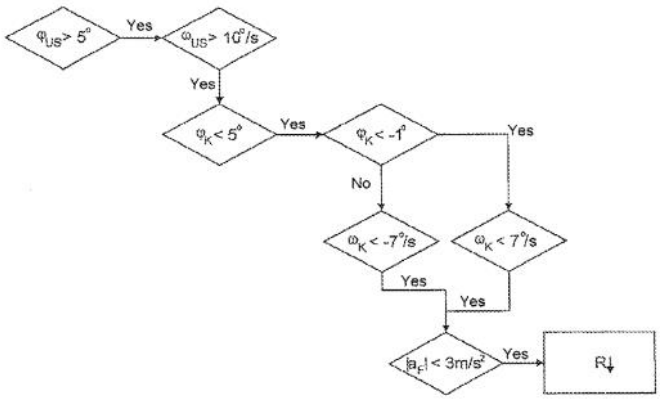

Figure 4

Figure 3

An invention relates to knee prothesis that employs a hydraulic damper to passively regulate the angular velocity or rotation artificial knee joint. It is remarkably similar to the logic used by our product C-leg. System is shown below designed at [19].

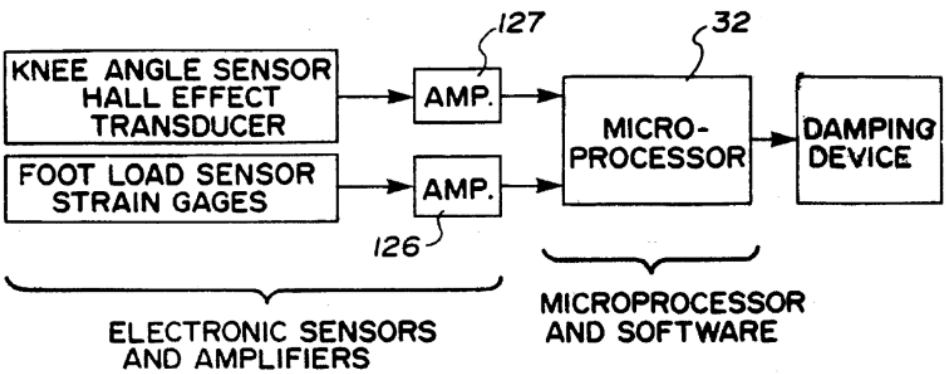

Figure 5

Similar piston and valve designs to C-leg are shown below.

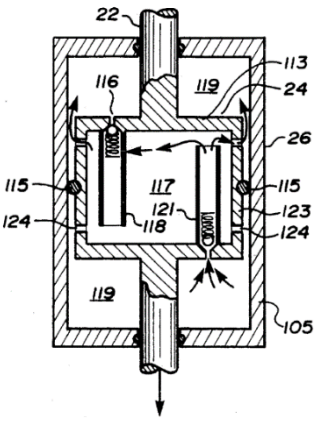

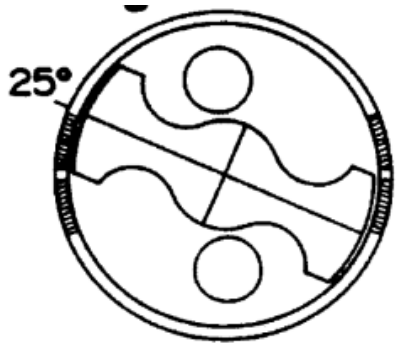

Figure 7

Figure 6

An invention which is a prosthetic knee provides a single axis of rotation and includes a hydraulic damping cylinder, a micro-processor, and sensors has a similar logic with C-leg. This Gait Cycle-Knee position graph of this design shown below will guide us with designing our control system [20].

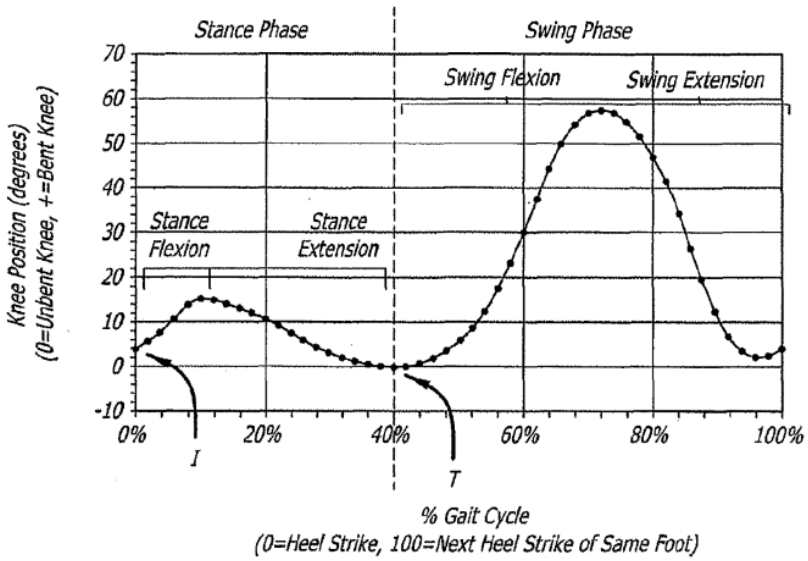

Figure 8

Knee angle, ankle angle, bending moment, angular and linear accelerations are measured by appropriate sensors in [17]. Obviously, more sensors give more data about the gait, thus it will be easier to detect the gait phase. However, sensors add cost and complexity to the system. Therefore, unnecessary sensor use should be avoided.

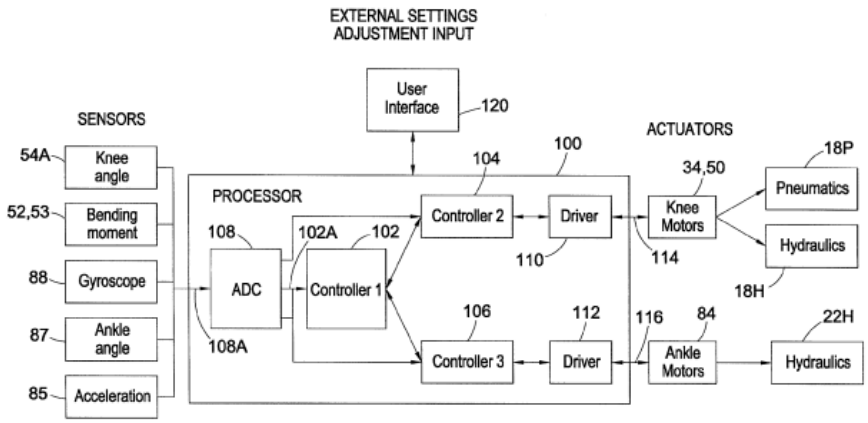

Figure 9

The phases of a healthy gait cycle are shown in [18]. We need to understand every phase of the gait to design a gait detection system and determining the adjusted system parameters.

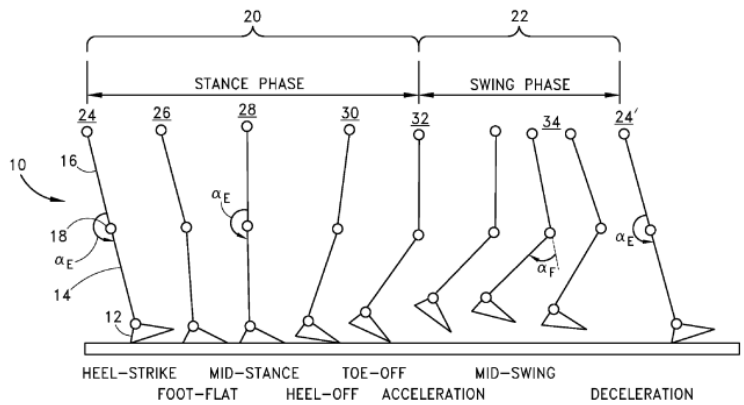

Figure 10

3.5 SUMMARY AND CONCLUSION

We analyzed and compared four different commercial products, which are C-leg (Ottobock), Orion (Blatchford), Rheo (Össur), and Genium (Ottobock). In addition, we benefited from 6 different patents with similar inventions used in C-leg.

According to articles and researches we investigated; several experiments show that C-leg (Ottobock) is superior in different aspects of a patient's daily life. Therefore, C-leg would be a reasonable choice to be used in our project. Designing a control system for C-leg may provide the best performance for patients. The differences between C-leg and other products mentioned in the Commercial Products part and the technology behind the device C-leg is explained in the State-of-the-Art Related Technologies part in 3 main categories: control strategies, mechanical control elements, and innovative technology. In the part of the patents, we significantly benefited from inventions that we think are similar to designs of systems in C-leg.

This survey enlarged our scope in lower-limb amputation and prosthetic knee joints. We realized that several methods were used and still using through the years, especially in sensors and actuator design. Although many ways may provide sufficient walking experience, only a few of them are capable of increasing the quality of life for amputees significantly.

4. PROJECT PLANNING & MANAGEMENT

4.1 INTRODUCTION

The project organizational planning, timeline and distribution of tasks is explained. The identification of tasks and their sub-tasks are prepared, and each member is assigned tasks according to their abilities and areas of specialization. The timeline and duration of each task is presented in the form of a Gantt chart.

4.2 ORGANIZATION OF THE PROJECT

During the design phase of the project, 6 main tasks were identified. They are literature survey, conceptual design, detailed design, modeling, manufacturing and documentation. The names of each group member and their initials is given in Table 1. Assigning tasks to members and setting time durations made it easier to control and follow the progress of the project.

Table 3 Team Member Names and Initials

1.	Ali Fuat Şahin (AFŞ)
2.	Can Uludoğan (CU)
3.	Egemen İlikmen (Eİ)
4.	Faysal Turkistani (FT)
5.	Hüsnü Furkan Evci (HFE)
6.	Mehmet Furkan Doğan (MFD)
7.	Osman Berkin İnci (OBİ)

4.3 EXPLANATION OF THE TASKS AND THEIR DEFINITIONS

4.3.1 Literature Survey

The aim of the literature survey is to collect information about different microprocessor controlled prosthetic knee joints MPKs, their working principals, advantages and disadvantages. This helped generate concepts, set project requirements and specifications. Sub-tasks and their duration were as follows:

Commercial Product Research (FT, OBİ)

Perform research on the different types of MPKs that are available commercially. The reason behind this is to understand the working principals behind products and where our product could stand in the market in terms of cost, quality and performance. This helps in deciding what areas to focus on improving in our project.

Start Date: 03.10.2022 Finish Date: 28.10.2022

Patent Research (MFD, HFE)

Research was carried out into the technologies and ideas behind the MPK products to get information on the origin of designs, their invention and who owns them. Furthermore, performing patent surveys avoids us from falling into legal complications.

Start Date: 22.10.2022 Finish Date: 28.10.2022

State of the Art Survey (CU, Eİ, AFŞ)
Research on the different and recent technologies available in the literature and the market related to the project is carried out. This helped improve our design targets and problem-solving approach.
Start Date: 22.10.2022 Finish Date: 28.10.2022

4.3.2. Conceptual Design
The aim of this process is to specify required functions and coming up with suitable concepts and then evaluating those possible concepts that might be used in our project.

Problem definition and Project specification (All members)

The problem and why this project is needed is clearly stated. After, the literature survey project requirements are specified according to these surveys.

Start Date: 12.10.2022 End Date: 19.10.2022

Functional Decomposition (All members)

Subfunctions that are required for this project are determined.

Start Date: 27.10.2022 End Date: 01.11.2022

Brain Storming (All members)

Thinking about the ways to improve the design concepts. To do that previously decided subfunctions are written and by order we enhanced each other's concepts. At the end of this process, we decided the concepts for subfunctions.

Start Date: 26.10.2022 End Date: 02.11.2022

Morphological Chart (All members)

Trying to figure out possible solutions for the essential functions.

Start Date: 03.11.2022 End Date: 06.11.2022

Assessment of Concepts (All Members)

After deciding the possible concepts for the required functions, choosing the best possible solution for the project. Writing down both positive and negative traits for each concept.

Start Date: 07.11.2022 End Date: 21.11.2022

4.3.4 Detailed Design
After determining the concepts, we need to finalize the design of those concepts. We can divide the tasks based on functions we need to implement.

Knee Angle Sensor (Eİ, OBİ, MFD)
Determining suitable sensor to detect knee angle which is a crucial input for control system to understand phases of walking.
Start Date: 11/11/2022 End Date: 25/11/2022

Force Measurement Sensor (FT, CU, HFE)
We need to measure forces and moments on the knee instantaneously to adapt to different walking conditions, so a force measurement sensor is decided.
Start Date: 04/11/2022 End Date: 11/11/2022

Valve Motor Control (AFŞ, Eİ)

Our control system benefits from the changing damping values while walking. To use these values on the control system, we use valves on motors.
Start Date: 02/12/2022 End Date: 09/12/2022

Control Strategy for Different Walking Speeds (AFŞ, MFD)
Deciding the most suitable control strategy which interprets sensor data and detects gait phase, movement speed and movement anomalies to reach smooth walking experience with appropriate response time.
Start Date: 12/12/2022 End Date: 14/01/2023

Microcontroller Selection (AFŞ, CU, HFE)
Deciding the most suitable micro control device for the system which will be the main controller of our control system and deciding if there is a need for another microcontroller.
Start Date: 11/11/2022 End Date: 25/11/2022

4.3.4.6 Battery and BMS Selection (FT, OBİ, Eİ)
Selecting appropriate batteries and module for the system.
Start Date: 25/11/2022 End Date: 09/12/2022

4.3.4.7 User Interface (AFŞ, MFD)
Creating a user interface to display remaining charge, walking modes, etc. Also, the user should be able to select its mode according to different situations such as walking, running.
Start Date: 14/01/2023 End Date: 21/01/2023

4.3.4.8 Experiments (AFŞ, MFD)
Testing processes for decided concepts.
Start Date: 09/01/2023 End Date: 28/01/2023

4.3.5 Supplying Material and Manufacturing

In this task, the process of gathering necessary materials for our control system and their assembly operations are conducted. Some materials are bought directly and tested before final usage.

Determination of Necessary Components (All Members)
Since we need to design a control system, different electronic components are needed. After literature research, decisions are made for selecting suitable sensors and controllers.
Start Date: 10/10/2022 End Date: 30/10/2022

Purchasing (CU, HFE, FT)
When we start to determine components to use, we start to get some of them by purchasing. Since some materials came from abroad, it took more time to have.
Start Date: 17/10/2022 End Date: 28/11/2022

Testing (MFD, AFŞ, HFE)
Some of the purchased products, especially sensors, are tested to check whether we can get healthy signals from them or not. Also, we analyzed their signal behaviors.
Start Date: 31/10/2022 End Date: 11/12/2022

Assembly (All Members)
It is the task of giving the final shape to the control system with all the components.
Start Date: 12/12/2022 End Date: 18/12/2022

4.4 Documentation

In the documentation process, the tasks which are done in the project are documented. Documentation is prepared to figure out the progress through all project steps. Documentation templates are given by the department, and reports and presentation prepared according to these templates.

R1-2-3-4-5 Reports (All Members)
Five R reports are prepared in total. R reports are prepared after some main tasks which are determined by the department. These tasks are literature survey, problem definition and project specifications, project planning, conceptual design and detailed design respectively.
Start Date: 20/10/2022 End Date: 06/01/2023

Final Report (All Members)
Final Report (FR) are compilation of the revised versions of previous reports (R1-R5). In addition, FR includes a comprehensive conclusion and final remarks on the tasks conducted as well as some additional sections.
Start Date: TBA End Date: TBA

Presentation (All Members)
The presentation of the project is prepared to present faculty members.
Start Date: TBA End Date: TBA

Poster of the Project (All Members)
The poster of the project is prepared to demonstrate product and production steps more clearly. It is presented in the final presentation.
Start Date: TBA End Date: TBA

4.5 Modeling

To complete the design control system, it is required to determine the properties and interactions of the physical parts. To determine these a number of mathematical models and analyses are used.

4.5.1 Solid modeling (CU, FT, MFD)

This is a crucial task since physical properties of the leg are required for many other tasks. Since we are using an already existing prosthetic leg accurate physical measurements are required to create a solid model. Thus, a 3D scanning machine with point cloud technology is used.
Start Date: 04/11/2022 End Date: 25/11/2022

4.5.2 Kinematic Analysis (MFD, Eİ, AFŞ, HFE)

In this task physical properties of the (dimensions, masses, moment of inertias) prosthetic leg is used along with the required motion to determine required forces to complete said motion. Then calculated forces are used to determine the required damping coefficients.
Start Date: 04/11/2022 End Date: 18/11/2022

4.5.3 Flow analysis (FT, OBİ)

The purpose of doing a flow analysis is to determine the required motor angles to achieve previously calculated damping coefficients. In order to achieve this a flow

analysis, have to be done using the geometry of the hydraulic cylinder and properties of hydraulic fluid.
Start Date: 13/11/2022 End Date: 04/12/2022

4.6 TIME TABLE

Table 4 Time table showing the overall distribution of the workload

TASK ID	DURATION (# WEEKS)	TEAM MEMBERS
1.a	1 week	FT, OBİ
1.b	1 week	MFD, HFE
1.c	1 week	CU, AFŞ, Eİ
2.a	1 week	All Members
2.b	1 week	All Members
2.c	1 week	All Members
2.d	1 week	All Members
2.e	2 weeks	All members
3.a	3 weeks	Eİ, OBİ, MFD
3.b	1 week	FT, CU, HFE
3.c	1 week	AFŞ, Eİ
3.d	4 weeks	AFŞ, MFD
3.e	2 weeks	AFŞ, CU, HFE
3.f	2 weeks	FT, OBİ, Eİ
3.g	1 week	AFŞ, MFD
3.h	3 weeks	All members
4.a	3 weeks	All members
4.b	6 weeks	CU, HFE, FT
4.c	6 weeks	MFD, AFŞ, HFE
4.d	1 week	All Members
5.a	7 weeks	All Members
5.b	TBA	All Members
5.c	TBA	All Members
5.d	TBA	All Members
6.a	3 weeks	CU, FT, MFD
6.b	2 weeks	MFD, Eİ, AFŞ, HFE
6.c	3 weeks	FT, OBİ

4.7 TIMELINE

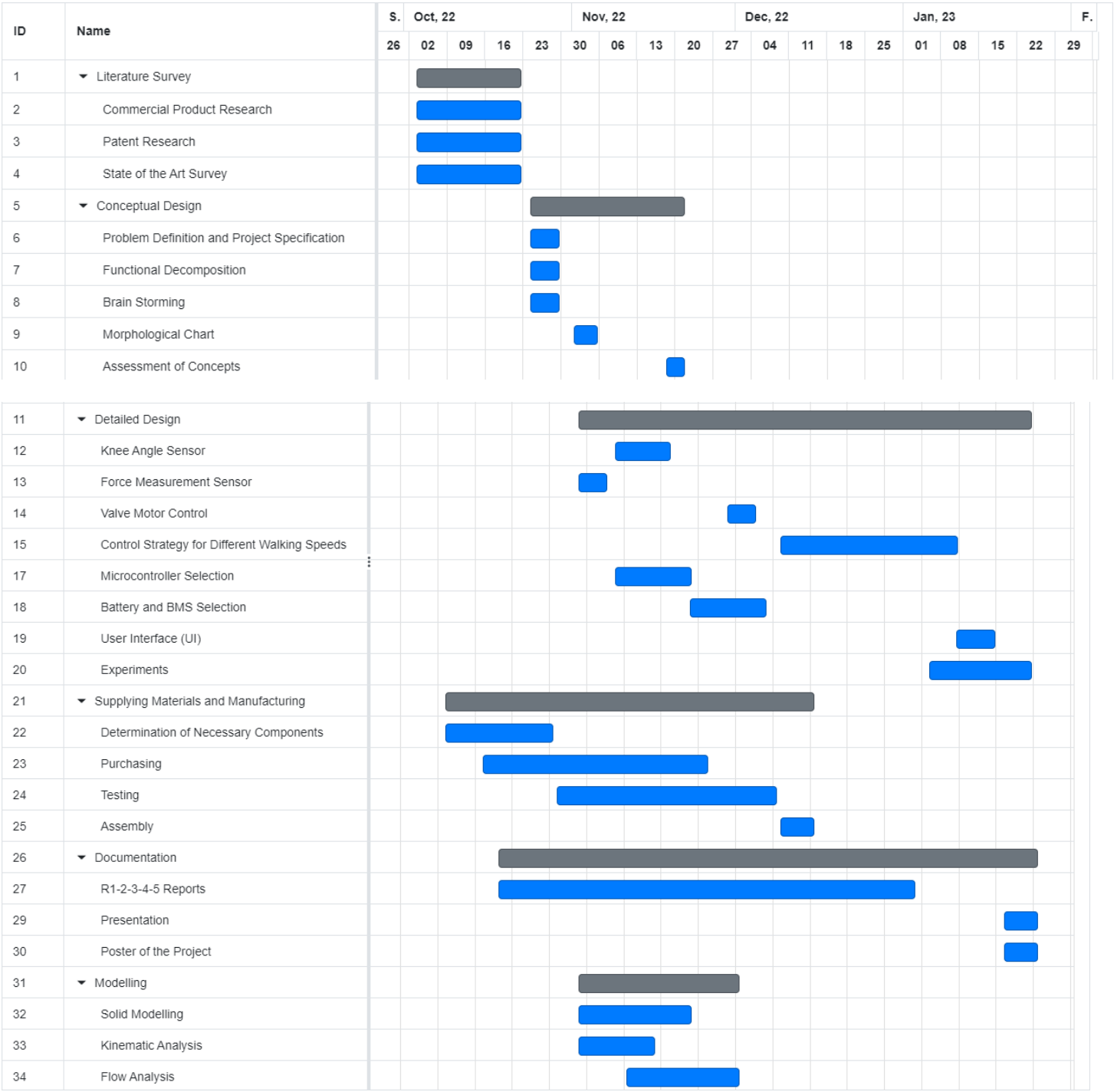

Figure 11. Gantt Chart

4.8 SUMMARY AND CONCLUSION

In this report we gave a description of the tasks that members must complete. We tried to distribute the tasks efficiently, according to members' wishes and area of specialization. We tried to be as flexible as possible in terms of tasks, and labor division to avoid inefficiency, since most of the workload will be in the future. Therefore, if any team member needs assistance, they can get it from other members in the group. The riskiest tasks in this project are measurement and detecting the knee angle and gait phase. Also preparing the algorithm and coding programs of the microprocessor. In case a physical model could not be delivered, virtual simulations of the working model will be presented. Some of the dates are set tentatively and could be changed according to the circumstances. In this process we plan to use MATLAB, SolidWorks, Simulink, ADAMS, ANSYS, Word, Excel. The Gantt chart was prepared to keep track of the timeline of the project's progress and to know which member has which task in hand.

5. CONCEPTUAL DESIGN

5.1 INTRODUCTION

In this report, alternative design concepts that are developed in conceptual design and concept evaluation workshops are presented. Comparison of concepts in system and component level are presented with the help of functional decomposition, morphological chart and decision matrices. Conceptual design process is presented below.

5.2 CONCEPT DEVELOPMENT AND PRESENTATION

5.2.1 Functional Decomposition Chart

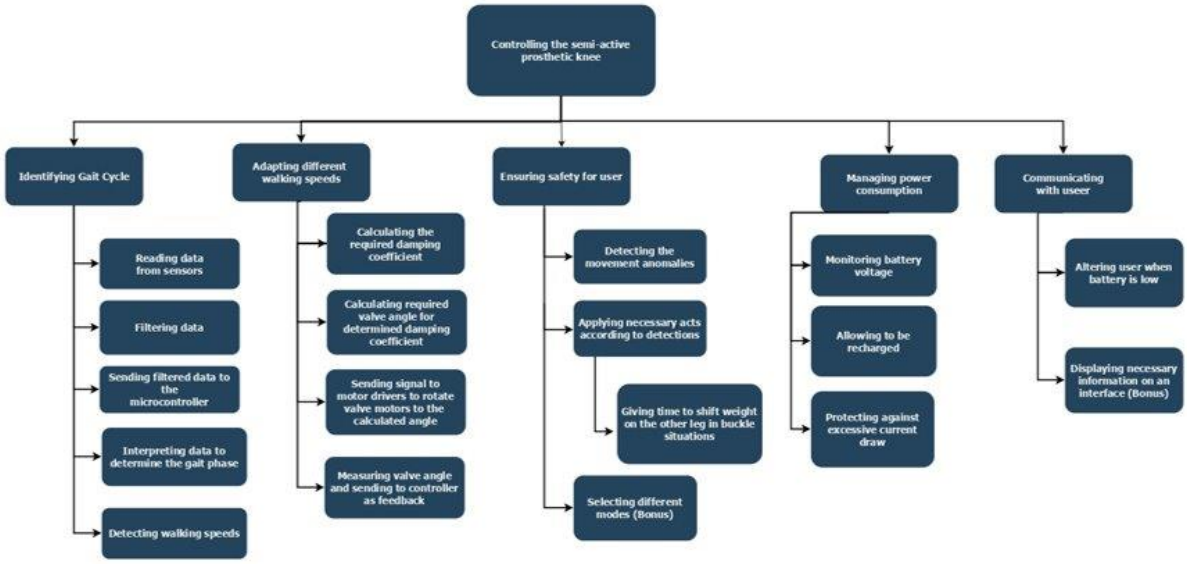

Figure 12: Functional Decomposition Chart

5.2.2 Functional Decomposition List

1. Identifying Gait Cycle
    a. Reading data from sensors
    b. Filtering data
    c. Sending filtered data to the microcontroller
    d. Interpreting data to determine the gait phase
    e. Detecting walking speeds
2. Adapting different walking speeds
    a. Calculating the required damping coefficient
    b. Calculating required valve angle for determined damping coefficient
    c. Sending signal to motor drivers to rotate valve motors to the calculated angle
    d. Measuring valve angle and sending to controller as feedback
3. Ensuring safety for user
    a. Detecting movement anomalies
    b. Applying necessary acts according to detection
    i. Giving time to shift weight on the other leg in buckle situations
    c. Selecting different modes (Bonus)

4. Managing power consumption
    a. Monitoring battery voltage
    b. Allowing to be recharged
    c. Protecting against excessive current draw
5. Communicating with user
    a. Altering user when battery is low
    b. Displaying necessary information on an interface (Bonus)

5.3 Morphological Chart

Table 5 Morphological Chart

Functions	Concepts			
Identifying Gait Phase and Calculating Valve Angle	Decision Tree	Artificial Neural Networks 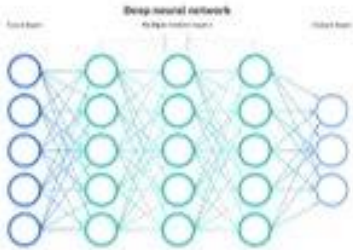	Evolutionary Algorithms 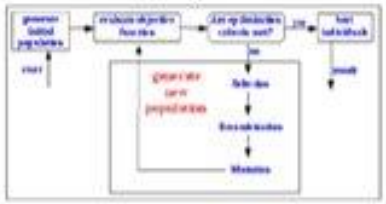	Combined System 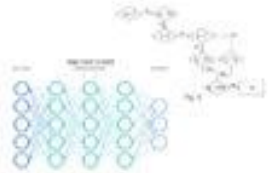
Controlling Valve Angles	PD 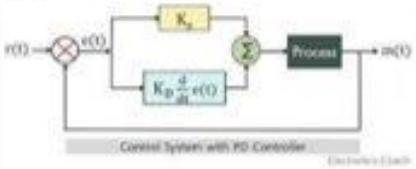	PID 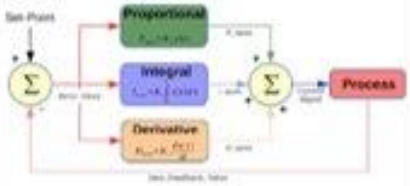	Fuzzy Logic 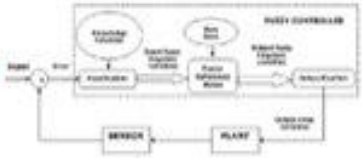	Combined System 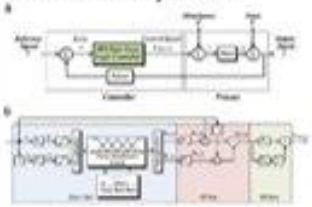
Ensuring Safety for User	By Predictive Confidence Level Approach 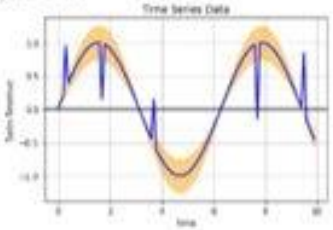	Statistical Profiling Approach 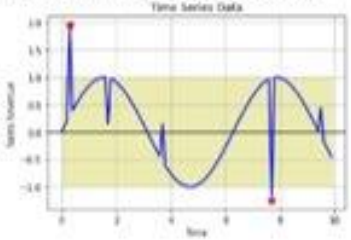	Clustering Based Unsupervised Approach 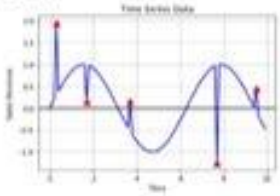	

Managing Power Consumption	BMS Module			
Communication with User	Buzzer	Vibration Motor	Mobile App	Combined System
Measuring Knee Angle	Incremental Encoder 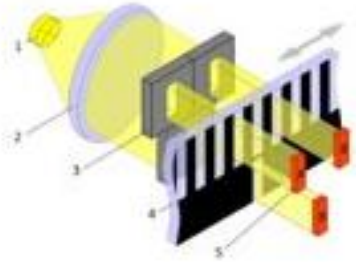	Absolute Encoder Optic Encoder 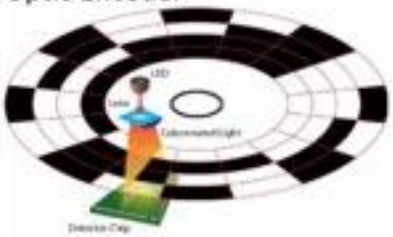	Magnetic Encoder 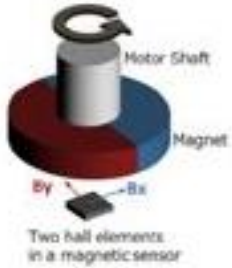	

Measuring the Ground Reactions	Active-Dummy Half Bridge System 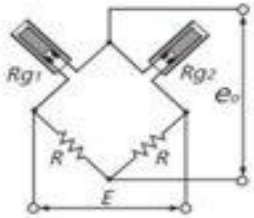	Orthogonal Active Full Bridge System 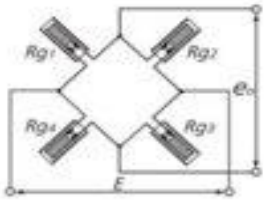	Active Quarter Bridge 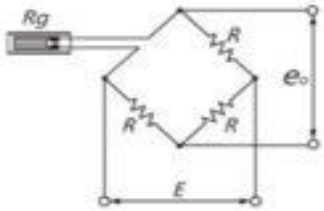	
Microcontroller	2 pico	1 pico + multiplexing	Arduino mega	STM32
Filtering	Low Pass 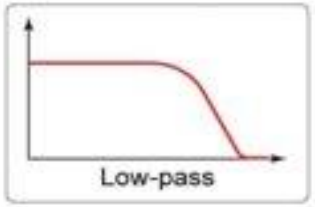	High Pass 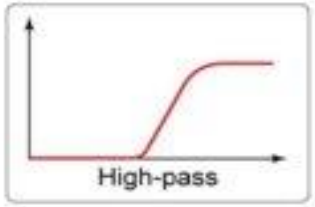	Band Pass 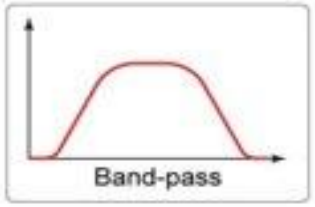	Band Stop 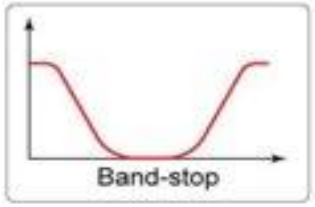

5.4 Identifying Gait Phase:

5.4.1 Decision Tree

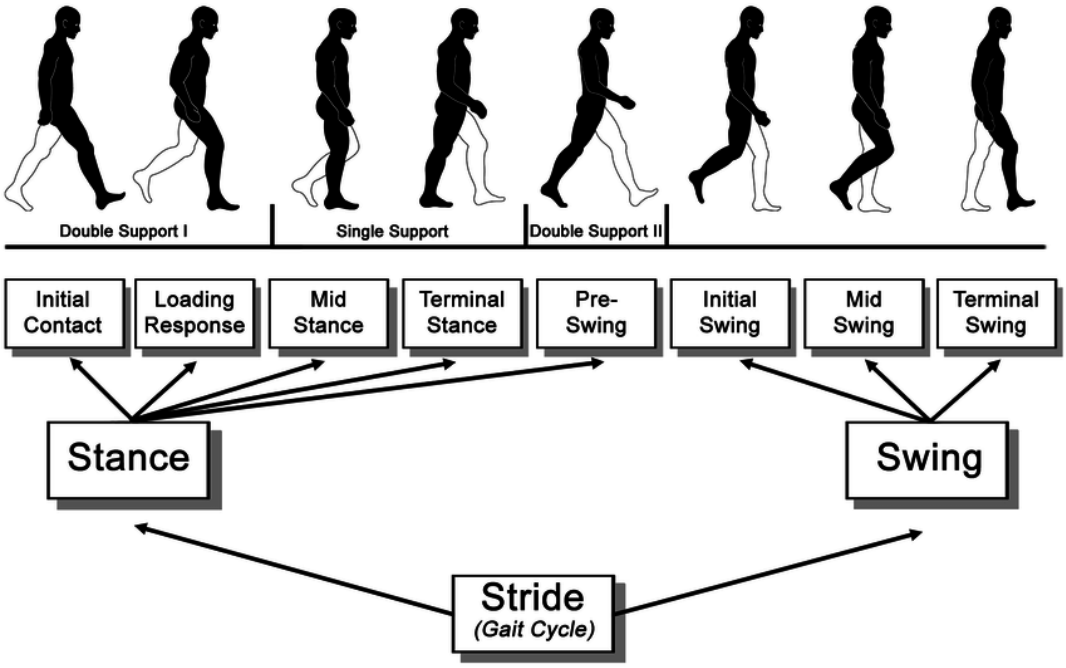

Figure 12: Example Decision Tree Algorithm for determining gait phases

Decision Tree algorithm is mainly based on the idea of classification and regression of problems to obtain all possible solutions to solve a problem or decision. The main goal is to create a learning environment for the control system by depending on learning simple decision rules inferred from prior data.

5.4.2 Artificial Neural Networks

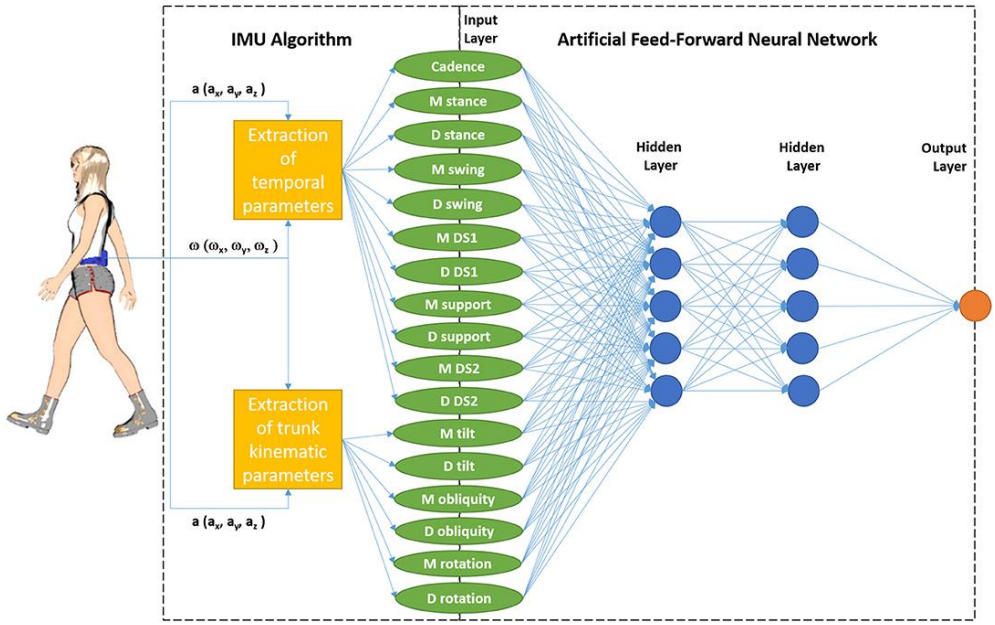

Figure 13: A Neural Network Algorithm used for controlling a microprocessor controlled prosthetic knee

Neural networks are developed for classifying and clustering sensor data based on the recognized patterns. It is a group of algorithms that recognizes the underlying relationship between a set of input data.

5.4.3 Evolutionary Algorithms

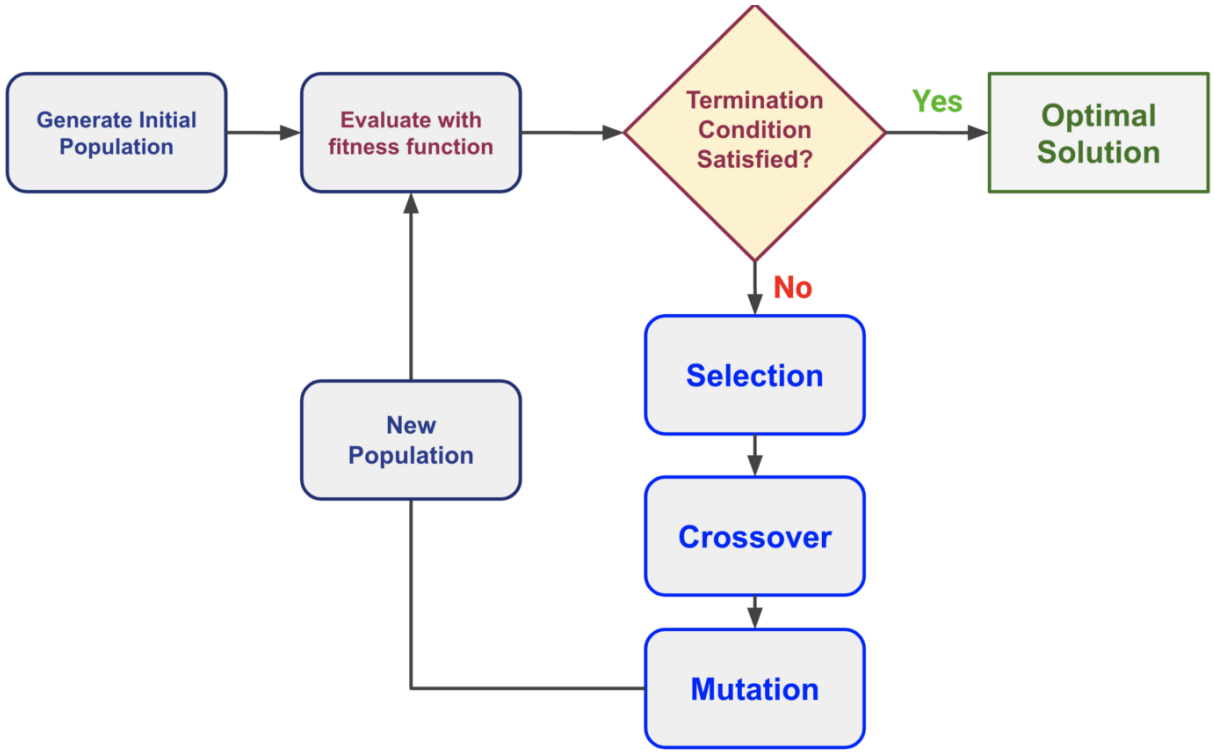

Figure 14:Flow chart of an evolutionary algorithm

Evolutionary algorithms are an unsupervised learning algorithm alternative to neural networks that are based on fitness functions instead of trained nodes. Most preferred type of evolutionary algorithms is genetic algorithm which seeks the solution in the form of the string of numbers by applying operators such as selection, crossover, and mutation.

5.4.4 Combined System

This is a possible concept which combines advantages of either artificial neural networks and decision tree or genetic algorithm and decision tree algorithms.

5.5 Controlling Valve Angles

5.5.1 PD Control

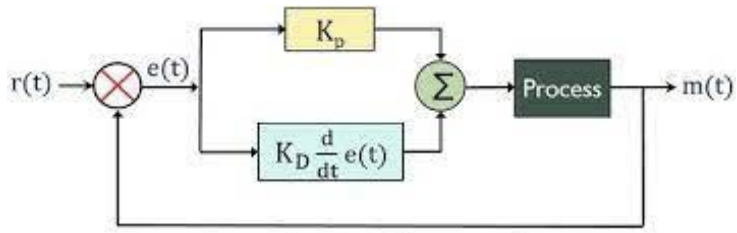

Figure 15: Block diagram of a feedback control system with PD controller

PD controller is based on error measurement of the sensor data and controlling the parameters with respect to variation and multiple of error data.

5.5.2 PID

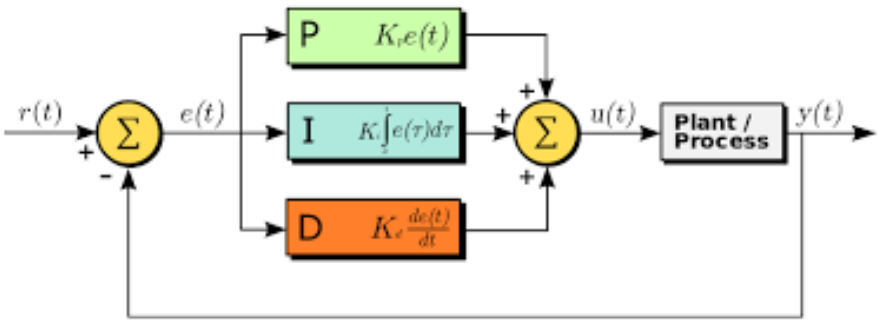

Figure 16: Block diagram of a feedback control system with PID controller

In addition to advantages of PD controller, PID controller adds an integrator to consider cumulative error to obtain a better steady state solution.

5.5.3 Fuzzy Logic

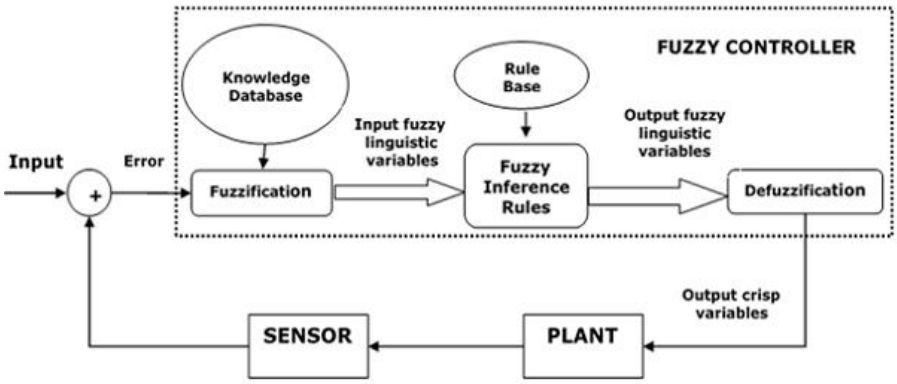

Figure 17: Block diagram of a feedback control system with a fuzzy logic controller

In fuzzy logic, rather than using absolute true and absolute false using fuzzification of logic values, degrees of truths are created. This makes control system more stable due to control parameters depending on significance of sensor data.

5.5.4 Combined System

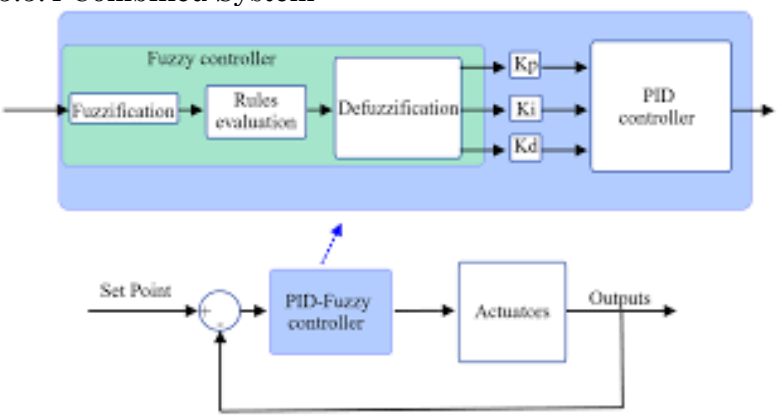

Figure 18: Block diagram of a feedback control system with a PID controller and a fuzzy logic controller combined

This is a possible concept to use PID and Fuzzy controllers in the same system to satisfy requirements of system by benefiting from advantages of both PID and Fuzzy Logic.

5.6 Ensuring Safety for User

5.6.1 Predictive Confidence Level Approach

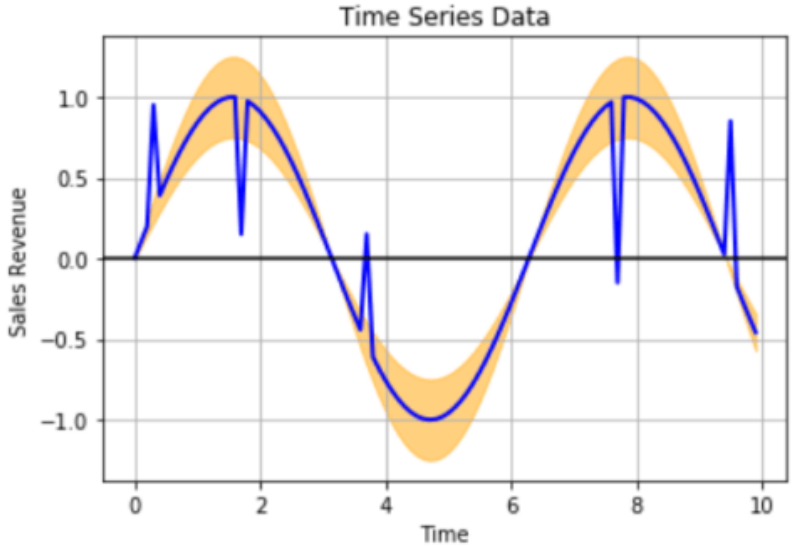

Figure 19: Time series graph for predictive confidence level approach

Predictive Confidence Level Approach is a supervised machine learning method to detect anomalies in a pattern. Since it is a supervised method, it needs historical data to detect anomaly in following pattern.

5.6.2 Statistical Profiling Approach

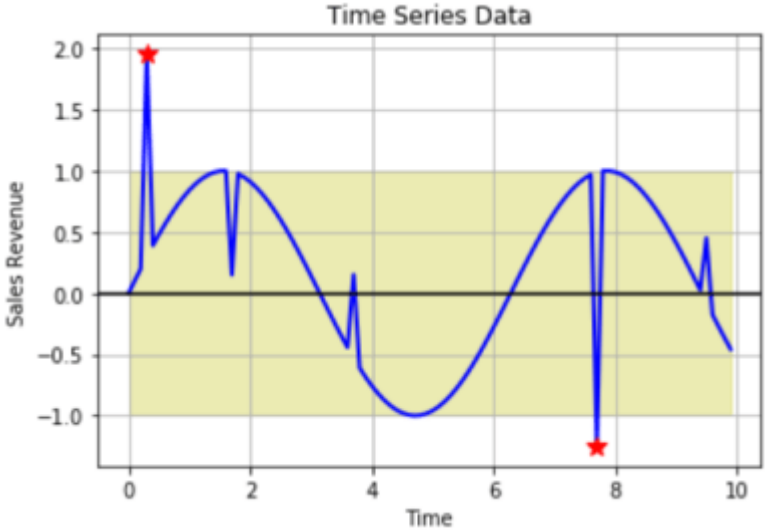

Figure 20: Time series graph for statistical profiling approach

Statistical Profiling Approach is also a supervised machine learning method which needs historical data. Also, it is the most precise method compared to

others. It calculates statistical information such as median and standard deviation of historical pattern for detection.

5.6.3 Clustering Based Unsupervised Approach

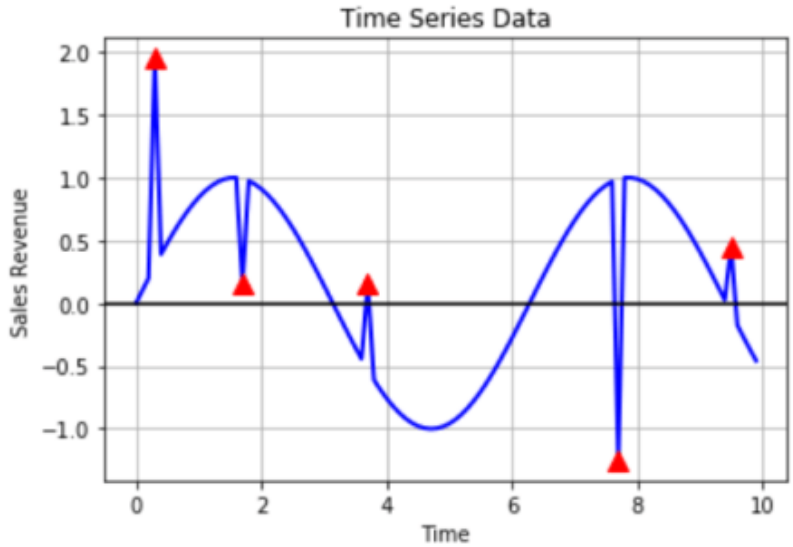

Figure 21: Time series graph for clustering based unsupervised approach

This is an unsupervised method of machine learning which is an alternative for supervised anomaly detection algorithms. Therefore, this approach does not need any historical data for detection. As opposed to supervised approaches, this approach can be used for time series data.

5.7 Managing Power Consumption

5.7.1 BMS Module

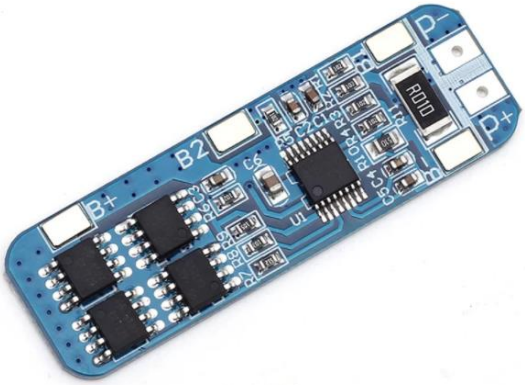

Figure 22: Battery Management System (BMS) Module for a single cell Li-Ion Battery

Battery Management System (BMS) is a technology dedicated to oversight of a battery pack. BMS module manages rechargeable cells by preserving from outside of its safe area, and controls its environment by authenticating and balancing.

5.8 Communication with User

5.8.1 Buzzer

Figure 23: A buzzer

Buzzer is an audio signaling device that includes alarm devices, timers to warn the user by generating a sound. It has mainly three types which are electromechanical, piezoelectric and mechanical buzzers.

5.8.2 Vibration Motor

Figure 24: A vibration motor

Vibration motor is a typical mechanical device that generates vibrations using a dc motor and an unbalanced mass on the motor shaft. It has variety of types and is mainly used in commercial products such as scanners, tools and medical instruments.

5.8.3 Mobile app

Figure 25: Mobile Phone Application

In our case mobile app is selected as a concept since it allows user to select different modes in addition to warn the user against possible problems. Mobile app is a versatile tool to communicate with the user and convenient to modify through changing the interface of the application.

5.8.4 Combined System

Combined system uses advantages of all three systems and can warn the user through all possible ways. Furthermore, in case a warning system fails user can still be warned through other systems. Mobile app supplies versatile mode selection, buzzer and vibration motor warns the user both with sound and vibration.

5.9 Measuring Knee Angle

5.9.1 Incremental Encoder

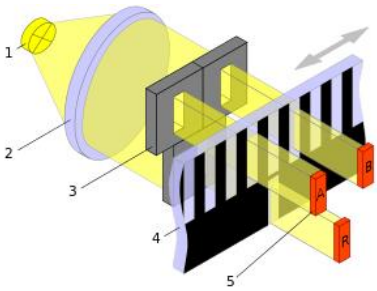

Figure 26: Figure explaining the functional principle of a optical incremental encode. As (4) moves shaded and lighted areas chances

It converts the angular motion of the knee joint into a digital code to identify the position the knee joint makes with the vertical. It works by changing angular position of the shaft into pulse signals using an optical disk. It gives 2 output signals which indicate the occurrence and direction of motion. Each pulse is an increment corresponding to a defined resolution. It does not measure absolute position.

5.9.2 Optical Encoder

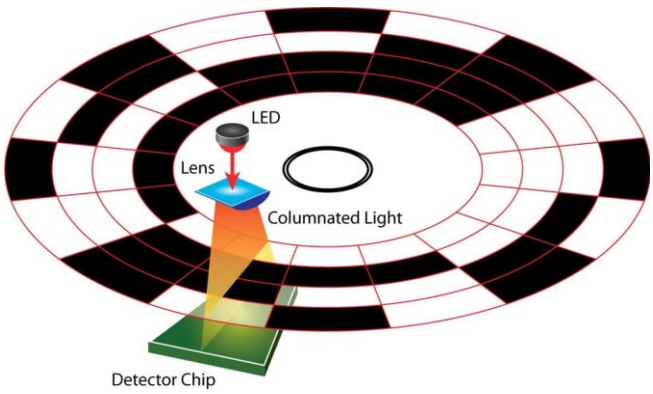

Figure 27:Figure showing the functional principle of a absolute optical encoder

It measures rotational motion using a shaft connected to a round disc which contains tracks of alternating opaque and transparent spots. A light source and an optical sensor are placed on opposite sides of each track. The light sensor emits pulses as the light source is disturbed by the pattern on the disc when the shaft rotates. At the disk every part has a different number in binary. By detecting the light for each section an absolute position of the disc can be determined.

5.9.3 Magnetic Encoder

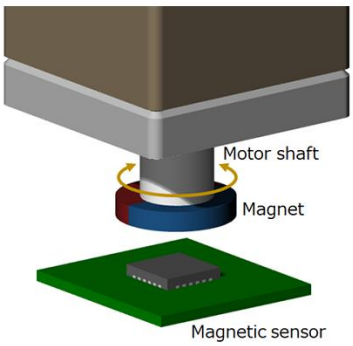

Figure 28: The physical composition of a magnetic encoder

It utilizes change in magnetic field and converts it to electrical signals to detect rotational position information. Consists of a magnet and a magnetic sensor. When the magnet that is fixed to the shaft rotates, the magnetic field direction measured by the magnetic sensor changes and thus encoder detects rotational motion.

5.10 Measuring the Ground Reaction Forces

The easiest way to measure force on a body is to use strain gauges since it doesn't take much space and we can correlate the strain to the ground reaction force after some calculations. Strain gauge is a resistor that changes its resistance when it is under an axial strain. It is happening because under the axial strain its resistive cross-sectional area decreases and its resistive length increases. Both decreases its resistance since:

$$R = \rho \cdot \frac{L}{A} \quad (1)$$

Where L: resistor length
A: resistor area
ρ: specific resistance

To determine the ground reaction force, we need to know the stains on the front and back sides of the leg. The average of those values gives us the axial force on the leg and the difference between the measurements gives the moment applying on the leg.

To achieve this, we need a system for measuring the axial strain on a solid body. Different configurations of strain gauges can be used for that purpose.

5.10.1 Active Quarter Bridge

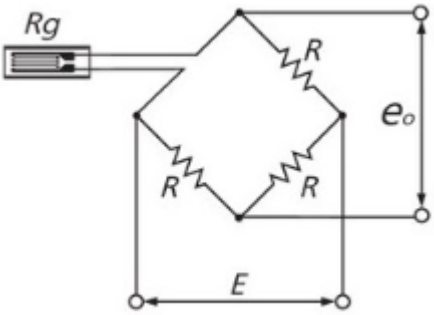

Figure 29: Circuit diagram showing the connections of an active quarter bridge system

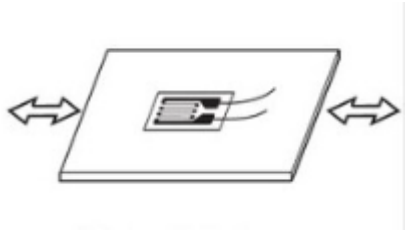

Figure 30: The physical positioning of the strain gauge used in active quarter bridge system

The simplest strain gauge configuration is the active quarter bridge configuration. In this configuration there is only one strain gauge. To measure the change in resistance, we need a circuit to transfer that change to the change in potential difference. We can achieve that by using a Wheatstone bridge with resistances same as the strain gauge. In that case output voltage can be calculated as:

$$e_0 = \frac{E}{4} \cdot \kappa_s \cdot \varepsilon_0 \tag{2}$$

Where e_0: output voltage
E: input voltage
κ_s: gauge factor
ε_0: strain

5.10.2 Orthogonal – Active Half Bridge System

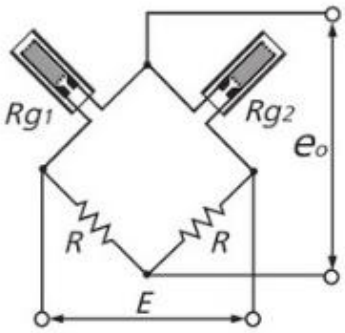

Figure 31: Circuit diagram showing the connections of an orthogonal active half bridge system

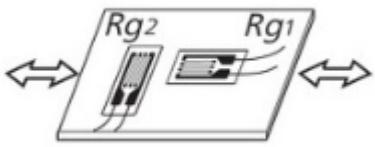

Figure 32: The physical positioning of the strain gauges used in orthogonal active half bridge system

To improve the active quarter bridge system, we can add an orthogonal strain gauge to the system instead of one of the resistors. This strain gauge doesn't measure the axial stress. What it does is to measure the expansion due to possible temperature variations. Since expansion is experienced by both strain gauges, connecting them this way cancels the temperature effects. Therefore, we can measure the strain without experiencing errors due to temperature changes.

This time, the output voltage can be measured as:

$$e_0 = \frac{(1+\nu)\cdot E}{4} \cdot \kappa_s \cdot \varepsilon_0 \tag{3}$$

Where e_0: output voltage
E: input voltage
κ_s: gauge factor
ε_0: strain
ν: Poisson's ratio

5.10.3 Orthogonal – Active Full Bridge System

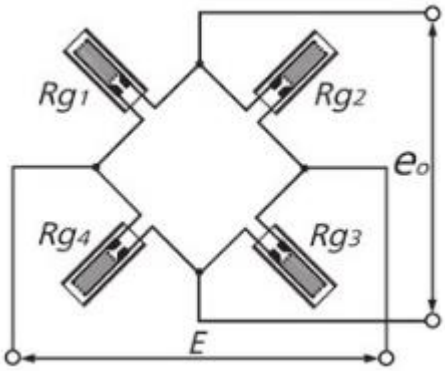

Figure 33: Circuit diagram showing the connections of an orthogonal active full bridge system,

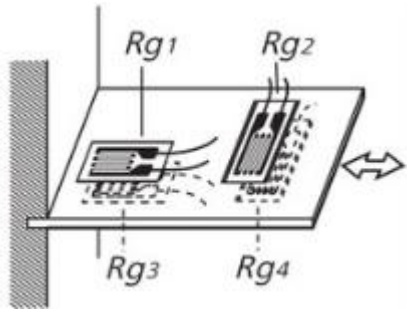

Figure 34: The physical positioning of the strain gauges used in orthogonal active full bridge system

To improve this design even further, we can change all the resistors with strain gauges. Inheriting the previous designs, allow this system to convert resistance change to potential change, and compensate the temperature variations. As an addition to those, the output voltage is increased special to this design. This is important for practical applications because the output voltage can be so low that it is hard to measure using a simple circuit.

The output voltage can be measured as:

$$e_0 = \frac{(1+\nu)\cdot E}{2} \cdot \kappa_s \cdot \varepsilon_0$$

(4)

Where e_0: output voltage
E: input voltage
κ_s: gauge factor
ε_0: strain
ν: Poisson's ratio

5.11 Microprocessor Selection

5.11.1 Raspberry Pi Pico

Raspberry Pi Pico is a RP2040 based microcontroller it is quite powerful for its price point. However, it only has 3 ADC channels which is its shortcoming to be used in this project therefore 2 of them might be used to accomplish the requirements of the project.

5.11.2 Raspberry Pi Pico and multiplexing

Since as discussed previously Raspberry Pi Pico only has 3 ADC channels, however, we need to read at least 5 analog values to fulfill our requirements. Multiplexing is a process in which a number of data are read by single channel. This method allows the microprocessor to read more than 3 analog data channels while having only 3 ADC channels. However, multiplexing reduces the sampling rate of the data.

5.11.3 Arduino Mega

This is a classic and powerful Arduino board which is based on ATmega2560.

5.11.2 STM32F103C8

stm32f103c8 is an arm-based microcontroller unit really powerful for its size and price point.

5.11.4 Arduino Nano

Arduino Nano is another classic Arduino board based on ATmega328. It is compact, cheap and available.

5.12 Filtering

- Low Pass: By definition, a low-pass filter is a circuit offering easy passage to low-frequency signals and difficult passage to high-frequency signals.
- High Pass: A high-pass filter's task is just the opposite of a low-pass filter: to offer easy passage of a high-frequency signal and difficult passage to a low-frequency signal.
- Band Pass: There are applications where a particular band, or spread, or frequencies need to be filtered from a wider range of mixed signals. Filter circuits can be designed to accomplish this task by combining the properties of low-pass and high-pass into a single filter. The result is called a band-pass filter.

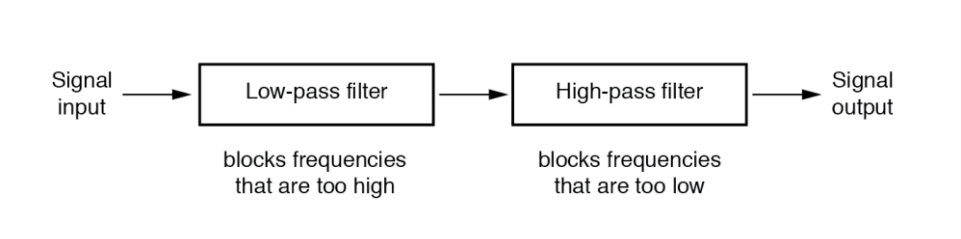

Figure 35: Block diagram explaining a band pass filter

- Band Stop: The band stop filter is formed when a low pass filter and a high pass filter are connected in parallel with each other. The main function of the band stop filter is eliminating or stopping the particular band of frequencies. The band stop filter is also referred with some other names like band-reject or notch or band elimination filter.

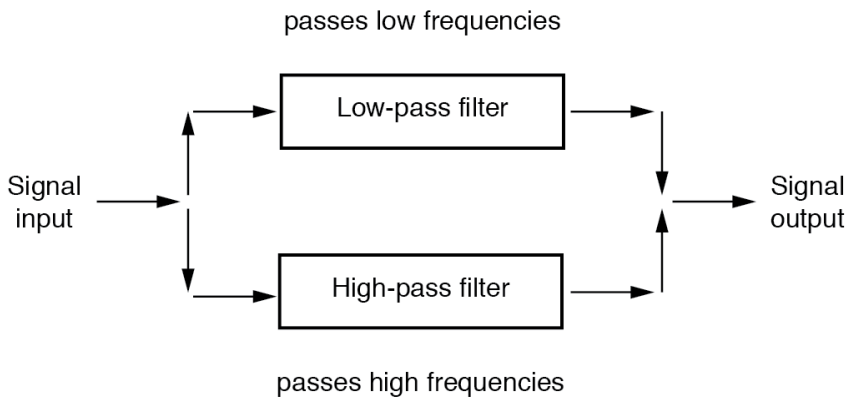

Figure 36: Block diagram for a band stop filter

5.13 EVALUATION OF CONCEPTS

This section presents the evaluation of 8 alternative concepts of the project and their explanation using Pugh's concept selection method, complete list of evaluation criteria, decision matrices of sub-functions and their weight factors. Finally, the best evaluated design concept is selected, and detailed explanation is provided.

5.13.1 Full List of Evaluation Criteria

This list is made according to the project requirements and design specifications.

Accuracy: The gait phase needs to be identified correctly to ensure a safe walking. To achieve that different sensors are being used. To determine the gait phase there are two sensors used on the C-Leg. Those are strain gauge and knee angle sensor. We should use them such that the

Precision: Precision shows the repeatability of the system. To ensure a safe walking, the right decisions should be made every step without a random error.

Data Measurement Speed: The prosthesis should adapt walking speeds up to 1.6 m/s as stated in the problem definition. To adapt such speed measuring data shouldn't take so much time.

Response Time: Fastly acquired sensor data is not enough for fast working of the system. Analyzing and using those data for controlling the valves should be fast as well. The selection of time effective control algorithms is essential for that purpose.

Ease of Implementation: The design process should also be optimized to successfully complete the project. Selection of the unnecessarily complex systems will increase the amount of time must be spent and decrease the chance of the project to be completed in time.

Cost: Like every project the amount of money can be spent for that project is limited to an extent.

Weight: Total weight of electronic hardware used should not exceed project requirements.

Power Consumption: The electronic components selected must consume power effectively such that the battery lasts for a complete day.

Safety: needs to be ensured so that the user is not harmed.

Reliability: The user should be able to stand upright when not moving and when walking on rough surfaces or obstacles.

5.13.2 Identifying gait phase and calculating valve angles

The Hierarchical Objective Tree

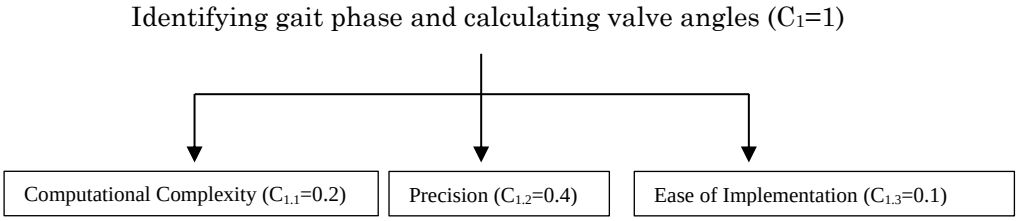

Figure 37: Hierarchical objective tree for identifying gait phase and calculating valve angles

Criteria

Computational Complexity: It shows the number of computations need to be done for each algorithm. Big O notation is used as a measure of that. The letters used in O notation on the table are:

n: size of the training data

m: feature count

f: fitness

m: mutation

c: crossover

Precision: We need not only fast but correct determination of the phase. To compare the performance of the algorithms, precision is used as a criterion. The magnitudes are determined using the experience we had and the general opinion of the literature.

Ease of Implementation: The ease of implementation concerns with the amount of additional work we need to do to use those algorithms. The biggest difficulty of using machine learning models is that they require a lot of data to train the system. The requirement of collecting additional data will increase the amount of time need to spend to implement an algorithm. Other than that, the experience (or the lack of experience) that we have in those algorithms are assessed for determining the magnitudes.

Table 6 Decision matrix for identifying gait phase and calculating valve angles

			Decision Tree			Artifical Neural Networks			Genetic Algorithm			GA + DT			ANN + DT		
Design Criterion	Weight Factor	Unit	Magnitude	Score	Rating	Magnitude	Score	Rating	Magnitude	Score	Rating	Magnitude	Score	Rating	Magnitude	Score	Rating
Computational Complexity	0.2	O notation	O(n*log(n) *m)	8	1.6	$O(n^5)$	4	0.8	O(O(f) * (O(m) + O(c)))	3	0.6	O(O(f) * (O(m) + O(c)))	1	0.2	$O(n^5)$	1	0.2
Precision	0.4	-	FAIR	6	2.4	GOOD	9	3.6	FAIR	6	2.4	GOOD	9	3.6	VERY GOOD	10	4
Ease of Implementation	0.4	-	GOOD	8	3.2	SATISFACTORY	5	2	SATISFACTORY	5	2	SATISFACTORY	5	2	TOLAERABLE	6	2.4
TOTAL					7.2			6.4			5			5.8			6.6

5.13.3 Controlling valve angles

The Hierarchical Objective Tree

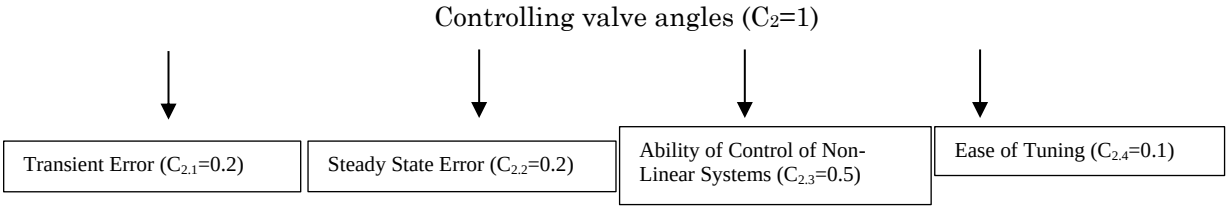

Criteria

Transient Error: During gait phase, valve angles should be adjusted immediately for providing required damping to user. For this reason, valve angles error should be minimized in the short periods. Transient error characteristics of controller determine these kinds of errors. For example, rise time, peak time or maximum overshoot criterion play an important role while adjusting valve angles.

Steady State Error: At some phases of gait cycle, steady state error of valve angles are important to giving correct response to the user. An undesired offset between reference input and controlled output in the steady state term may cause the inefficient or over damping characteristic.

Ability of Control of Non-Linear Systems: In the prosthetics knee, the system is operated with hydraulic power. In hydraulics, nonlinearity plays a significant role. So that, our control system should be able to be compatible with non-linear systems.

Ease of Tuning: Tuning controller is crucial to control a dynamic system. With respect to time cost, tuning should not be too complex. Instead of complex tuning algorithms, simple and efficient tuning methods are preferred for the sake of the time management.

Table 7: Decision matrix for controlling valve angle

			PD			PID			Fuzzy Logic			Combined System		
Design Criterion	Weight Factor	Unit	Magnitude	Score	Rating	Magnitude	Score	Rating	Magnitude	Score	Rating	Magnitude	Score	Rating
Transient Error	0.2	-	Very Good	8	2.4	Very Good	8	2.4	Excellent	9	1.8	Excellent	9	2.7
Steady State Error	0.2	-	Tolerable	4	0.8	Excellent	9	1.8	Excellent	9	1.8	Excellent	9	1.8
Ability of Control of Non-Linear Systems	0.5	Experience	Tolerable	4	2	Tolerable	4	2	Excellent	9	4.5	Ideal	10	5
Ease of Tuning	0.1	Experience	Very Good	8	0.8	Good	7	0.7	Tolerable	4	0.4	Poor	3	0.3
TOTAL					6			6.9			8.5			9.8

5.13.4 Ensuring safety for user

The Hierarchical Objective Tree

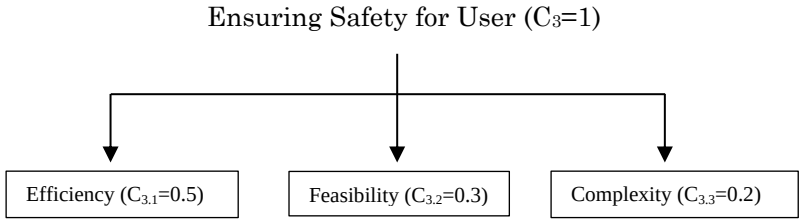

Figure 38: Hierarchical objective tree for ensuring safety for user

Criteria

Efficiency: This criterion is related to accuracy of anomaly detection. Since supervised methods use historical data, they are more suitable to check anomalies in gait phase, so they have better grades. Predictive confidence method uses time series forecasting, while statistical profiling method uses statistical data of historical pattern such as median, and standard deviation. Therefore, statistical profiling method gives us most accurate results.

Feasibility: This criterion defines the possibility of applying each method for detecting anomalies in a gait cycle. This means that how they adapt to general profile of gait cycle. Although it is possible to get satisfied results with clustering and predictive methods, statistical profiling method works well with volatile series. Gait cycle can be volatile in walking experience, so statistical method is the most feasible method.

Complexity: This criterion is related to apply method through machine learning process. Statistical method has better grades in other criterions. However, it is the most complex one to apply in aspects of creating its programming. Other methods have less complexity without significant differences.

Table 8: Decision matrix for ensuring safety for user

			Predictive Confidience			Statistical Profiling			Clustering Based		
Design Criterion	Weight Factor	Unit	Magnitude	Score	Rating	Magnitude	Score	Rating	Magnitude	Score	Rating
Efficiency	0.5	Experience	Good	7	3.5	Very Good	10	5	Satisfactory	5	2.5
Feasibility	0.3	Experience	Good	7	2.1	Very Good	10	3	Good	7	2.1
Complexity	0.2	Experience	Good	7	1.4	Tolerable	4	0.8	Good	7	1.4
Total					7			8.8			6

5.13.5 Measuring Ground Reaction Forces

The Hierarchical Objective Tree

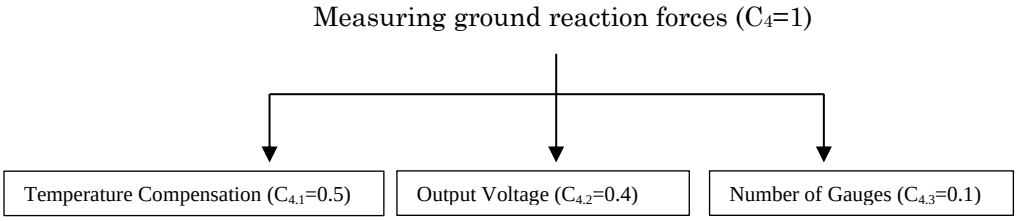

Figure 39: Hierarchical objective tree for measuring ground reaction forces

Criteria

Temperature Compensation: The product should be used in different air conditions. Therefore, the sensor measurements shouldn't be affected by temperature differences.

Output Voltage: Output voltage is where we will get information from the sensor. If the voltage level is so low, measuring it will require additional circuitry thus adds cost and complexity to the project.

Number of Gauges: Adding more gauges to the system can increase the total cost of the system. Its percentage is not as high as the others since strain gauges can be bought in pre-configurated packages with a minimal cost increase.

Table 9: Decision matrix for measuring ground reaction forces

Design Criterion	Weight Factor	Unit	Active Quarter Bridge			Orthogonal Active Half Bridge System			Orthogonal Active Full Bridge System		
			Magnitude	Score	Rating	Magnitude	Score	Rating	Magnitude	Score	Rating
Temperature Compensation	0.5	Availability	No	0	0	Yes	10	5	Yes	10	5
Output Voltage	0.4	Multiplier	x 1	4	1.6	x (1 + v)	6	2.4	x 2 (1 + v)	10	4
Number of Gauges (Cost)	0.1	Number	1	10	1	2	5	0.5	4	3	0.3
Total					2.6			7.9			9.3

5.13.6 Microcontroller

The Hierarchical Objective Tree

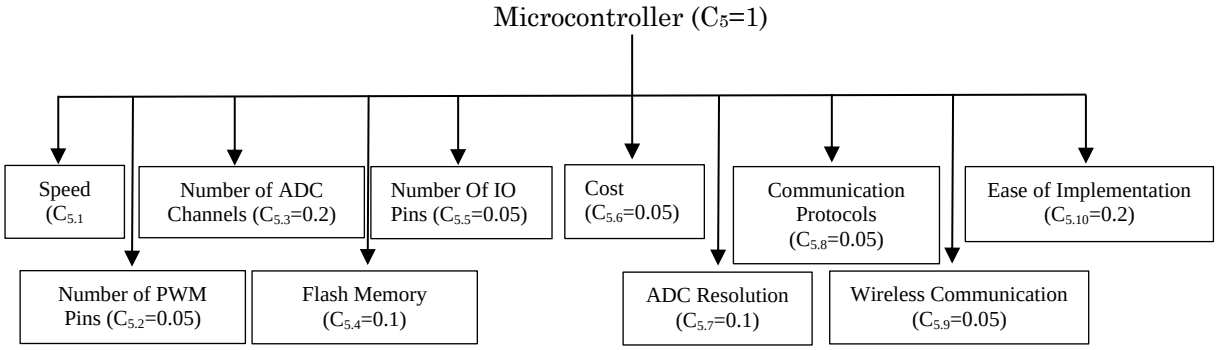

Figure 40: Hierarchical objective tree for microcontroller selection

Criteria

Speed: This criterion is the clock speed of the microcontroller, and this is an important criterion considering the speed of the microprocessor directly correlates with the response time of the overall system.

Number of PWM Pins: Most of the actuators that are used in the project require PWM input to work so microprocessor needs to provide at least 5 PWM outputs.

Number of ADC channels: In order to achieve the requirements of the project we need to read at least 5 analog data. Thus, a minimum of 5 ADC channels is needed.

Flash Memory: Flash memory refers to the memory that is available on the microprocessor to hold variables, functions, instructions and so on. A bigger flash memory means the ability to hold longer codes which might come in handy while using machine learning algorithms.

Number of I/O pins: These pins are able to read and send single binary data to/from actuators/sensors. So, if there is a need for reading or sending digital data these pins could be used.

Cost: Cost of the microprocessors.

ADC Resolution: This parameter directly correlates with the ability of the microprocessor to read necessary analog data accurately. If the resolution is high, there are less errors in the readings.

Communication Protocols: Since some sensors and actuators communicate via set protocols, a microprocessor which supports these protocols is a plus.

Wireless Communication: Wireless communication of the microcontroller could be used to build a smartphone user interface, or it could be useful while building and testing our control system for debugging purposes.

Ease of Implementation: This parameter is the measure of the ability of our team to implement the microprocessor in a way that fulfils the requirements. This includes our familiarity with the coding environment or earlier experience with the microprocessor or the technique.

Table 10: Decision matrix for microcontroller selection

Design Criterion	Weight Factor	Unit	2 Raspberry Pi Pico			Raspberry Pi Pico + Multiplexing			Arduino Mega			STM32			Arduino Nano		
			Magnitude	Score	Rating	Magnitude	Score	Rating	Magnitude	Score	Rating	Magnitude	Score	Rating	Magnitude	Score	Rating
Speed	0.15	MHz	133	10	1.5	133	10	1.5	16	8	1.2	72	9	1.35	16	8	1.2
Number of PWM Pins	0.05	-	32	10	0.5	16	10	0.5	15	10	0.5	15	10	0.5	6	10	0.5
Number of ADC channels	0.2	-	6	9	1.8	3+	9	1.8	16	10	2	16	10	2	8	10	2
Flash Memory	0.1	kB	4000	10	1	2000	9.5	0.95	256	9	0.9	64	8	0.8	32	7	0.7
Number of I/O Pins	0.05	-	46	10	0.5	23	10	0.5	54	10	0.5	37	10	0.5	14	10	0.5
Cost	0.05	₺	351.54	8	0.4	175.77	9	0.45	371.32	8	0.4	131.83	9	0.45	112.16	9	0.45
ADC Resolution	0.1	bit	12	10	1	12	10	1	10	9	0.9	12	10	1	10	9	0.9
Communication Protocols	0.05	-	UART I2C SPI	10	0.5	UART I2C SPI	10	0.5	SPI UART I2C	10	0.5	SPI USART I2C CAN USB 2.0	10	0.5	SPI UART I2C	10	0.5
Wireless Communication	0.05	-	Yes	10	0.5	Yes	10	0.5	NO	0	0	NO	0	0	NO	0	0
Ease of Implementation	0.2	-	-	7	1.4	-	5	1	-	10	2	-	5	1	-	10	2
Total					9.1			8.7			8.9			8.1			8.75

5.13.7 Filtering

The Hierarchical Objective Tree

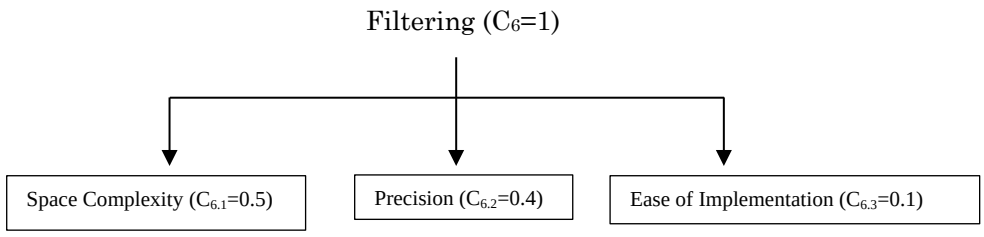

Figure 41: Hierarchical objective tree for filtering

Criteria

Space Complexity: This criterion is the space that filtering algorithm takes in the microprocessor. It is important to have a small space complexity because the memory of the microprocessor is not too large.

Precision: To have precise results is always what engineers want, however as we try to get more precise results the time to obtain it, and the space algorithm takes increases. Therefore, deciding the optimal way is what we preferred.

Ease of Implementation: This criterion is about how easy it is to imply the found solution to the whole system. The low pass filtering system is slightly easier to apply to our system when it is compared to other digital filtering methods.

Table 11 : Decision matrix for filtering

Design Criterion	Weight Factor	Unit	Low Pass Filtering			High Pass Filtering			Bandpass Filtering			Bandstop Filtering		
			Magnitude	Score	Rating	Magnitude	Score	Rating	Magnitude	Score	Rating	Magnitude	Score	Rating
Space Complexity	0.2	Byte	Lower	7	1.4	Lower	7	1.4	Higher	5	1	Higher	5	1
Precision	0.35	Experience	Medium	5	1.75	High	6	2.1	Excellent	8	2.8	Very Good	8	2.8
Ease of Implementation	0.45	Experience	Very Good	6	2.7	Very Good	5	2.25	Low	4	1.8	Low	4	1.8
Total					5.85			5.75			5.6			5.6

5.13.8 Measuring Knee Angle

The Hierarchical Objective Tree for this function is given in

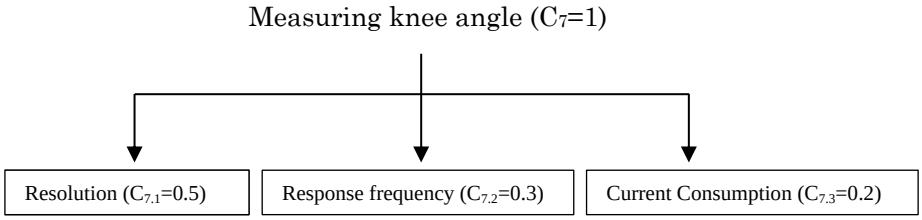

Figure 42: Hierarchical objective tree for measuring knee angle

Criteria

Resolution: This is the number of pulses per revolution the encoder can record. It is the most important criterion because if the resolution is insufficient, encoder will not provide effective feedback to the controller and the damping system will not work properly.

Response Frequency: The maximum frequency that the encoder can provide output through the output channels. Higher frequency response is wanted to give proper control commands to the motor.

Current Consumption: Sensors that consume low power are preferred to effectively manage power consumption for one complete usage cycle.

Table 12: Decision matrix for measuring knee angle

			Incremental Encoder			Optical Encoder			Magnetic Encoder		
Design Criterion	Weight Factor	Unit	Magnitude	Score	Rating	Magnitude	Score	Rating	Magnitude	Score	Rating
Resolution	0.5	PPR	100-2000	5	2.5	100-6000	8	4	5000	7	3.5
Response frequency	0.3	KHz	<300	4	1.2	<200	3	0.9	<1000	8	2.4
Current Consumption	0.2	mA	<60	7	1.4	<100	4	0.8	<60	7	1.4
TOTAL					5.1			5.7			7.3

5.13.9 Communication with User

Criteria

Current Consumption: Current consumption of used components in communication is important due to power consumption constraints of the control system design. It is determined from various datasheets and given a small weight factor relative to notification effect.

Notification Effect: This criterion is the main branch of communication with user concept since components may need to alert user in an emergency situation to prevent an injury or failure of the system. Evaluation of this criteria is based on how strong stimulating effect of the component is in terms of previous user experiences.

Table 13 : Decision matrix for communication with user

Design Criterion	Weight Factor	Unit	Buzzer			Vibration Motor			Mobile App			Combined System		
			Magnitude	Score	Rating	Magnitude	Score	Rating	Magnitude	Score	Rating	Magnitude	Score	Rating
Current Consumption	0.2	mA	30 to 100	5	1	12 to 35	6	1.2	10 to 30	6.5	1.3	52 to 165	3	0.6
Notification Effect	0.8	Experience	Fair	5	4	Fair	6	4.8	Good	7	5.6	High	9	7.2
Total					5			6			6.9			7.8

5.14 Overall Design Concepts and Their Evaluation

Table 14: Overall design concepts

	1	2	3	4	5	6	7	8
Identifying Gait Phase and Calculating Valve Angle	Artificial Neural Networks	Genetic Algorithm	Decision Tree	GA+DT	ANN+DT	Decision Tree	ANN+DT	Artificial Neural Networks
Controlling Valve Angles	PID	Fuzzy Logic	Combined System	PID	Fuzzy Logic	Combined System	Fuzzy Logic	Combined System
Ensuring Safety for Users	Predictive Confidince Level Approach	Clustering Based Unsupervise d	Statistical Profiling Approach	Predictive Confidince Level Approach	Statistical Profiling Approach	Clustering Based Unsupervised	Statistical Profiling Approach	Clustering Based Unsupervi sed
Managing Power Consumption	BMS Module	BMS Module	BMS Module	BMS Module	BMS Module	BMS Module	BMS Module	BMS Module
Communication with User	Combined System	Mobile App	Combined System	Vibration Motor	Buzzer	Vibration Motor	Mobile App	Buzzer
Measuring Knee Angle	Incremental Encoder	Optic Encoder	Magnetic Encoder	Incremental Encoder	Optic Encoder	Magnetic Encoder	Optic Encoder	Magnetic Encoder
Measuring the Ground Reactions	Orthogonal Active Full Bridge System	Orthogonal Active Half Bridge System	Orthogonal Active Full Bridge System	Orthogonal Active Half Bridge System	Orthogonal Active Full Bridge System	Orthogonal Active Half Bridge System	Orthogonal Active Full Bridge System	Orthogona l Active Half Bridge System
Microcontroller	2 Raspberry Pi Pico	2 Raspberry Pi Pico	2 Raspberry Pi Pico	Arduino Mega	Arduino Nano	Arduino Nano	Raspberry Pi Pico + Multiplexing	Arduino Mega
Filtering	High Pass	High Pass	Low Pass	Low Pass	Bandpass	Bandpass	Bandstop	Bandstop

Table 15: Overall points for each concept

	1	2	3	4	5	6	7	8
Identifying Gait Phase and Calculating Valve Angle	6.4	5	7.2	5.8	6.6	7.2	6.6	6.4
Controlling Valve Angles	6.9	8.5	9.8	6.9	8.5	9.8	8.5	9.8
Ensuring Safety for Users	7	6	8.8	7	8.8	6	8.8	6
Managing Power Consumption	10	10	10	10	10	10	10	10
Communication with User	7.8	6.9	7.8	6	5	6	6.9	5
Measuring Knee Angle	5.1	5.7	7.3	5.1	5.7	7.3	5.7	7.3
Measuring the Ground Reactions	9.3	7.9	9.3	7.9	9.3	7.9	9.3	7.9
Microcontroller	9.1	9.1	9.1	8.9	8.75	8.75	8.7	8.9
Filtering	5.75	5.75	5.85	5.85	5.6	5.6	5.6	5.6
TOTAL	67.35	64.85	75.15	63.45	68.25	68.55	70.1	66.9

5.15 THE BEST CONCEPT

Table 16: Overall design concepts and the selected one shown in green

	1	2	3	4	5	6	7	8
Identifying Gait Phase and Calculating Valve Angle	Artificial Neural Networks	Genetic Algorithm	Decision Tree	GA+DT	ANN+DT	Decision Tree	ANN+DT	Artificial Neural Networks
Controlling Valve Angles	PID	Fuzzy Logic	Combined System	PID	Fuzzy Logic	Combined System	Fuzzy Logic	Combined System
Ensuring Safety for Users	Predictive Confidince Level Approach	Clustering Based Unsupervised	Statistical Profiling Approach	Predictive Confidince Level Approach	Statistical Profiling Approach	Clustering Based Unsupervised	Statistical Profiling Approach	Clustering Based Unsupervised
Managing Power Consumption	BMS Module	BMS Module	BMS Module	BMS Module	BMS Module	BMS Module	BMS Module	BMS Module
Communication with User	Combined System	Mobile App	Combined System	Vibration Motor	Buzzer	Vibration Motor	Mobile App	Buzzer
Measuring Knee Angle	Incremental Encoder	Optic Encoder	Magnetic Encoder	Incremental Encoder	Optic Encoder	Magnetic Encoder	Optic Encoder	Magnetic Encoder
Measuring the Ground Reactions	Orthogonal Active Full Bridge System	Orthogonal Active Half Bridge System	Orthogonal Active Full Bridge System	Orthogonal Active Half Bridge System	Orthogonal Active Full Bridge System	Orthogonal Active Half Bridge System	Orthogonal Active Full Bridge System	Orthogonal Active Half Bridge System
Microcontroller	2 Raspberry Pi Pico	2 Raspberry Pi Pico	2 Raspberry Pi Pico	Arduino Mega	Arduino Nano	Arduino Nano	Raspberry Pi Pico + Multiplexing	Arduino Mega
Filtering	High Pass	High Pass	Low Pass	Low Pass	Bandpass	Bandpass	Bandstop	Bandstop

These solution concepts are chosen with the method of numerically evaluating the concepts. To begin with, the **decision tree** was more advantageous in criterions of computational complexity and ease of implementation compared to its competitors by far. In precision criteria, decision tree was not very advantageous however after rating each method decision tree was chosen. For controlling valve angles, we decided to use a **combined system**. The combined system had a low potential for transient error and steady state error compared to other concepts, but it is terrible on ease of tuning. Despite that because of the points it gathered from other criterions combined system was chosen. **Statistical profiling** approach is chosen for ensuring safety for users because of the points it gathered from efficiency and feasibility. In terms of complexity statistical profiling approach was too complex however this design criterion has a low weight factor, therefore this approach was chosen. For managing power consumption **BMS Module** was the only applicable solution by us because we did not compare with other solutions. For communication with user, we chose **combined system** despite of its current consumption its notification effect advantage was too high therefore we chose combined system for this criterion. For measuring knee angle, **magnetic encoder** was the primary choice of ours. For response frequency criterion it is significantly advantageous. However, for resolution criterion all candidates were close in terms of points. In addition, magnetic encoder was advantageous for current consumption, so we chose magnetic encoder for our design. For measuring the ground reactions there were two options and best possible solution was chosen as

orthogonal active full bridge system. While choosing a microcontroller system we considered the factors of speed, number of PWM pins, Number of ADC channels, flash memory, number of I/O pins, cost, ADC resolution, communication protocols, wireless communication, ease of implementation. The most important factors were ease of implementation and number of ADC channels followed by speed. The rating results were too close. However, by a small difference **2 Rasberry Pi Pico** was chosen as the best possible solution. For the filtering, we looked for digital filtering methods and reached 4 different methods. High-pass filtering, Low-pass filtering, Band-pass filtering, and Band-stop filtering. We compared these methods according to their space complexity, ease of implementation, and precision. While band-pass filtering is more precise, it is difficult to imply and also has a high space complexity. Its competitor low pass filtering is much easier to imply and has a low space complexity, and an acceptable precision rate. Therefore, we chose to apply **low-pass filtering**. After combining all those best possible methods for each sub-function best possible combination is visible.

5.16 SUMMARY AND CONCLUSION

Before starting all the processes that is necessary to complete this project, we had to define the problem. After we defined the problem, a solution was necessary. Firstly, in order to complete this project, we tried to create a suitable functional decomposition of the project that was assigned to us. Following that, we designed some concepts by brainstorming to each of these functions. During this brainstorming session every single group member delivered his contribution. That helped us to choose a path from lots of possible ones. After that, we applied an evaluation process to subfunctions of the decomposed functions. Generally, we set 3 different evaluation criteria for each subfunction, and we rated the possible solutions of subfunctions to decide the best combination of solutions. Therefore, we cleared our mind for the solutions that are needed to be applied. Following that we plan to conduct kinematic and flow analysis. Depending on those analysis we have to design the control system. The design of control of control system will be done based on system of equations accompanied with analyses.

6. DETAILED DESIGN

6.1. INTRODUCTION

Details of the prosthetic knee's control system design are discussed. The ways to test the requirements have been stated. The components of the design system include Raspberry Pi Pico which will be the microcontroller. DC motors connected to the valves control the damping effect provided to the piston stroke. Strain gauges attached to the prosthetic leg tube to measure ground reaction forces. Magnetic encoders to measure knee angle variations and a battery system to provide energy to the system. In order to create a proper design, we prepared models. The models were healthy walking model, prosthetics walking model, hydraulic model of the piston, and control system model. For healthy walking model and prosthetic walking model MATLAB was used. For hydraulic model of the piston and control system model Simulink was used.

Furthermore, tests that were and will be conducted for model verification and failure prevention are described. For spring stiffness determination, load applied and deflection is measured to model the piston. For ESAR, foot stiffness measurements, load applied, and deflection were measured to model walking with the prosthetic knee. For leg center of mass and inertia measurement, a two-axis balancing experiment was conducted for walking with prosthetics model. We weighed the prosthetic leg and obtained its weight for walking with prosthetics model creation. For knee joint damping measurement. For moment of inertia measurement, we freely swan the leg, this value will be used for walking with prosthetics model. For material determination of the strain gauge holder, spectrochemical analysis was conducted to learn the physical characteristics of the material. Further tests will be carried out, those are walking speed test to check if the system can respond to different walking speeds, standing test to check if the piston can provide enough support during stance phase. Power test to check if the battery can provide energy for one working day. Weight test to see if weight requirements are satisfied. Response time measurement to check for lag and delay problems.

6.2 PROPERTIES OF DESIGNED SYSTEM

6.2.1 Operating Principle

The control system for a micro-controlled semi-active prosthetic knee is designed to mimic the functions of a natural knee joint as much as possible. This control system is responsible for regulating the damping effect applied by the knee joint to the movement of the user according to the walking pattern to allow smooth natural walking.

Operation Principle is based on using sensors and control algorithms to detect the walking phase and then control the movement of the knee joint accordingly. The system adapts to an individual's gait cycle by taking advantage of the hydraulics mechanism controlled by a micro-controller through DC motors. The sensors consist of strain gauges on a tube near to the ankle and a knee angle sensor. Also, there is another magnetic field sensor that detects valve openings driven by DC motors.

Strain gauges measure stress above the foot component while the knee angle sensor records the angle made with the vertical and angular velocity of the knee joint. Using this data, the system decides which phase of the gait cycle the user is in. Then it will set DC motors to reach correct damping in the hydraulic system by changing valve openings. The system recognizes the correct opening for the detected phase by using magnetic field sensors on the valves. Setting correct damping values through the gait cycle provides a smooth walking experience and is the main objective of the design.

6.2.2 Important aspects of design

The control system is designed for a specific product, the C-Leg from Ottobock. Design choices were made to make a robust control system for this product. While identifying the gait cycle, decision tree algorithms was used to reduce complexity and get accurate results. It is one of the most used algorithms in micro-controlled prosthetic knees.

To control valve angles, a combination of PID and Fuzzy Logic algorithms were found to be the most appropriate. Although PID has less complexity and ease of use, it is a robust algorithm for certain input-output systems. In prosthetic knees, control parameters may change for each user and it is hard to have a fixed input-output system. Therefore, a combination of PID algorithm and Fuzzy Logic which is able to handle input variables that are imprecise and uncertain which is the case for prosthetic knee control is used.

To ensure the safety of users, machine learning and statistical profiling approach is implemented. This approach uses supervised data to detect anomalies in a time series. It compares stored data and current data in statistical values such as median and standard deviation. As opposed to it has complexity in the application, it is one of the most accurate methods of anomaly detection. Hence, it can detect an anomaly in a walking pattern and can take action against stumbling situations.

BMS module is used in the battery system. It will improve the battery's performance and help to extend its lifespan. Also, it can monitor the battery for potential safety issues, such as power outages, and take action to protect the battery. In addition, it will reduce maintenance costs for the user because of these advantages.

The control system has some communication devices to alert the user such as a buzzer and vibration motor. In case of a low battery, it can alert the user and user will be aware of the situation. The user can input their weight, height and footsize through the mobile application and the control system will adjust walking settings accordingly.

For measuring knee angle, a magnetic encoder is used to measure the position of the knee. These magnetic encoders are relatively immune to environmental factors such as dirt and moisture. Also, they are capable of providing a high resolution which makes it an appropriate selection that requires precise position control. In addition, they have long lifespans and low failure rates, so they are a reliable choice. Furthermore, they can be used in non-contact operations, so they cannot cause any damage or wear with time.

To measure ground reactions, full bridge strain gauges are used. Since they provide four points of reference, they can compensate temperature effects and give more accurate measurements compared to other strain gauges. Also, they are more sensitive compared to others, so they allow detection of very small strains. In addition, they are more stable than other types which means they can be used over a long period of time.

For filtering the data that comes from the sensors, low-pass filtering is used. From literature survey it was found that there is not much difference between filtering methods. The main reason of this selection is related to the ease of implementation of low pass filtering compared to others. Also, it can effectively remove high-frequency noise in signals, which will be the case for the detected data. It will provide smooth signals to process, and these signals will give better outputs in the control system. Hence, avoiding negative effects of noise on sensor data.

Finally, 2 Raspberry Pi Picos are used as microcontrollers. Since it does not have enough ADC channels, 2 of them are needed. It is a low-cost, low-power, and flexible platform for developing projects. Also, it is one of the fastest micro-controllers in the market with 133 Mhz speed.

6.2.3 The system and subsystems

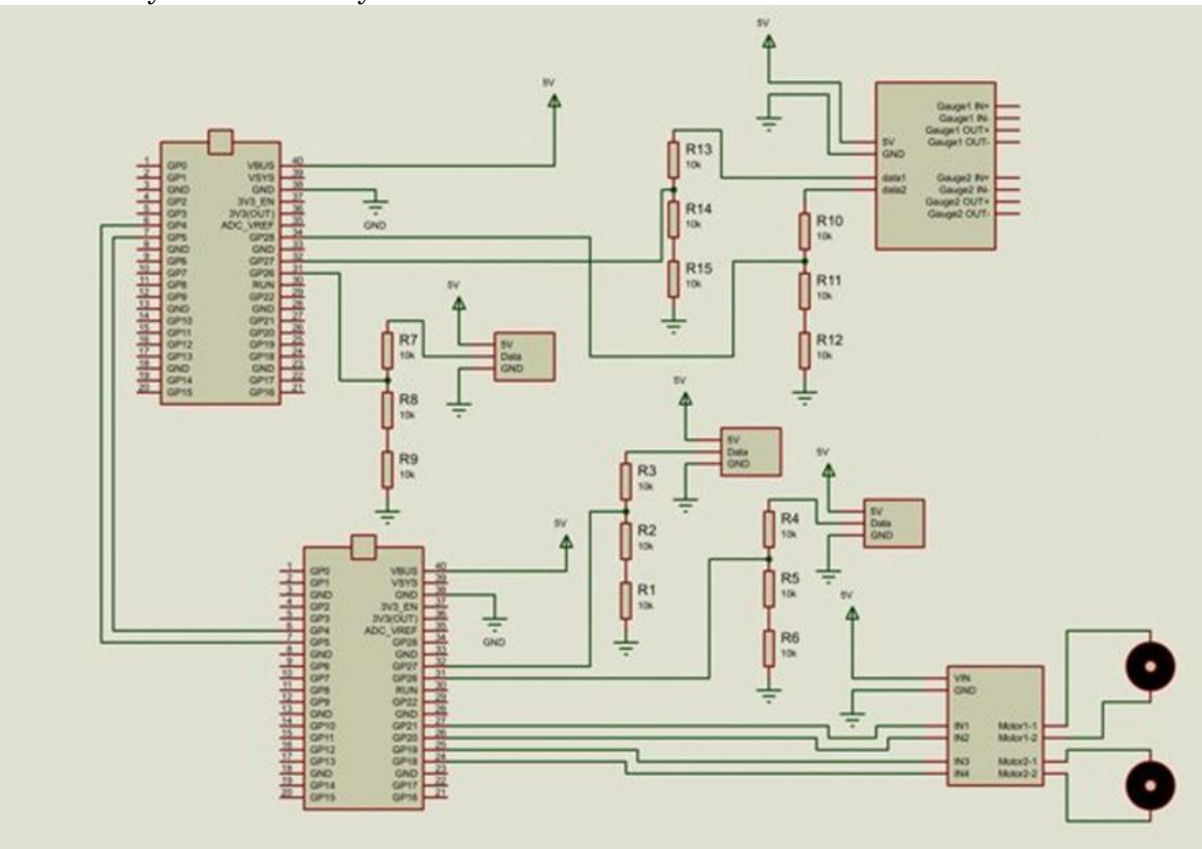

Figure 43: Circuit diagram of the system

The system consists of the following components:

- Raspberry Pi Pico:

It is microcontroller in which the control algorithm is embedded. Also, the sensors will be connected to it.

- DC Motors:

They are connected to valves, and they are responsible for setting the valve openings for a specific damping value.

- Strain gauges:

They are on the tube for measuring ground forces.

- Magnetic Encoders:

These are responsible for measuring knee angle for phase detection and detecting rotation made by DC motors on valve openings.

- Battery System:

It will provide the necessary power that the whole system needs.

6.3 ENGINEERING CALCULATIONS

ENGINEERING MODELS

Models	Assumptions	Software(s) Used
Healthy Walking Model	• The angles will fallow a similar path for different walking speeds • Ratios of leg parts to the hight are constant for different people • Forces during a gait cycle are linearly scalable based on the weight • Kinematic and kinetic variables are periodic during multiple gait cycles	MATLAB
Prosthesis Walking Model	• Prosthesis will act as a pendulum at the swing phase • ESAR foot can be modeled as a constant stiffness joint • Piston can be modeled with a lumped spring and a lumped damper in parallel • Inertia of the piston can be neglected	MATLAB
Hydraulic Model of the Piston	• Hydraulic system can be modeled using lumped parameter elements • Mass of the piston can be neglected	Simulink
Control System Model	• The knee angle and the strains on the leg can be measured linearly • The response time of the controller can be neglected	Simulink

6.3.1 Healthy Walking Model

To simulate a prosthetic leg, healthy gait cycle should be understood properly. To get a better understanding of the human gait cycle, the kinematic and kinetic data obtained by David A. Winter in his Biomechanics and Motor Control of Human Movement**Error! Reference source not found.** is used. In his book, kinematic and kinetic data of a gait cycle of a person is presented.

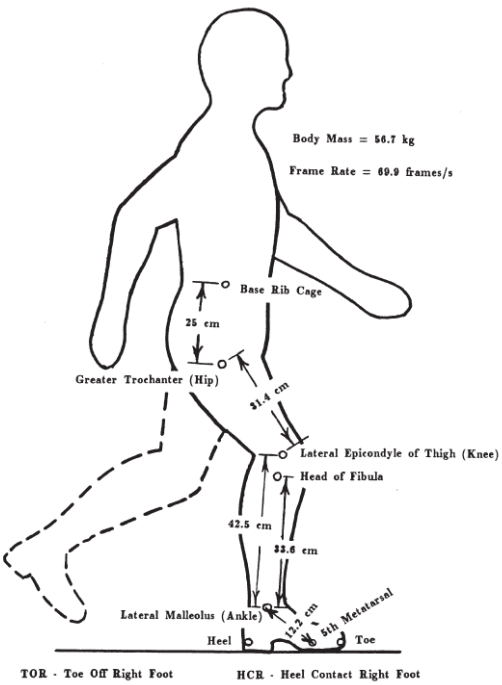

Figure 44: : Link lengths, weight and frame rate information for the data obtained by David A. Winter

Using the data given, a gait cycle model is created for persons with different heights, weights, and different walking speeds. To extend the data to more than one gait cycles, a function is fitted to the data using Fourier Series. Using the data Fourier series analysis equation is used to calculate the Fourier series coefficients.

$$a_k = \frac{1}{T} \cdot \int_0^T F \cdot e^{-i \cdot k \cdot \omega_0 \cdot t} \cdot dt$$

(5)

where a_k: k^{th} Fourier series coefficient

F: kinematic or kinetic data

T: Gait period

ω_0: Angular frequency$\left(\frac{2\pi}{T}\right)$

After calculating the Fourier series coefficients, we can use Fourier series synthesis equation to create a continouous and periodic function for gait cycle data.

$$F_f(t) = \sum_{k=-n}^{n} |a_k| \cdot \cos\left(k \cdot 2\pi \cdot t + \varphi_k\right)$$

(6)

where a_k: k^{th} Fourier series coefficient

$F_f(t)$: Function fitted to kinematic or kinetic data

φ_k: Phase shift $(\angle a_k)$

This procedure can be applied to every kinematic and kinetic data presented in the tables since all of them should be a periodic function during constant speed walking. However, this procedure alone gives only the functions for a specific person walking at a specific walking speed. To extend this model to every person walking at every speed, we can scale the results. To get the gait cycle for a different walking speeds, time axis can be scaled using the ratio of the walking speeds. To get the forces for persons with different weights, forces can be scaled using the ratio of the weights. Lastly, to get the positions of the joints for persons with different heights, we can use the body segment lenght to persons height ratios presented in Winter's book**Error! Reference source not found.**.

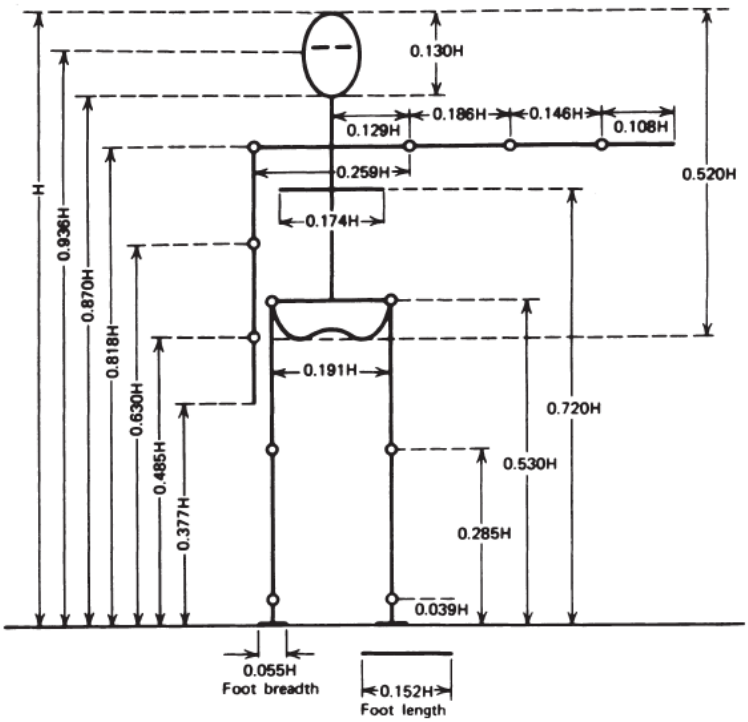

Figure 45: Body segment leghts as a fraction of persons height H

6.3.2 Prosthesis Walking Model

After creating a model for healthy walking of a human being, we can simulate the prosthesis using that model. We can write the equation of motion (EOM) of the prosthesis as:

$$I(\ddot{\theta}_{hip} - \ddot{\theta}_{knee}) + mgL_{cm}\sin(\theta_{hip} - \theta_{knee}) + c_{knee}(\dot{\theta}_{hip} - \dot{\theta}_{knee}) + c_{piston}b(\dot{\theta}_{hip} - \dot{\theta}_{knee})\sin(\alpha) + k_{piston}b \cdot \theta \cdot \sin(\alpha) = 0$$

(7)

where I: moment of inertia of the prosthesis around knee axis

θ_{hip}: Hip angle

θ_{knee}: Knee angle

m: Total mass of the prosthesis

L_{cm}: Distance between the center of mass of the prosthsis and the knee axis

c_{knee}: Damping coefficient of the knee joint

c_{piston}: Damping coefficient of the piston

a: Distance between piston upper joint and the knee axis

b: Distance between piston lower joint and the knee axis

α:The angle between piston and the leg

sin (α) can be found directly using the cosine and sine theorems:

$$\sin(\alpha) = \frac{a \cdot \sin\left(\frac{\pi}{2} - \theta_{knee}\right)}{\sqrt{a^2 + b^2 - 2 \cdot a \cdot b \cdot \cos\left(\frac{\pi}{2} - \theta_{knee}\right)}}$$

(8)

This differential equation is non-linear and complicated to solve by hand. However, numerical methods can be used to calculate the response of the leg. This equation is derived for the swing phase of the gait. In order to calculate the stance phase as well, ESAR foot can be modelled as a spring. That way ground reaction forces can be found.

6.3.3 Hydraulic Model of the Piston

In this analysis, calculation of damping coefficients for different orifice openings is aimed. Analysis is made in the Simulink environment. The following equation is used for damping coefficient calculation:

$$F = c \cdot V$$

(9)

where “F” is the force on the piston, “V” is the velocity of the piston and “c“ is the damping coefficient. In simulation setup, hydraulics elements of the C Leg are defined by using Simscape Fluids Library of Simulink. Following blocks from that library are used:

- Double-Acting Hydraulic Cylinder
- Pressure Sensor
- Fixed Orifice x2
- Check Valve x2
- Spring Loaded Accumulator
- Ideal Translational Velocity Source
- Translational Spring

- Hydraulic Fluid
- Mechanical Translational Reference
- PS-Simulink Converter
- Simulink-PS Converter

Also, following standard simulink blocks are used:

- Scope
- Ramp
- Gain
- Divide

The hydraulics scheme of C Leg is constructed in the Simulink as Fig.4.

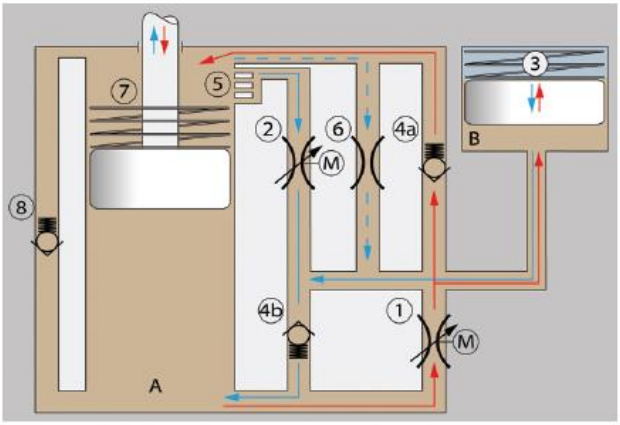

Figure 46: Hydraulic schematic of C-leg

The constructed Simulink block diagram:

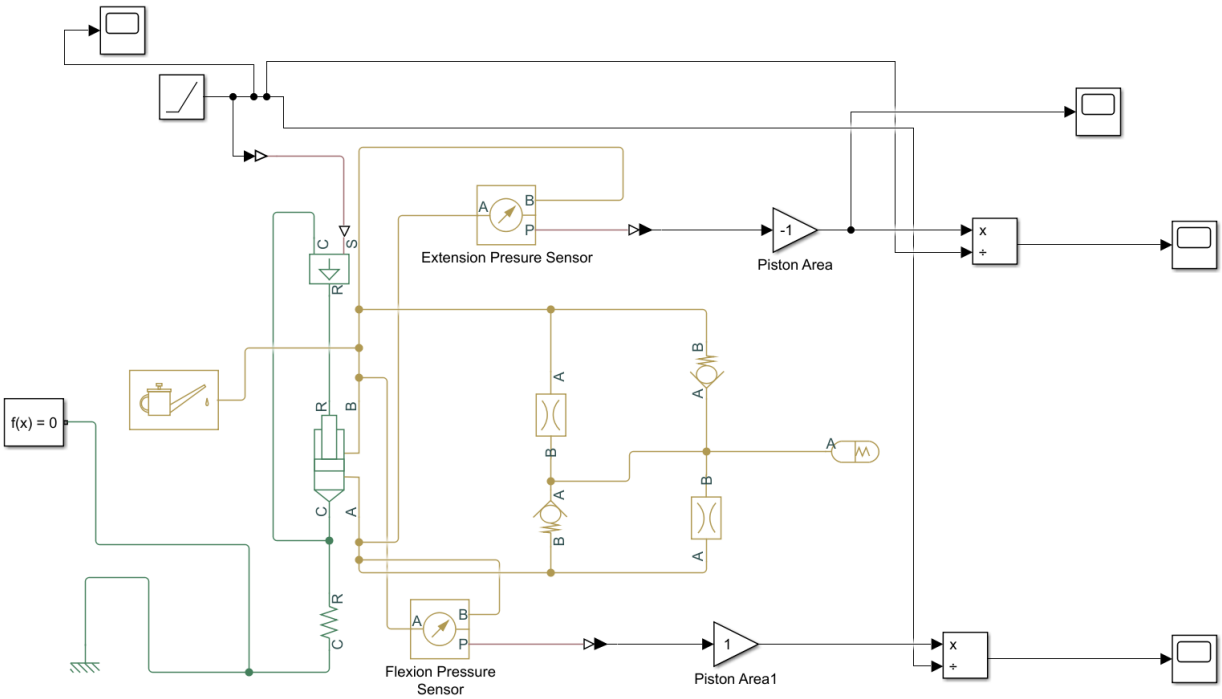

Figure 47: Simulink Block Diagram for Hydraulic System

Before starting the simulation, some necessary parameters have to be determined to represent the real system . Following parameters are determined:

- Stiffness of the piston spring (28854 N/mm)
- Piston area of upper side (490.8739 mm^2)
- Piston area of lower side (412.3341 mm^2)
- Piston stroke (32 mm)
- Dead volumes of two portion (981 mm^3 and 824 mm^3)
- Accumulator fluid chamber capacity
- Accumulator preload pressure
- Hydraulic fluid (SAE 30)

In the beginning of the simulation, an arbitrary ramp function is given as input piston velocity in the unit of [m/s]. The main goal of this is to determine the damping characteristic for a linear input. This function is fed into the piston by using ideal translational velocity source block. After defining the input, the force the piston needs is to be determined from the simulation. The force on the piston cylinder is the product of the pressure difference between the upper and lower volume of the piston and the corresponding piston area (The piston area for extension and flexion area is different because of piston rod). The pressure difference is measured by using pressure sensor block. The output of the pressure sensor is multiplied with piston area. Then, the force is divided by the piston velocity which is the input of the whole simulation. These two signals are divided by using divide block. Output of the division is the damping coefficient which is the output of the analysis.

6.3.4 Control System Model

In the control system we have modelled a fuzzy tree. In the fuzzy tree, we have three fuzzy interference systems (FIS) and 4 different inputs such as knee angle, speed, strain and system response error. Initially, we input knee angle and strain into the first FIC according to their respective membership functions given as follows.

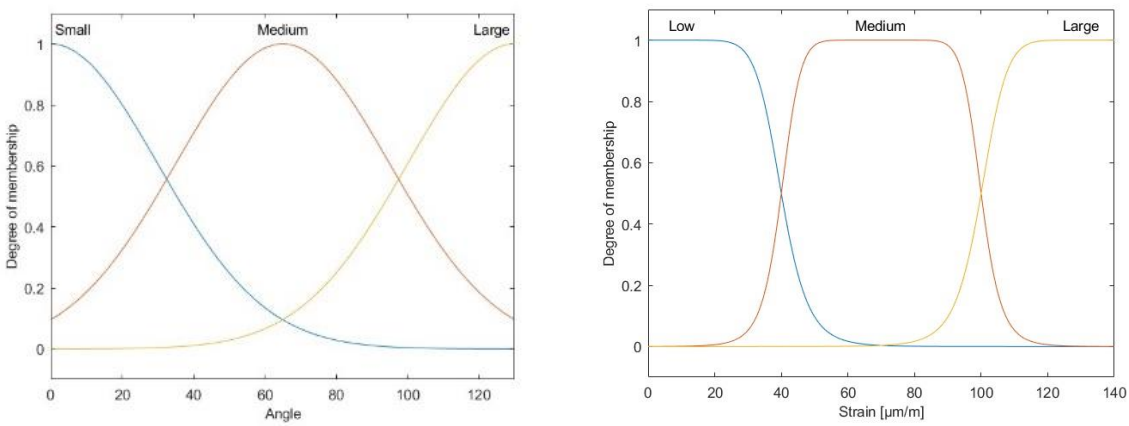

Figure 48 : Membership Functions for The First Fuzzy Interference System

According to the given membership function and predetermined rules, FIS system interprets the data using centroid rule. Output of the first FIS determines gait cycle position. Output can be plotted using 5 membership functions as follows.

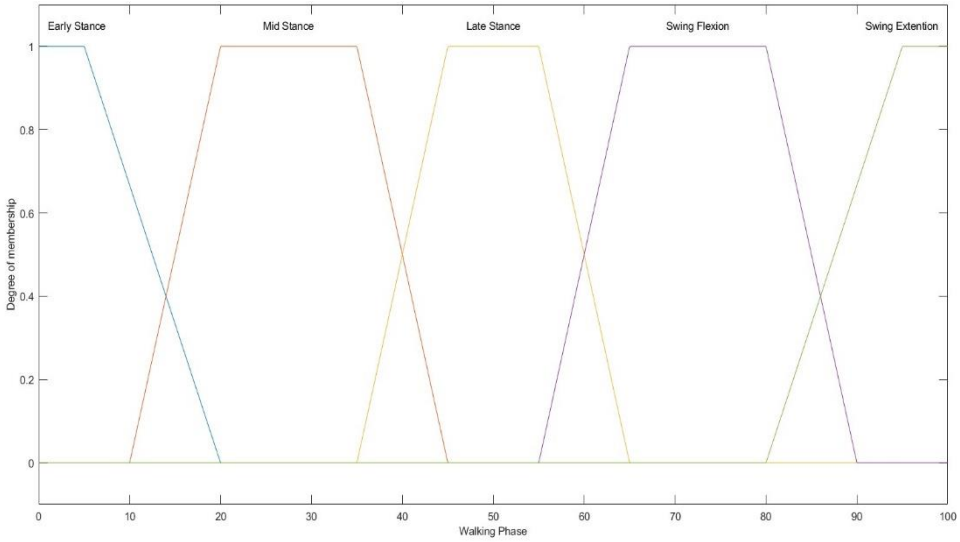

Figure 49 : Output Membership Function of Gait Phase

Note that walking phase is written in terms of percentage which shows how much of a step is the user completed. This output and velocity input from magnetic field sensor is fed into the second FIC. For velocity there are 5 membership functions given as follows.

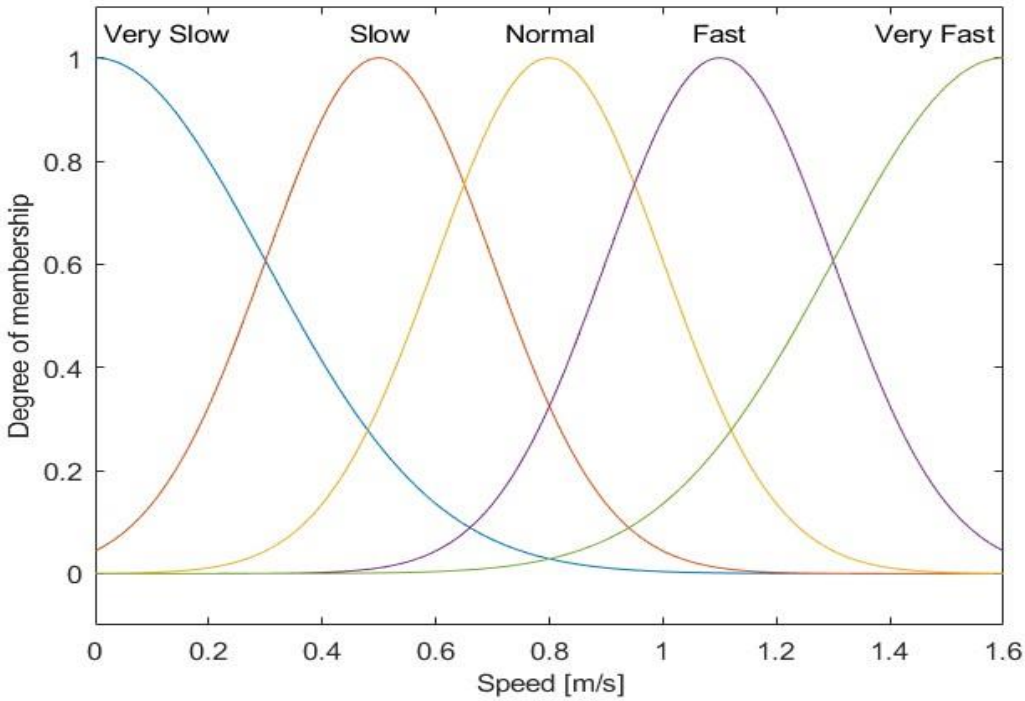

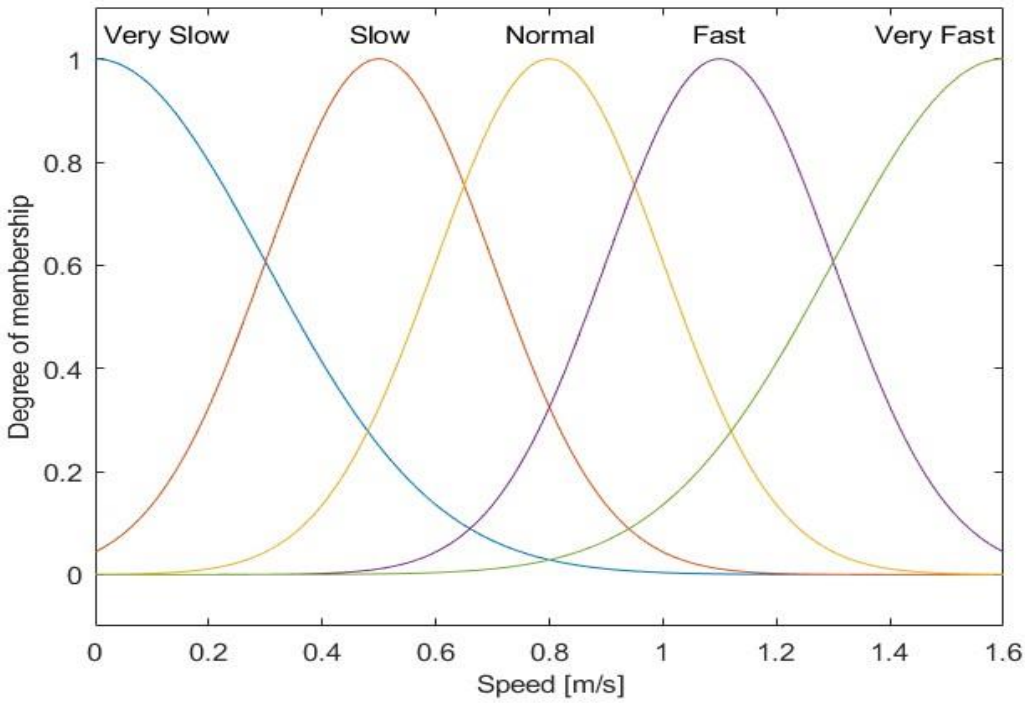

Figure 50: Input Membership Function for Velocity

Combining these inputs second FIS outputs precalculated required damping coefficient as follows.

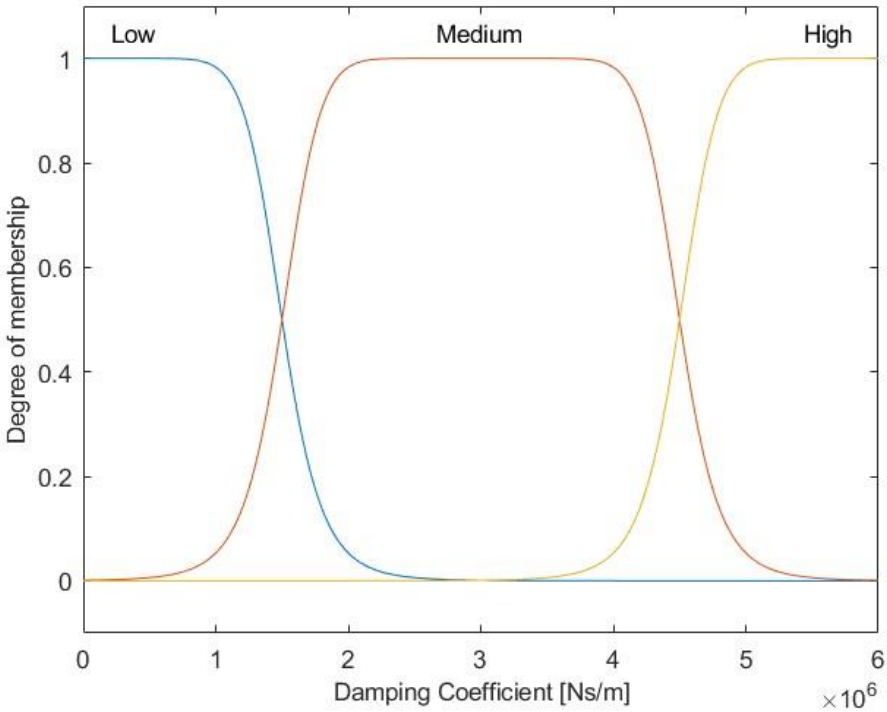

Figure 51: Precalculated System Damping Coefficient

This damping coefficient output is corrected inside the third FIS by calculating anomalies using the knowledge base and feedback system response with statistical profiling approach and final output is reached. Furhermore, in this process 3 fuzzy interference systems and numerous membership functions are used. Therefore, to shrink the solution domain, genetic algorithm is used. This not only decreases response time of the system but also gives more accurate results.

6.3.5 Calculation of Valve Opening for Different Motor Angles

The main goal of this simulation is calculating valve opening areas for different motor angles. The simulation is made in the Simulink environment by using Simscape toolbox. Before the simulation, the CAD models of the valve components of the C Leg are drawn using SolidWorks. Then, these CAD models are imported into Simulink to simulate valve motion. The other requirements of the simulation is to fit a curve for valve openings for different shaft angles. The total range of motor motion is 90 degrees in the C Leg. The shaft is adjusted for every 3 degrees on Solidworks and the valve opening is measured for that particular shaft angle. The motor angles and corresponding opening areas are tabulated in Microsoft Excel. Data is imported to MATLAB and a curve is fitted for this data by using MATLAB Curve Fitting Toolbox.

In the simscape simulation following blocks are used to simulate valve motion:

- World Frame
- Mechanism Configuration
- Rigid Transform
- File Solid

- Revolute Joint
- Matlab Function
- PS-Simulink Converter

The output of the revolute joint which is the position of the joint in degrees is fed into MATLAB function to obtain valve opening for a particular motor angle. The simulink block diagram of the simulation is provided in the following.

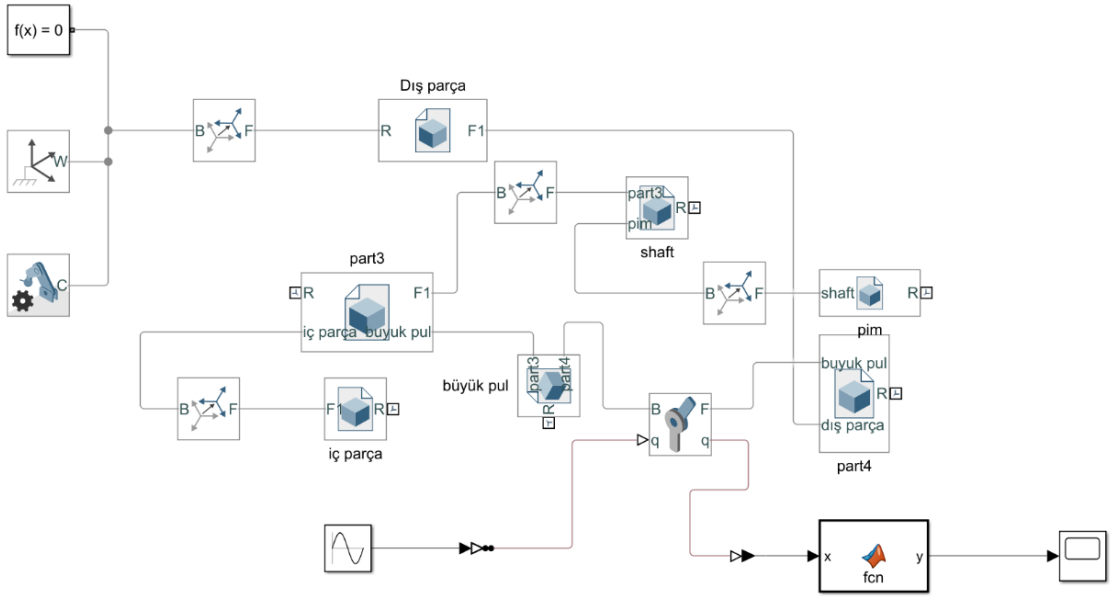

Figure 52: Simulink Block Diagram for Calculating Motor Angles

Thanks to this simulation, the valve opening for different motor angles can be calculated.

6.4 ANALYSES

Analysis	Performance Criteria Target	Assumptions	Software(s) Used
Strain Analysis of the Lower Leg	Measuring the measurable amount of strain (Performance Criteria Target)	• Small deflections • Linear elastic deflections • The system is static during loading	MATLAB, Mathcad
Stress Analysis of the Lower Leg	Avoiding plastic deformation at the lower leg (Potential Failure)	• Linear elastic deflections • The system is static during loading	Solidworks Simulation
Flow Analysis of the Valves	Avoiding Piston not maintaining the required damping (Potential Failure)	• Input velocity of the fluid is the same as the piston velocity	ANSYS Fluent

6.4.1 Strain Analysis of the Lower Leg

Strain analysis of the lower leg is mainly performed on MATLAB. Firsly, using previous researches, for various weights plots of ground reaction forces are generated. For stain analysis, maximum weight (130kg) supported by the knee is used. Then, for each phase of the gait cycle, strain calculations are performed on the critical part of the lower leg. Using these data, maximum and minimum strain values are obtained and it is seen that strain gage will work inside its linear range.

6.4.2 Stress Analysis of the Lower Leg

For stress analysis, initially critical parts of the lower leg is determined and most critical part is found by comparing strongest candidates. In stress analysis of the lower leg, fatigue, impact and force analyses are performed using maximum supported weight.

Using an optimization procedure adequate factor of safety is calculated without sacrificing strain value on the strain gages.

6.4.3 Flow Analysis of the Valves

For the fluid dynamic analysis of the valve which controls the damping coefficient provided by the hydraulic piston valve system, ANSYS Fluent was used and the geometry of the valve is modeled and constructed as shown in Figure 11. Inlet is defined as the hole on the left and outlet is the hole on the right side. By rotating the inner valve component, flow rate can be modified.

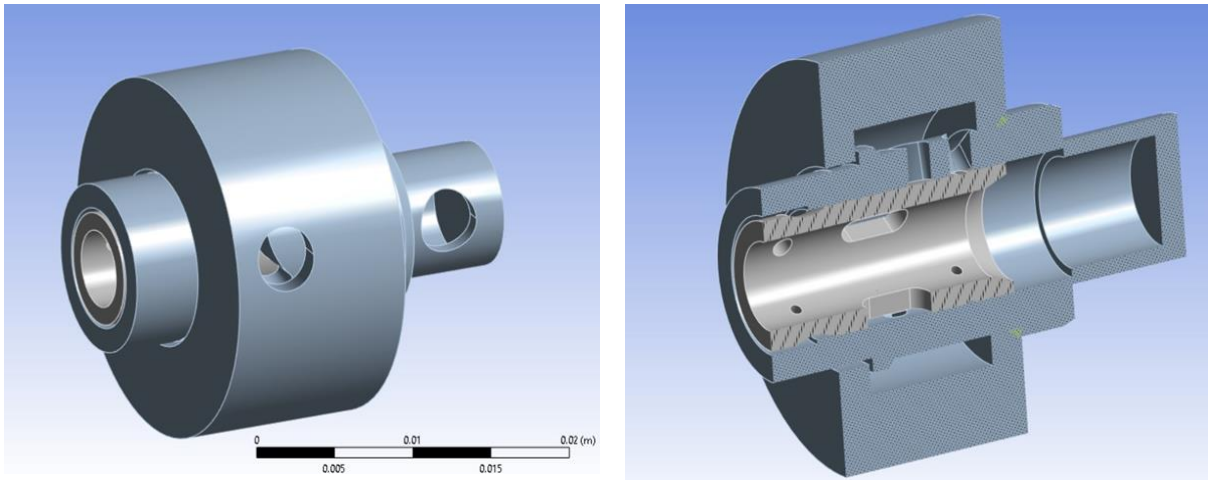

Figure 53: Simplified Valve Geometry and Section View

The aim of this analysis is to understand the characteristics of the fluid flow through the valve and to check for the most critical case when the inlet is fully open whether this valve provides the necessary damping to the knee motion or not. A fluid volume body is created as shown in Figure 12. This model represents the domain through which fluid flows inside the valve.

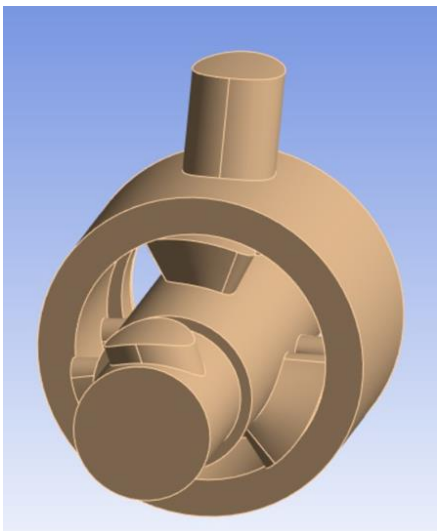

Figure 54: Fluid Body Volume

6.5 TESTS

Tests Conducted for Modeling Purposes

Test	Mehod	Aim
Spring Stiffness Measurement	Applying load and measuring the deflection	Piston Modeling
ESAR Foot Stiffness Measurement	Applying load and measuring the deflection	Prosthesis Walking Modeling
Leg Center of Mass Measurement	Balancing on two different axes	Prosthesis Walking Modeling
Weighing the leg assembly	Weighing using a scale	Prosthesis Walking Modeling
Knee joint damping measurement	Free swinging of the leg, logarithmic decrement	Prosthesis Walking Modeling
Leg Moment of Inertia Measurement	Free swinging of the leg	Prosthesis Walking Modeling
Material determination of the strain gauge holder	Spectrochemical analysis	Determination of the physical characteristics of the material

6.5.1 Spring Stiffness Measurement

In order to determine the spring stiffness which is used in the C-Leg piston, two methods are followed. Firstly, the spring coefficient was calculated by using online tools. In this software, wire diameter, outer diameter, free length and number of active coils of the spring should be defined to the calculator. Then, spring coefficient can be obtained. From this software spring stiffnes coefficient is 28,854 N/mm.

Afterwards, the physical experiment is made in the sponsor company Proted test environment. In this environment, the setup is set for loading and unloading to spring. The required force for determined deflection of the spring was checked and it is compared with stiffnes coefficient which is obtained from software. There is a small difference approximately 10-15 Newtons for this force. This difference is caused by frictions, measurement errors etc. Thus, spring stiffnes coefficient is used as 28,854 N/mm for analyses.

6.5.2 Energy Storage and Return (ESAR) Foot Stiffness Measurement

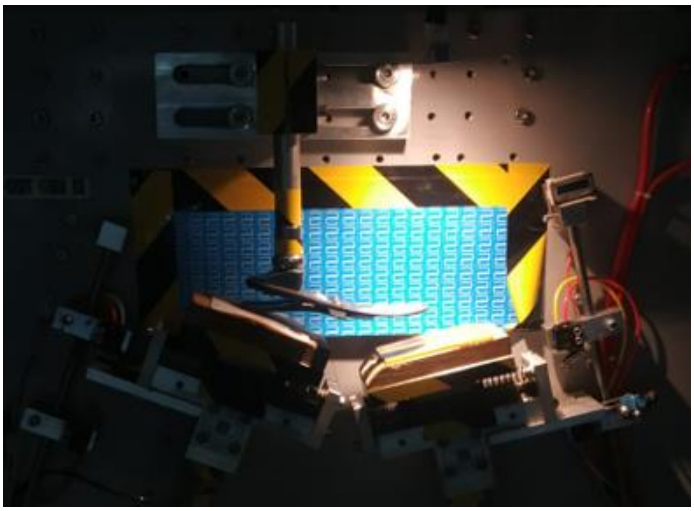

Figure 55: Foot Stiffness Test Mechanism

ESAR foot stiffness measurement has been completed by using machine shown on the figure above. Force is applied 93 kg-f on both heel and tip of the foot. We observed 0.5 – 1.0 cm vertical displacement on the heel, and 1.0 – 1.5 cm vertical displacement on the tip. Variation is due to different material characteristics of each foot. An average value can be used for general calculations.

Note that plate that apply force to heel makes an angle 21 degree with the ground, while other plate makes an angle 14 degree.

6.5.3 Leg Center of Mass Measurement

Center of mass of an object is on the axis that it can balance. Therefore balancing an object on three different axes will determine the position of the center of mass in 3d space. Since C-leg is symmetrical in one axis, two balance axes are enough to determine the position of the center of mass. The intersection of those axis is the center of mass of the prosthesis. We need the distance of the center of mass from the knee joint axis to use in the prosthesis walking model.

6.5.4 Knee Joint Damping Measurement

To find the damping of the knee joint, an experiment is conducted such that the leg swings freely. A low pass filter is applied to raw data to eliminate the noise. Damping coefficient is calculated using logarithmic decrement method.

$$\delta = \frac{1}{n}\ln\frac{\theta(t)}{\theta(t+nT)} = 0.807$$

(10)

$$\xi = \frac{1}{\sqrt{1+\left(\frac{2\pi}{\delta}\right)^2}} = 0.127$$

(11)

$$c = \xi \cdot c_c = \xi \cdot 2 \cdot \sqrt{m \cdot g \cdot L_{cm} \cdot I} = 0.018\ N \cdot s$$

(12)

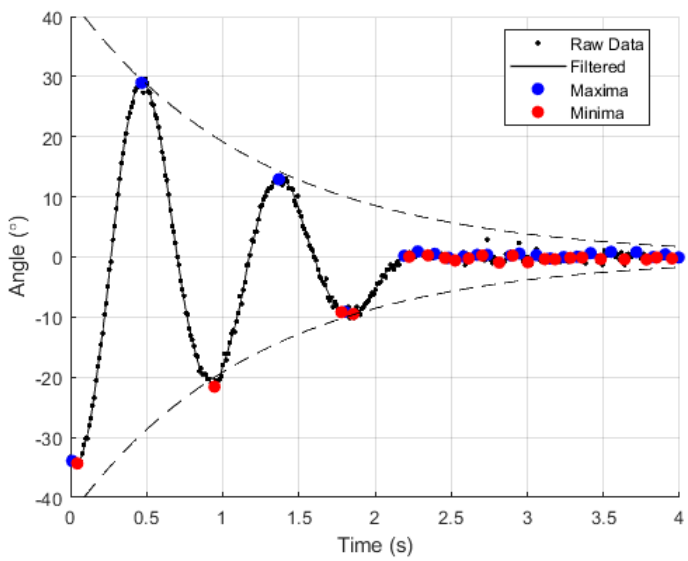

Figure 56: Angle for free swing of the leg showing raw and filtered data as well as local extrema

6.5.5 Leg Moment of Inertia Measurement

Using the same experiment, we can determine the moment of inertia of the leg by trying to find a fit to the data. The EOM of the system can be written as:

$$I \cdot \ddot{\theta} + c \cdot \dot{\theta} + mgL_{cm} \cdot \sin(\theta) = 0$$

(13)

This equation can be solved numerically using MATLAB. The results can be seen at the figure below. The initial guess for the moment of inertia can be taken by solving the differential equation by assuming a small angle.

$$I_i = \frac{T^2}{4\pi^2} \cdot mg \cdot L_{cm}$$

(14)

The damping coefficient can be taken from logarithmic decrement calculations. The results can be seen in the figure below.

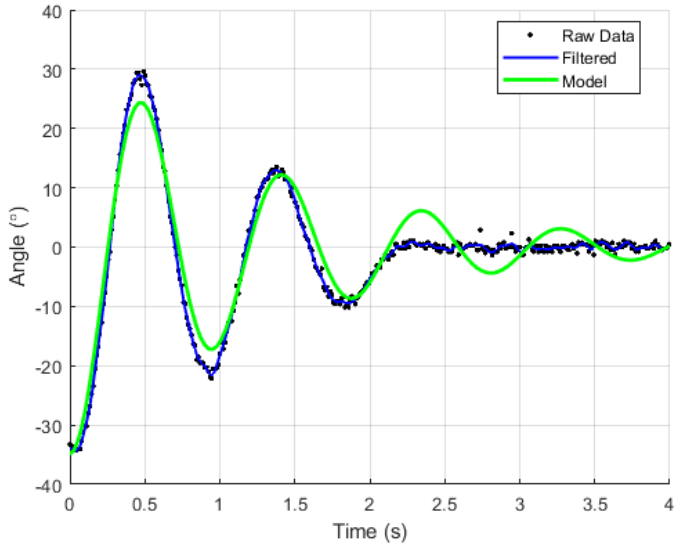

Figure 57: Angle for free swing of the leg showing raw and filtered data as well as mathematical model created

6.5.6 Material Determination of the Strain Gauge Holder

First, we analyzed the material of Strain Gauge Holder on C-Leg, then we decided the material used in C-Leg as Aluminum 2024 from alloy values.

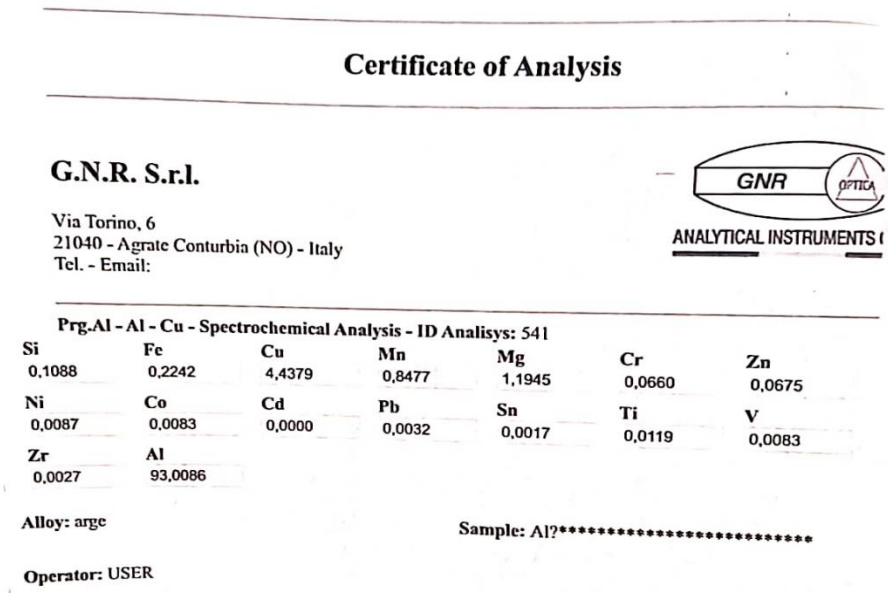

Certificate of Analysis

G.N.R. S.r.l.

Via Torino, 6
21040 - Agrate Conturbia (NO) - Italy
Tel. - Email:

GNR OPTICA
ANALYTICAL INSTRUMENTS

Prg.Al - Al - Cu - Spectrochemical Analysis - ID Analisys: 541

Si	Fe	Cu	Mn	Mg	Cr	Zn
0,1088	0,2242	4,4379	0,8477	1,1945	0,0660	0,0675
Ni	**Co**	**Cd**	**Pb**	**Sn**	**Ti**	**V**
0,0087	0,0083	0,0000	0,0032	0,0017	0,0119	0,0083
Zr	**Al**					
0,0027	93,0086					

Alloy: arge

Sample: Al?**********

Operator: USER

Figure 58: Spectrochemical Analysis Results

Although we found the material as Aluminum 2024, we couldn't decide which tampered version of this. In addition, our sponsor uses Aluminum 7075 in their products. Therefore, we compared two materials, and realized that all versions of Aluminum 7075 is have higher tensile and yield strength values. As a result, we have decided to use Aluminum 7075 which is profitable and safe.

6.6 Tests That Will be Conducted to Assess the System Performance

Test	Mehod	Aim
Walking Speed Test	Physical Test Using Parallel Bars	Checking if the system can respond for different walking speeds
Standing Test	Physical Test Using Parallel Bars	Checking if the pistons can maintain enough support for standing
Power Test	Measuring the power usage for one gait cycle	Checking if the battery would last for a day
Weighing	Weighing using a scale	Checking the weight requirement
Response Time Measurement	Measuring the time it takes to run a cycle of the loop using timer interrupt	Checking the response time requirement

6.6.1 Walking Speed Test – The user will be asked to walk along a path while holding on to parallel bars. They will be asked to walk at speeds ranging from 1 to 1.6 m/s and the prosthetic knee will be observed to check if it provides the necessary damping and support and can adapt to the different speeds.

6.6.2 Standing Test – The user will stand between two parallel bars for safety precautions. The user will stand still with their body load on the knee in full extension and if the piston does not move causing the knee to go to flexion it passes the test. Another test is the user will stand in a squatting position and the piston must provide enough support to prevent the user from falling.

6.6.3 Power Test - A Watt meter will be used. The prosthetic knee will be plugged to the watt meter and the user will be asked to walk and the energy consumption for 5 gait cycles will be measured and an average estimation for 15000 steps power consumption will be calculated. The battery size should be sufficient enough to provide the estimated power needed.

6.6.4 Weighing – Using a mass balance, all the electronic parts and sensors will be weighed and the sum must not exceed 300 grams.

6.6.5 Response Time Measurement – To measure the response time of the control system internal clock of the microcontrollers will be used. Since there are 2 microcontrollers, one taking necessary inputs to determine gait phase and running the decision-making algorithm other controlling the valve angles accordingly. A manual command will be sent to the first microcontroller about the mechanical position of the system and current value of the internal clock will be saved. Using the received information first microcontroller will calculate necessary damping values and send instructions along with saved time value. Then, the second microcontroller will execute the command and check the magnetic sensors to see if the desired valve angles are achieved. When real value of the angle is sufficiently close to the instructed angle microcontroller will save its current time and find out the difference between 2 saved times to find out how long 1 command execution cycle takes. This value is essentially the response time of the whole system.

6.7 Design Decisions

Design Decision	Value	Decision Method
Strain Gauge Holder Material	Al7075 - T6	Stress and Strain Calculations
Strain Gauge Holder Position	75 mm	Stress and Strain Calculations
Tolerance Between Strain Gauge Holder and the Tube	30.2 H5/h5	Clearance Calculations
Strain Gauge	Geoants 350Ω Full Bridge Strain Gauge	Strain Gauge Calculations
Magnetic Encoder	KMZ10C	Accuracy Needs

6.8 ANALYSIS RESULTS

6.8.1 Healthy Walking Model

We can get both kinematic and kinetic measurements using this model. It will be helpful to see the desired shapes of the measurements that will be measured by sensors. We have two sensors on the leg for determining the gait phase. The magnetic encoder measures the angle between thigh and the lower leg, i.e. knee angle. The other angle measurement that is important for walking with prosthesis is the ankle angle. Both plots show the filtered data and Fourier series fit on top of each other.

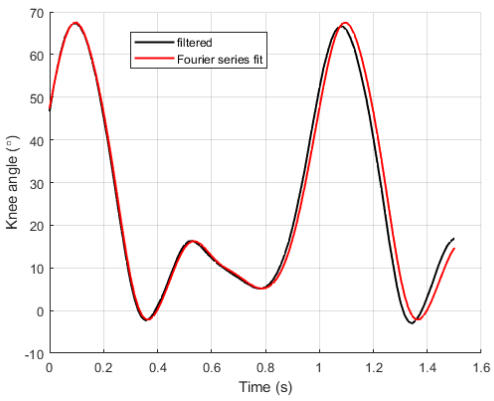

Figure 59: Knee angle in one gait cycle

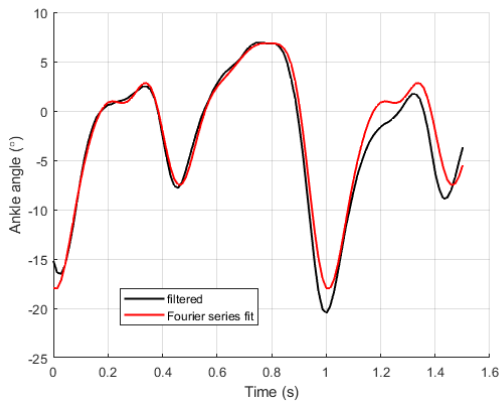

Figure 60: Ankle angle in one gait cycle

The movement of the piston is also critical since it is the part we have some control on it. The below plots shows the piston length and piston velocity in one gait cycle. Using those plots, we determined the most critical point for the piston on the gait cycle. For maximum walking speed of 1.6 m/s, the maximum piston velocity in extension direction is 0.142 m/s, while the maximum piston velocity in flexion direction is 0.185 m/s.

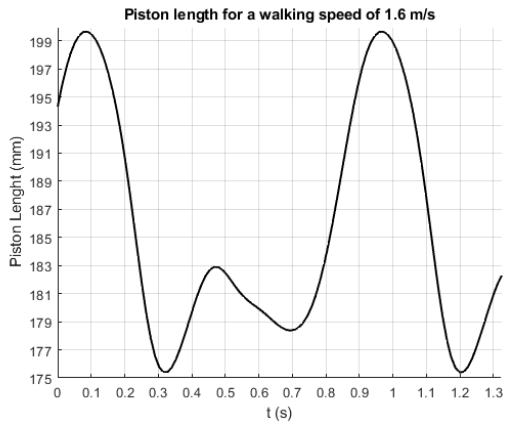

Figure 61: Piston length in one gait cycle

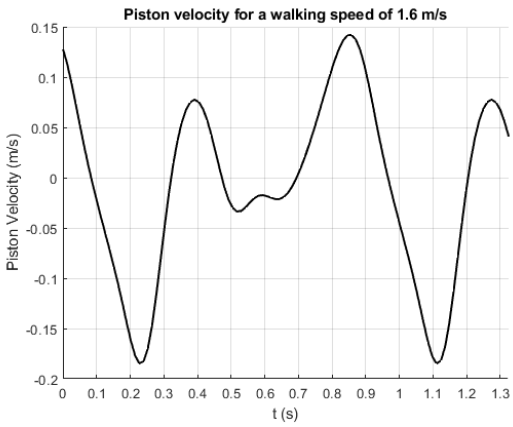

Figure 62: Ankle angle in one gait cycle

The ground reaction forces are important while designing the weight carrying parts. The health walking model can be used to asses the ground reaction forces if the prosthesis can be controlled perfectly. Those forces can be used to determine the most critical point on the lower leg when walking.

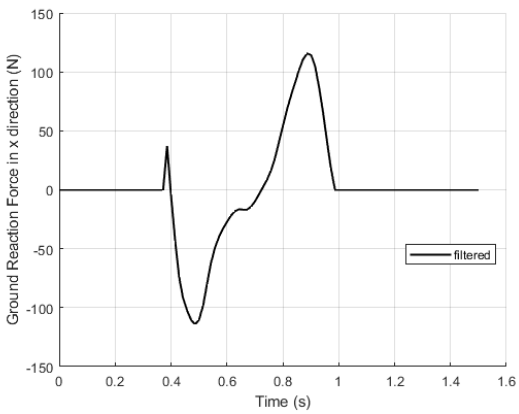

Figure 63: Ground reaction force parallel to the ground for one gait cycle

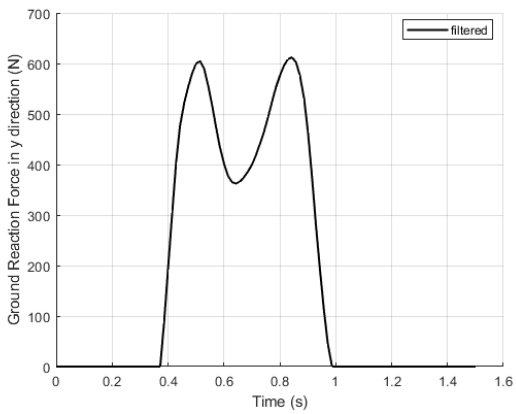

Figure 64: Ground reaction force perpendicular to the ground for one gait cycle

6.8.2 Stress Strain Analysis of the Lower Leg

Using the ground reaction forces obtained by the healhy walking model, we can calculate the strain on the strain gauges assuming linear elastic deflection on all parts. The results shows the most critical point for both strain gauges. They are approximately at the same time,which is the late half of the stance phase. Those values are calculated for a 135 kg person walking at 1.6 m/s to determine the most critical point.

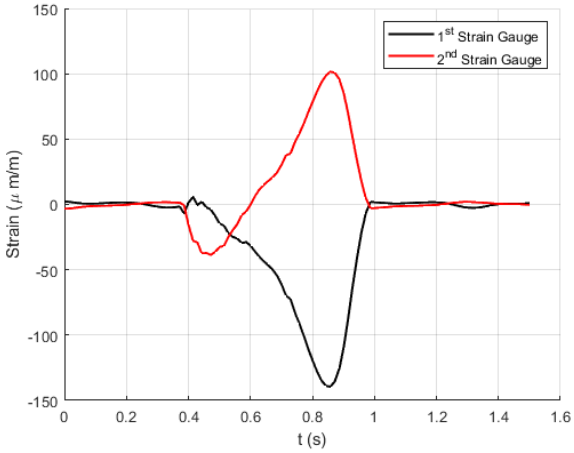

Figure 65: Strains on strain gauges in one gait cycle

Strain at the most critical part is the strain that we can measure at normal walking case. It is also the point where the leg is most probable to fail. Therefore, this point can be calculate to determine the strain gauge distance. The below plots shows the factor of safety and the maximum strain at the most critical point.

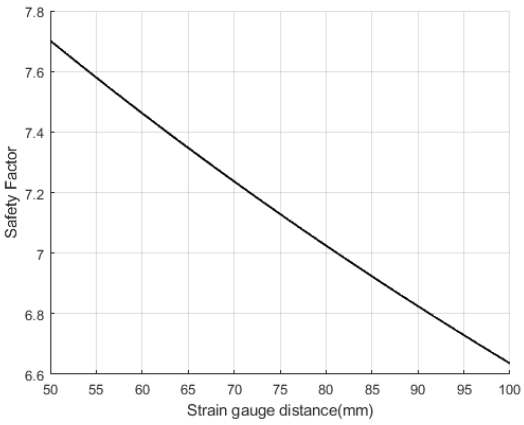

Figure 66: Factor of Safety of the leg based on strain gauge distance from the below

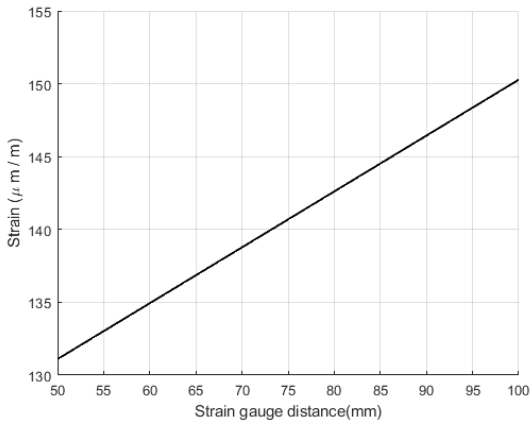

Figure 67: Maximum strain on strain gauges based on strain gauge distance from the below

The above results are checked using a commercial finite element analysis software. The results are parallel to the ones calculated in MATLAB.

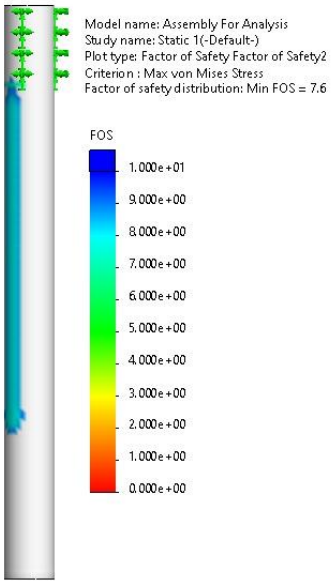

Figure 68: Factor of safety plot on the tube located at the lower leg

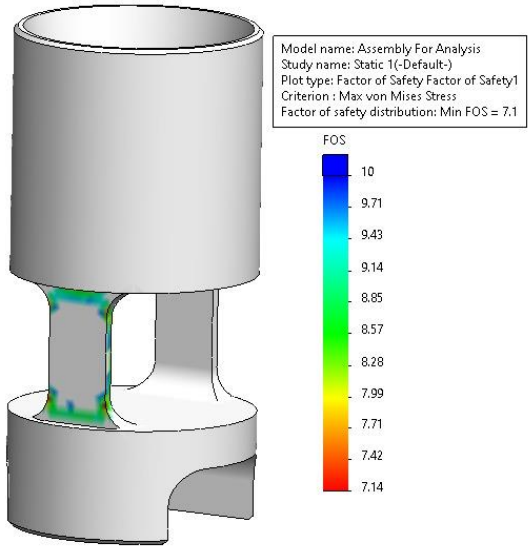

Figure 69: Factor of safety plot of the strain gauge holder part

6.8.3 Analysis of the Hydraulic System's Servovalve

The maximum piston velocity obtained during the gait cycle was 0.16 m/s and this was given as an inlet boundary condition with the valve inlet having the maximum orifice size. The system was modeled as turbulent and run as steady state. Figure 28 of the velocity contour plot shows that the velocity increases as it goes through the main channel reaching the outlet with a velocity of approximately 0.45 m/s. This increase in velocity is due to the pressure losses inside the valve. The obtained outlet velocity shows that this valve can provide the necessary damping for the most critical case. Assuming this outlet velocity of 0.45 m/s decreases as it flows through the pipes and round corners, the flow rate will decrease by the time it hits the piston and the 0.16 m/s flow can be obtained. Figure 29 shows the streamlines of the flow based on the velocity. There is a smooth flow with no backflow.

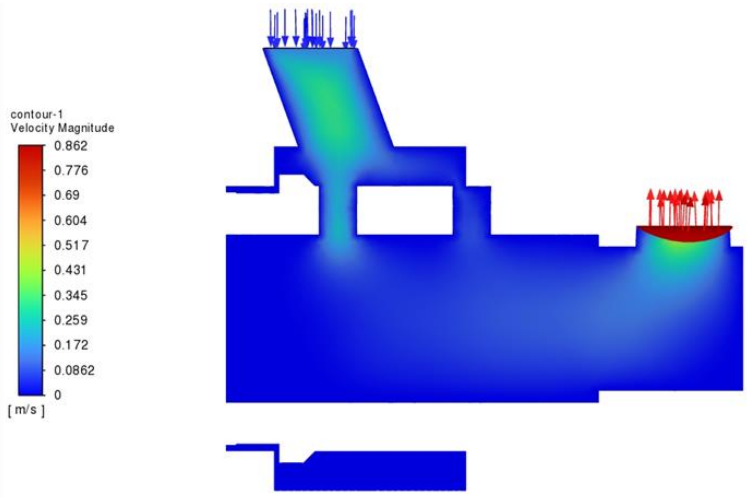

Figure 70: Velocity Contour Plot

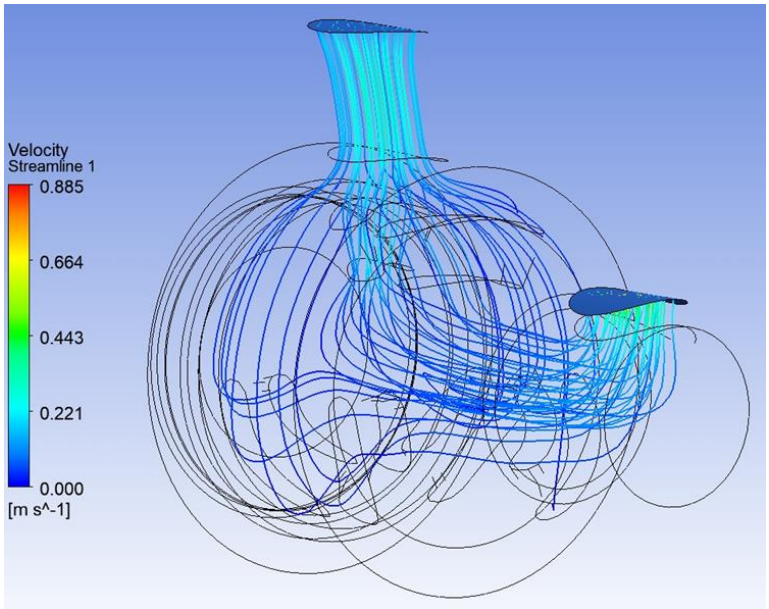

Figure 71 : Streamlines Plot

Figure 30 shows the pressure distribution of the fluid inside the valve. With average inlet pressure of 0.3 MPa and outlet pressure 29 KPa. Pressure decreases due to the losses caused by the geometry of the valve, sharp edges and corners.

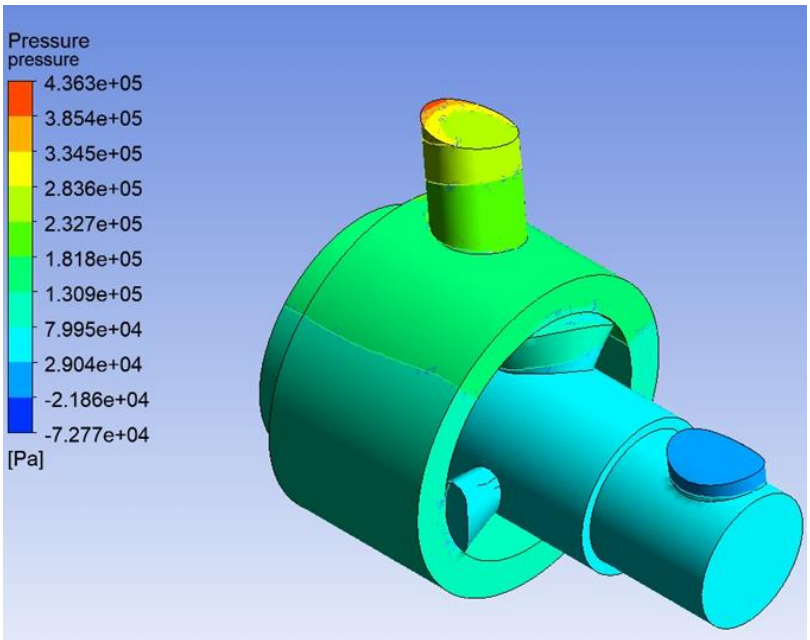

Figure 72: Pressure Contour Plot

6.8.4 Simulink Results

Instead of variable orifice, the fixed orifice is used in the simulation. Thus, the iteration process is required to represent the valve characteristic for whole range of orifice areas. For the 0.1 mm^2 orifice area, damping coefficient graph is provided in the Figure 31.

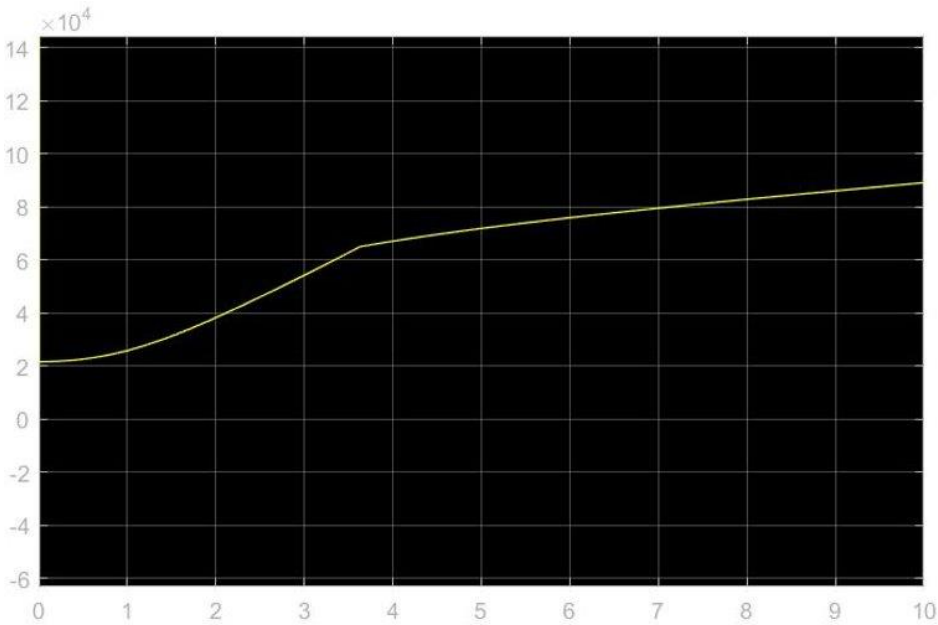

Figure 73:Variation of Damping Coefficient with Given Ramp Velocity Input

Where the horizontal axis is time in seconds [s] and the vertical axis is the damping coefficient in [N*m/s].
After 3.5 s there is almost linear variation of the damping coefficient with time upto 10 s.

6.8.5 Calculation of Valve Openings Results

To calculate valve openings, MATLAB Curve Fitting Toolbox was used. The fourier series method was selected as fitting method. The following figure represents the results of fitting.

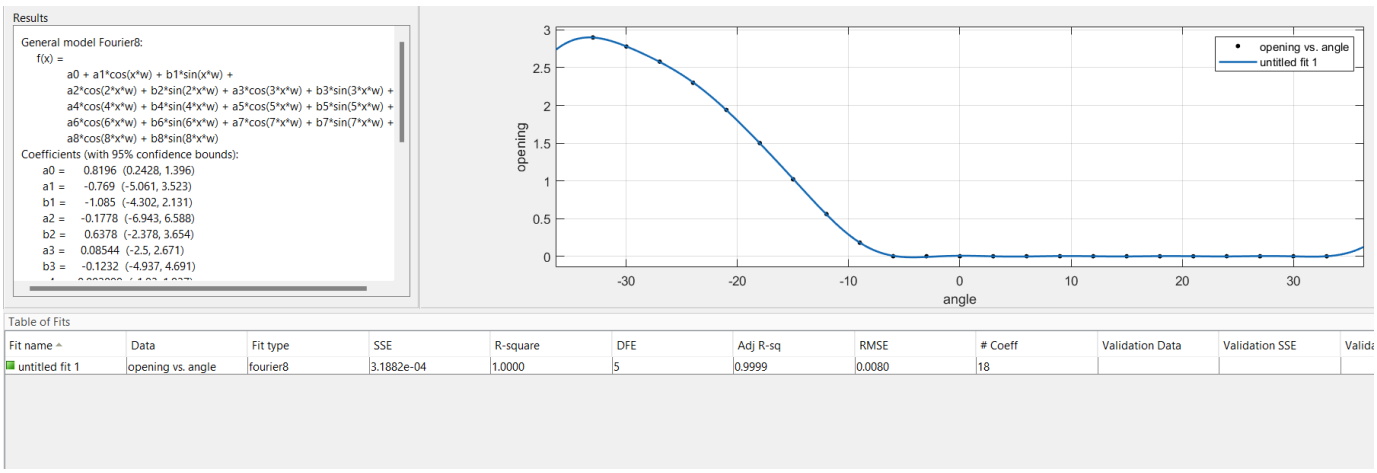

Figure 74: Curve Fitting for Valve Opening

Since the R value equals to 1.00, fourier series expansion with 8 terms are sufficient. According to analysis results, valve opens for only rotation to one side. The signs are chosen arbitrarily. With increasing motor rotation angle the valve opening area

increases. For positive motor angles the valve is closed. The maximum valve openings are 2.98 mm^2 for approximately -35 degrees motor angle.

6.9 DISCUSSION OF CONTROL ALGORITHMS AND SOFTWARE

In the control system of semi-active knee prosthesis, control system and decision algorithms are mainly based on previous knowledge depending on research and fuzzy inference systems. Following is the simplified version of the block diagram of the control system.

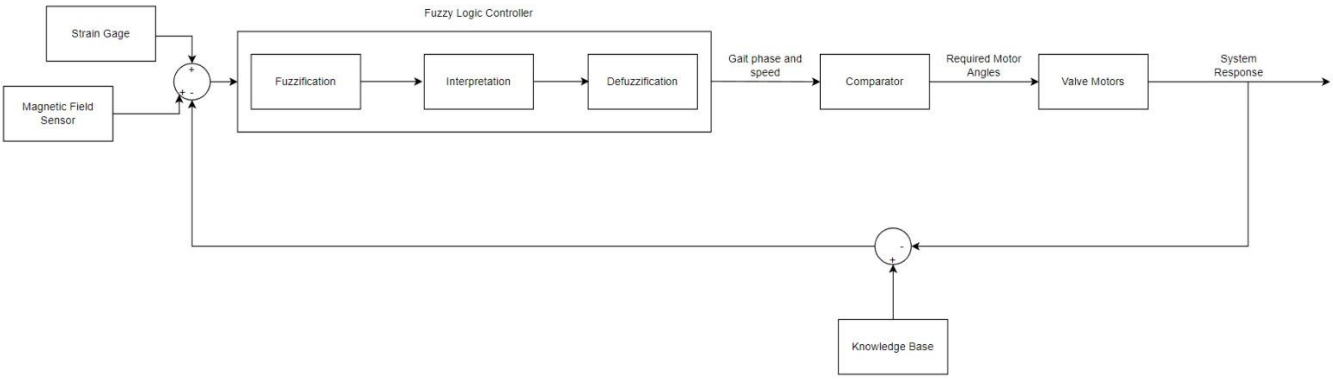

Figure 75: Block Diagram of the Control System

Control system consists of 3 main parts. Fuzzy logic controller (FLC) and comparator blocks are embedded in our microcontrollers. Knowledge base depends on previous research about kinematic analysis of human gait cycle.

Initially, inputs from strain gages and magnetic field sensor are filtered to get rid of noises in the data. From two sensors mainly three different data, which are knee angle, knee angular velocity and ground reaction forces, are interpreted. These data are feed into FLC to determine corresponding gait phase and speed. Then, FLC output is transmitted into the comparator to determine required damping coefficient and corresponding valve motor angles. This interpretation is based on previous fluid and geometry analyses done on the piston valve system. Afterwards, valve motors are driven to the required motor angles by using motor drivers and absolute encoders. Finally, system response is compared with knowledge base that is obtained through machine learning and using statistical profiling approach anomalies in the system response are fed back into the control system.

Following figure demonstrates FLC tree structure.

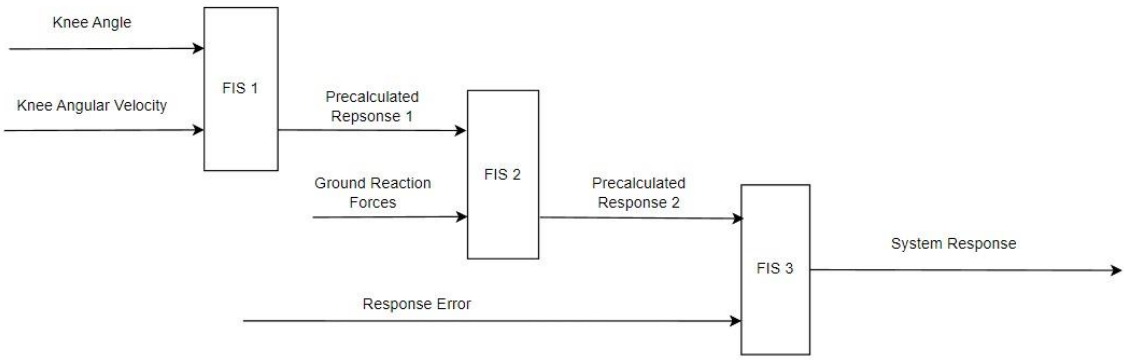

Figure 76: Incremental Fuzzy Tree

In this controller, incremental structure is used to simplify solution domain. Initially, controller takes knee angle and knee angular velocity inputs to the first fuzzy inference system and using corresponding membership functions and rules, outputs first precalculated response. Secondly, this precalculated response is given to the second fuzzy inference system with ground reaction forces to obtain corrected precalculated response. Finally, response error, which is calculated from difference between the system response and the knowledge base, final system response is obtained. During this process, membership functions are evaluated depending on the predetermined rules using genetic algorithm to obtain the quickest possible result. While knowledge base and system response is compared and anomalies in the response are calculated using statistical profiling approach.

6.10 OPTIMIZATION

Optimization process is done on strain gage positioning and lower leg thickness. Strain gage positioning is important such that load function creates strains in strain gages linear range and also part should not fail in extreme points of the load function. Initially, based on previous research and kinematic analysis of the knee joint, ground reaction forces are obtained. Then, values are stored in arrays and rotating coordinate system is defined to calculate forces and moments in x, y and z directions. Afterwards, for different assembly positions of the strain gage part and lower leg, stresses and strains are calculated on critical position of the assembly. Accordingly, factor of safety and strain values on strain gages versus strain gage part position and strain on strain gage versus time of the gait cycle are plotted. Finally, from the graphs optimum position and thickness of the parts are found by iterations. Resulting graphs are given as follows.

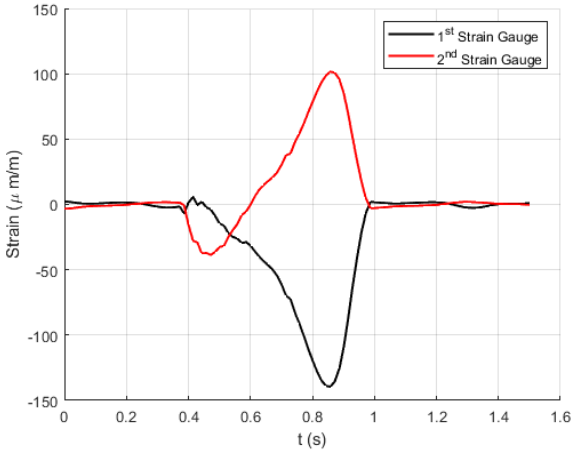

Figure 77: Strains on strain gauges in one gait cycle

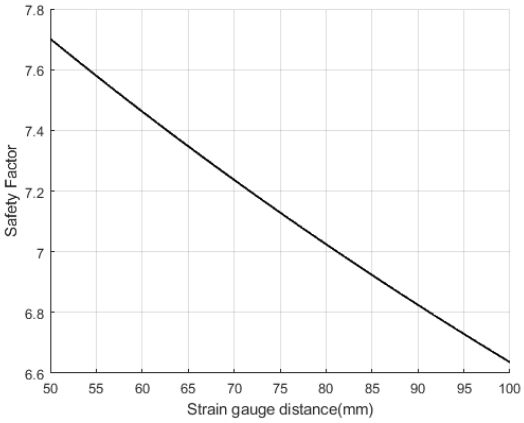

Figure 78: Factor of Safety of the leg based on strain gauge distance from the below

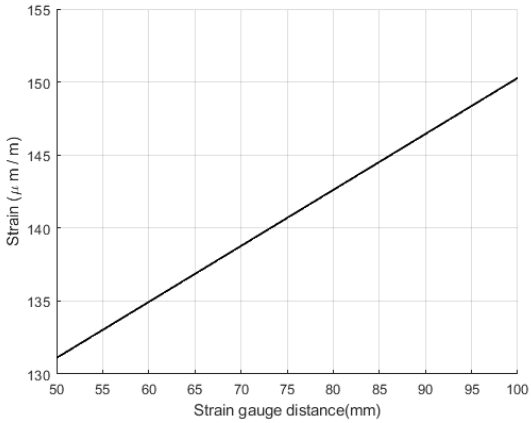

Figure 79: Maximum strain on strain gauges based on strain gauge distance from the below

From the graphs one can see that factor of safety decreases as the distance between ankle increases; however, maximum strain in a gait cycle on the strain gages does not increase significantly and stays in the linear range for all distances. Therefore, for both ease of assembly and safety, strain gage part is assembled closest to the ankle.

6.11 SYSTEM TO BE MANUFACTURED

Mechanics:

Since we design a control system for a specific product C-Leg, there are a few mechanicals system to be manufactured or purchased. A tube for holding strain gauge and a pipe for lower leg will be manufactured.

Figure 80: Rigid Models of Strain Gage Holder and Outer Pipe

See the Appendix for route sheets and technical drawings

Electronics:

One of the main parts of our project is the electronics, which are necessary for our microcontroller to communicate with and control the system. Our microprocessor as well as some complimentary electronic parts will be hand soldered to a piece of perfboard. And our microcontroller will be programmed manually. However, for a large volume production rp2040 chip could be used directly along with all the complementary parts on a single PCB.

Additionally, for amplifying the outputs of strain gauges another PCB is designed and manufactured.

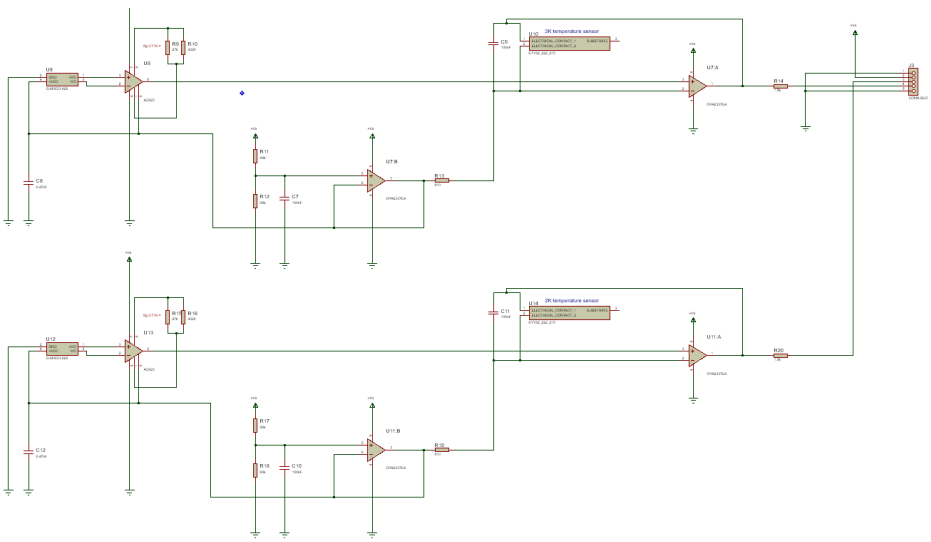

Figure 81: Strain Gage Amplifier Circuit

6.12 SUSTAINABILITY ANALYSIS

Sustainability analysis of the 2 mechanical parts is performed by SOLIDWORKS and report can be found in the Appendix Part. Rest of the system consists of electronic parts and their sustainably analysis is as follows.

a. Design for manufacture

Small amount of assembly will be done for electronic parts. This will consist of hand soldering some electronic parts. For larger volume productions printed circuit boards could be used.

For Li-ion batteries during manufacturing according to the assesments by Ellingsen et al. approximately 170 kg CO2-eq are emitted per kWh of battery capacity[3]. Meaning that with 2 18650 Li-ion batteries corresponding 3.8 kg of carbon emission

b. Design for distribution

Since the control system neither weighs much nor takes up significant volume it's effect on distribution is negligible compared to the complete prosthetic leg.

c. Design for use

During use, only environmental effects will be the electricity usage of the system, which will be maximum of 25Wh per day which corresponds to 9.3 g of carbon emission.

d. Design for retirement of the product

After the lifespan of the product has been completed it is preferable for some parts to be reused which may be possible for the programmable microprocessors, however for most other parts in the system this is not suitable and best solution is to recycle materials.

For Li-ion batteries recycling process can reach a recycling rate over 55%, and the only losses are related to the organics that cannot be recovered[2].

In case of the printed circuit boards on the product it is only possible to recycle a small portion of them in order to extract some valuable metals including copper[4].

6.13 TEST PLAN

Table 17 Table of Test Plans

Requirement	Specification	Description of the test	Equipment needed	Analysis Method
The control system of the prosthetic knee should identify the phase in the gait cycle and should be adjustable for different walking speeds.	It should allow patients to walk at a self-selected speed of up to 1.6 m/s.	Test with patients	Parallel Bars	SIMULINK
It should allow patients to stand without moving.	It should allow patients to stand without moving.	Test with patients	Parallel Bars	Checking if there is satisfactory damping in standing position by fluid control in SIMULINK.
The control system should work with effective energy consumption.	It should allow patients to walk approximately 15,000 steps with a velocity of 1.6 m/s with a full charge.	Current consumption in both standby and gait phases	Ammeter and oscilloscope	Summation of max and min power consumptions given in data sheets of the used components.
The system should be light enough to carry whole day	The total weight of the control system should be less than 300 grams.	Weighing the product	Scale with a resolution of 0.1 kg	-
Response time of the sytem should be small enugh to work properly	The delay of the response of the control system must be less than 5ms.	Given specific parameters and measuring time passed both externally and internally.	Real time clock	Control system simulation in SIMULINK
The leg should allow enough flexion	It should allow patients to rotate their knees at different angles, which are between 0 and 130 degrees.	Checking damping values in the given range of motion.	Parallel Bars	Flow analysis in Fluent, ANSYS and fluid control in SIMULINK

As mentioned in the introduction there are some sets of tests that are already conducted and will be conducted not just requirements. For spring stiffness determination, a load applied, and deflection is measured to model the piston. For ESAR, foot stiffness measurements, a load applied, and deflection were measured to model walking with the prosthetic knee. For leg center of mass and inertia measurement, a two-axis balancing experiment was conducted for creation of walking with prosthetics model. Prosthetic leg was weighed. Since, the weight of the leg is needed while modelling walking with prosthetics. For knee joint damping measurement, and for moment of inertia measurement the leg was freely swan, after that team solved the differential equation analytically using MATLAB. The result was needed for walking with prosthetics model. For material determination of the strain gauge holder, spectrochemical analysis was conducted to learn the physical characteristics of the material.

In the future tests will be carried out, those are walking speed test to check if the system can respond to different walking speeds, standing test to check if the piston can provide enough support during stance phase. Power test to check if the battery can provide energy for one working day. Weight test to see if weight requirements are satisfied. Response time measurement to check for lag and delay problems.

In addition to those tests that are mentioned above there are essential requirements that must be tested. Firstly, the control system of the prosthetic knee should identify the phase in the gait cycle and should be adjustable for different speeds. To test this patient will walk directly and failure will be checked visually. Requirement criteria is the allowing patients walk up to 1.6 m/s. Equipment will be the parallel bars and SIMULINK will be used.

Also, it is required that patients must be able to stand without moving. This requirement will be tested with the patients. Needed equipment for this test is parallel

bars. The test will be conducted in SIMULINK by checking if there is satisfactory damping value while patient stands still from the control algorithm that is created in SIMULINK.

One other requirement is the effective energy consumption of the control system. Specifically our design should allow patients to walk approximately 15,000 steps with a velocity of 1.6m/s while it is fully charged. Energy consumption can be calculated from the current consumption of the gait phases and also the phase of standing still. To measure them an amperemeter and oscilloscope will be used. Summation of maximum and minimum power consumption values will be dealt to data sheets of the used component.

The next requirement is stated as to obtain weight of the system must be light enough to carry whole day. By weighing the leg, it should be made less than 300 grams. Equipment that will be used has to be with a resolution of 0.1 kg.

Next requirement of the system is to have a short response time to get the system work properly, and accurately. To specifically indicate the requirement, response time of the control system must be less than 5 ms. Experiment will be conducted with a real time clock, which will be used for measuring both external and internal response times for a specifically given parameters. The simulation of this experiment will be done in SIMULINK.

One other requirement of this design is to have enough flexion allowance from the leg. To be specific, prosthetic leg should allow patients to rotate their knees in different angles. The interval will be 0 to 130 degrees. During the testing stage damping values in the given range of motion will be checked from flow analysis in Fluent, ANSYS, and fluid control in SIMULINK.

6.14 STANDARDS USED FOR DESIGN PROCEDURES and PERFORMANCE EVALUATION

6.14.1 Design Standards

In this project, mainly prosthesis standards are used. The used standards are listed below:

- ***ISO/TS 16955:2016,*** **Prosthetics — Quantification of physical parameters of ankle foot devices and foot unit.**
- ***ISO 13405-1:2015,*** **Prosthetics and orthotics — Classification and description of prosthetic components — Part 1: Classification of prosthetic components**
- ***ISO 13405-2:2015,*** **Prosthetics and orthotics — Classification and description of prosthetic components — Part 2: Description of lower limb prosthetic components**
- ***ISO 128-1:2003*****, Technical drawings—General principles of presentation—Part 1: Introduction and index**,

- ***ISO 129,*** **Technical drawings -- Indication of dimensions and tolerances,**
- ***ISO 286-2:2010,*** **Geometrical product specifications (GPS) -- ISO code system for tolerances on linear sizes -- Part 2: Tables of standard tolerance classes and limit deviations for holes and shafts,** This standard is used for dimensioning of shafts and housing diametric tolerances and their representations with some letters and numbers for minimum and maximum limits of the diameter of bearing seats. Also other this standard is used for representing the amount of tight fits used in our project.
- ***ASME Y14.5-2009 [Revision of ASME Y14.5 M-1994(R2004)],*** **Dimensioning and tolerancing – Engineering drawing and related documentation practices.**

6.14.2 Performance and Test Standards

In order to perform test and check whether design meets the standards or not, the following ISO standards are used.

- ***ISO/TR 22676:2006*****, Prosthetics — Testing of ankle-foot devices and foot units — Guidance on the application of the test loading conditions of ISO 22675 and on the design of appropriate test equipment**

- ***ISO 10328:2016*****, Prosthetics — Structural testing of lower-limb prostheses — Requirements and test methods**

- ***ISO 22675:2016*****, Prosthetics — Testing of ankle-foot devices and foot units — Requirements and test methods**

6.15 DISCUSSIONS AND CONCLUSIONS

Our design has five main functions. Identifying gait cycle, adapting different walking speeds, ensuring safety for user, managing power consumption, and communicating with user.

For the subfunctions of these main functions we decided to use concepts. For identifying gait phase and calculating valve angle we decided to use decision tree, for controlling valve angles we decided to use combined system. For ensuring safety for users it was decided to use statistical profiling approach. For managing power consumption it was decided to use BMS module. For communicating with user optimum solution was indicated as using combined system. For measuring knee angle using magnetic encoder was decided. For measuring ground reactions using orthogonal active full bridge system was decided. For microcontroller using 2 Raspberry Pi Pico was decided. For filtering choice was made from using Low pass filtering.

For analytical modelling of the design some simulations , and physical experiments were conducted. For inertia measurement a physical experiment has been made, and from there an analytical solution from the differential equation of the body

was obtained it was conducted to get the value of moment of inertia. For a healthy person's walking simulation MATLAB was used. For understanding the fluid behavior in the valve a CFD simulation was conducted from the ANSYS. For valve opening simulation we firstly obtained the required motor angle data from the SOLIDWORKS and then by using this data we transformed it into a mathematical function in MATLAB by curve fitting. For stiffness measurement a physical experiment was conducted and a force was applied to piston and measured its deflection.

If we were forced to re-start the design process all over again our approach would not drastically shift. After all, the team has decided in this limited time the best possible functions, solutions and tests that will be conducted to check them. If the desire is to get more precise and accurate solutions, it is matter of time limitation, not making every single choice all over again.

7. Discussion

Before starting all the processes that is necessary to complete this project, we had to define the problem. The problem that is confronted was the unergonomic adjustment of the prosthetic knee's kinematic motion. After we defined this problem, the solution was to create a semi-active knee that is able to adjust itself according to users walking motion. To enact adjustability of the leg to different situations, a controllable damping coefficient with hydraulic piston cylinder system is used in order to control the kinematic motion of the leg to make the motion more efficient for the user. The project has been mainly based on the control system the design of the hydraulic piston.

Firstly, in order to complete this project, team tried to create a suitable functional decomposition of the project that was assigned to us. Following that, each member of the team designed some concepts by brainstorming to each of these functions. During this brainstorming session every single group member delivered his contribution. That helped us to choose a path from lots of possible ones. After that, we applied an evaluation process to subfunctions of the decomposed functions. Generally, we set 3 different evaluation criteria for each subfunction, and we rated the possible solutions of subfunctions to decide the best combination of solutions. Therefore, we cleared our mind for the solutions to be applied. Following that we planned to conduct kinematic and fluid analysis. Depending on those analysis we had to design the control system. The design of control of control system has been done based on system of equations accompanied with analyses.

The design has five main functions. Identifying gait cycle, adapting different walking speeds, ensuring safety for user, managing power consumption, and communicating with user.

For the subfunctions of these main functions we decided to apply various concepts. For identifying gait phase and calculating valve angle we decided to use decision tree, and used combined system which includes PID and fuzzy logic to control valve angles. For ensuring safety of the users it was decided to use statistical profiling approach. For managing power consumption, it was decided to use BMS module. For communicating with user optimum solution was indicated as using combined system including vibration motor, buzzer and mobile app. For measuring knee angle using magnetic encoder was decided. For measuring ground reactions, using orthogonal active full bridge strain gage system was decided. For microcontroller, using 2 Raspberry Pi Pico was decided. For filtering the choice was made from using Low pass filtering.

For analytical modelling of the design some simulations and physical experiments were conducted. For inertia measurement a physical experiment has been made, and from there an analytical solution from the differential equation of the body was obtained to get the value of moment of inertia. For a healthy person's walking simulation MATLAB was used. For understanding the fluid behavior in the valve, a CFD simulation was conducted from the ANSYS. For valve opening simulation we firstly obtained the required motor angle data from the SOLIDWORKS and then by using this data we transformed it into a mathematical function in MATLAB by curve fitting. For stiffness measurement a physical experiment was conducted, and a force was applied to piston and measured its deflection.

For this project, the manufactured pieces were the outer pipe and the strain gauge holder. The reason to manufacture the pipe was to get a connecting element that will be placed between prosthetic knee and prosthetic foot. This pipe is also useful for adjusting different leg lengths in the production procedure. The real help of this pipe is that it results with a strain that is easy to analyze. The reason behind the production of

strain gauge holder was to obtain higher strain rates, with that way one could achieve more precise values from strain gauge sensor. This piece is placed inside the outer pipe and glued. Three copies of the strain gauge holder were manufactured in Proted. At the beginning, the strain gauge holder that was manufactured had a curvature problem on its face at the beginning therefore, the team has decided that using a part with a curvature problem was not appropriate. Following that a new part has been produced to evade this problem. These two parts that were produced achieves their objectives properly.

The project design of the microprocessor controlled prosthetic knee works with simple electronic components. The power supply comes from a battery that is placed on a prosthetic leg. Since the energy consumption of this project is considerably low, it does not do harm to the environment a lot caused by energy generation. The rest of the system does not hold a potential harm to environment directly. However, by indirect ways such as during manufacturing of product or the materials that were used during this procedure may cause minimal damages to environment.

8. Conclusion

The prosthetic knee design is effective in providing adaptive movement for the user and can meet user's basic needs and preferences. The materials that are used in prosthetic knee design are suitable for intended purposes and they are compatible with human biology. A prosthetic knee must meet the strict safety and performance requirements, and it must be comfortable for the user. The design must improve the quality of life of the user and it must help the user to regain their mobility. After all the studies that were performed, one can conclude that semi-active prosthetic knee is more beneficial than passive prosthetic knee, as it can adjust to the user's needs and activity level, which results in more adaptive and natural movement.

9. References

[1] C. Lansade et al., "Mobility and satisfaction with a microprocessor-controlled knee in moderately active amputees: A multi-centric randomized crossover trial," Ann. Phys. Rehabil. Med., vol. 61, no. 5, 2018, doi: 10.1016/j.rehab.2018.04.003.

[2] M. Windrich, M. Grimmer, O. Christ, S. Rinderknecht, and P. Beckerle, "Active lower limb prosthetics: A systematic review of design issues and solutions," BioMedical Engineering Online, vol. 15. 2016, doi: 10.1186/s12938-016-0284-9.

[3] M. Bellmann, T. M. Köhler, and T. Schmalz, "Comparative biomechanical evaluation of two technologically different microprocessor-controlled prosthetic knee joints in safety-relevant daily-life situations," Biomed. Tech., vol. 64, no. 4, 2019, doi: 10.1515/bmt-2018-0026.

[4] J. Thiele, B. Westebbe, M. Bellmann, and M. Kraft, "Designs and performance of microprocessorcontrolled knee joints," Biomed. Tech., vol. 59, no. 1, 2014, doi: 10.1515/bmt-2013-0069.

[5] P. J. R. Theeven, B. Hemmen, P. R. G. Brink, R. J. E. M. Smeets, and H. A. M. Seelen, "Measures and procedures utilized to determine the added value of microprocessor-controlled prosthetic knee joints: A systematic review," BMC Musculoskelet. Disord., vol. 14, 2013, doi: 10.1186/1471-2474-14-333.

[6] Y. Jia et al., "A numerical feasibility study of kinetic energy harvesting from lower limb prosthetics," Energies, vol. 12, no. 20, 2019, doi: 10.3390/en12203824.

[7] W. Cao, H. Yu, W. Chen, Q. Meng, and C. Chen, "Design and Evaluation of a Novel Microprocessor-Controlled Prosthetic Knee," IEEE Access, vol. 7, 2019, doi: 10.1109/ACCESS.2019.2957823.

[8] M. I. Awad et al., "Towards a Smart Semi-Active Prosthetic Leg: Preliminary Assessment and Testing," in IFAC-PapersOnLine, 2016, vol. 49, no. 21, doi: 10.1016/j.ifacol.2016.10.539.

[9] C. Chen, M. Hanson, R. Chaturvedi, S. Mattke, R. Hillestad, and H. H. Liu, "Economic benefits of microprocessor controlled prosthetic knees: A modeling study," J. Neuroeng. Rehabil., vol. 15, 2018, doi: 10.1186/s12984-018-0405-8.

[10] J. H. Campbell, P. M. Stevens, and S. R. Wurdeman, "OASIS 1: Retrospective analysis of four different microprocessor knee types," J. Rehabil. Assist. Technol. Eng., vol. 7, 2020, doi: 10.1177/2055668320968476.

[11] M. McGrath, P. Laszczak, S. Zahedi, and D. Moser, "Microprocessor knees with 'standing support' and articulating, hydraulic ankles improve balance control and inter-limb loading during quiet standing," J. Rehabil. Assist. Technol. Eng., vol. 5, 2018, doi: 10.1177/2055668318795396.

[12] B. Laschowski and J. Andrysek, "Electromechanical design of robotic transfemoral prostheses," in Proceedings of the ASME Design Engineering Technical Conference, 2018, vol. 5A-2018, doi: 10.1115/detc2018-85234.

[13] M. P. Mileusnic, L. Rettinger, M. J. Highsmith, and A. Hahn, "Benefits of the Genium microprocessor controlled prosthetic knee on ambulation, mobility, activities of daily living and quality of life: a systematic literature review," Disability and Rehabilitation: Assistive Technology, vol. 16, no. 5. 2021, doi: 10.1080/17483107.2019.1648570.

[14] S: H. Petrofsky, W. G. Gruesbeck, "Computer Controlled Hydraulic Resistance for a Prosthesis and Other Aparatus", United States Patent 6113642, Sep. 5, 2000

[15] R. Auberger, M. Seyr, C. Mandl, D. Seifert, H. Dietl, "Method for Controlling an Artificial Orthotcor Prosthetic Knee Joint", United States Patent 14911549, Jul 7. 2014

[16] M. S. Zahedi, N. Stech, D. Moser, A. J. Sykes, "Lower Limb Prosthesis", United States Patent 14364637, Dec.12, 2012

[17] H. M. Herr, A. Wilkenfeld, O. Bleck, "Control System for Prosthetic Knee", United States Patents 11868941, Oct. 8, 2007

[18] K. B. James, "System for Controlling Artificial Knee Joint Action in an Above Knee Prosthesis", United States Patent 341127, Nov. 18, 1994

[19] P. Micheal, B. Charles, "Computer controlled prosthetic knee device", European Patent 14166804.6, 28.07.2006

[20] D. A. Winter, Biomechanics and motor control of human movement. Wiley, 2009.

[21] Amin, Mario & Salgado, Mario & Usai, Lorenzo & Ellingsen, Linda & Pan, Qiaoyan & Strømman, Anders. (2019). Comparative Life Cycle Assessment of a Novel Al-Ion and a Li-Ion Battery for Stationary Applications. Materials. 12. 10.3390/ma12193270.

[22] Ghassan Zubi, Rodolfo Dufo-López, Monica Carvalho, Guzay Pasaoglu, The lithium-ion battery: State of the art and future perspectives, Renewable and Sustainable Energy Reviews, Volume 89, 2018, Pages 292-308, ISSN 1364-0321, https://doi.org/10.1016/j.rser.2018.03.002

[23] André Canal Marques, José-María Cabrera, Célia de Fraga Malfatti, Printed circuit boards: A review on the perspective of sustainability, Journal of Environmental Management, Volume 131, 2013, Pages 298-306, ISSN 0301-4797, https://doi.org/10.1016/j.jenvman.2013.10.003

10 Appendix

APPENDIX A – WORKING DRAWINGS

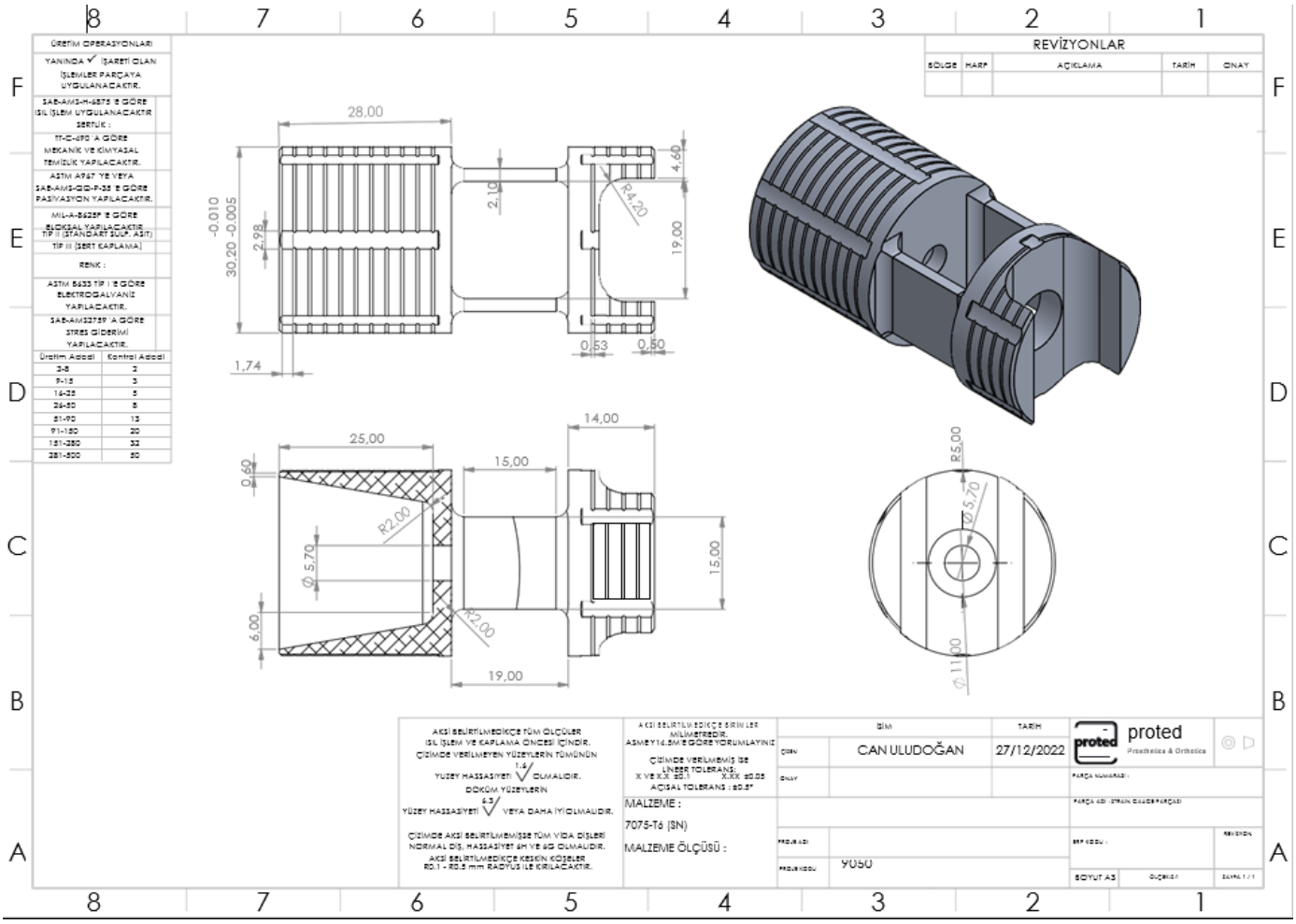

Figure 40: Technical Drawing of Strain Gage Holder

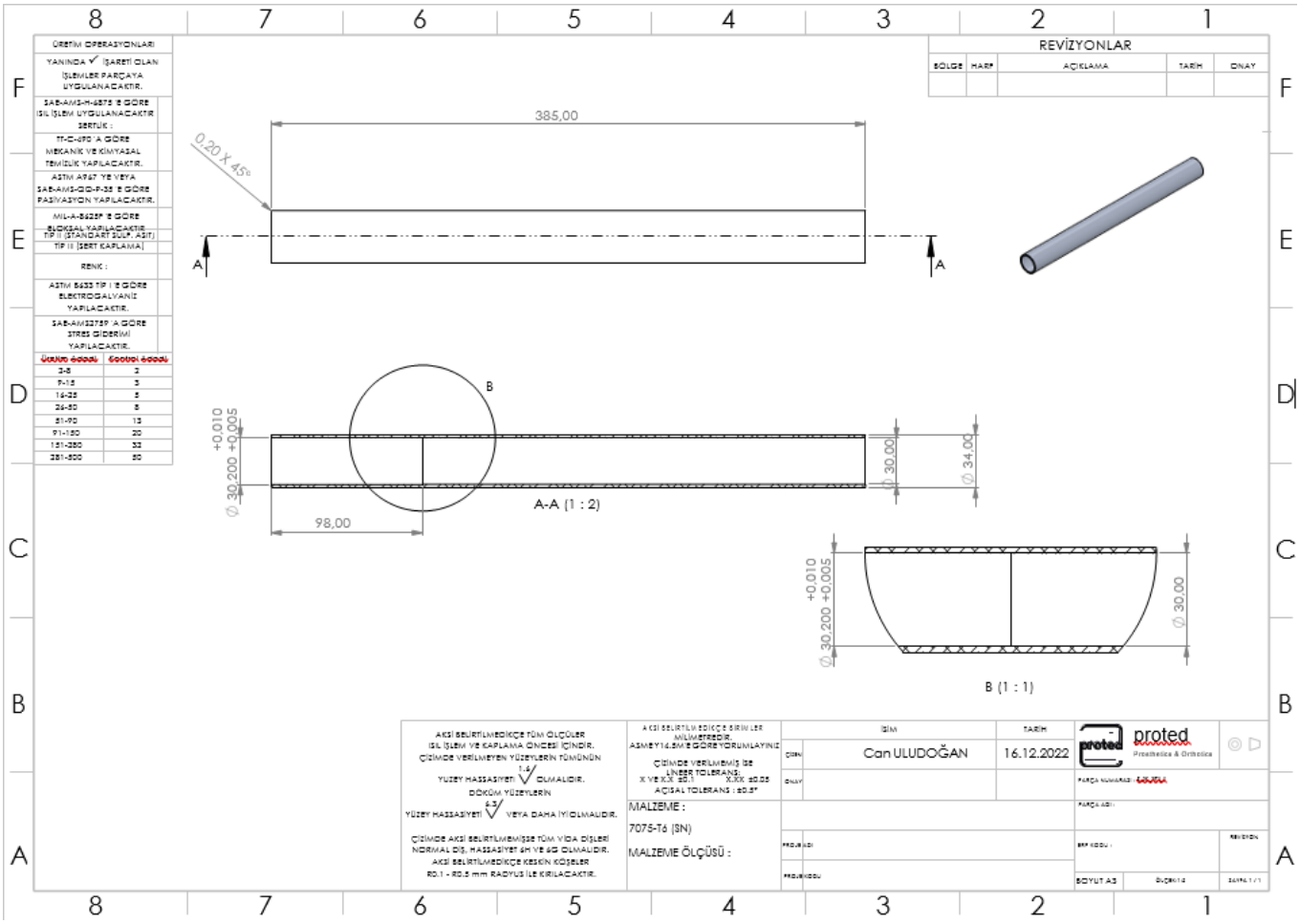

Figure 41: Technical Drawing of Outer Pipe

APPENDIX B – ROUTE SHEETS

Name of the part :	Strain Gauge Holder		
Part Number:	1		
Quantity to be manufactured:	8		
Material used:	Aluminum 7075		
Operation No:	**Description of the operation**	**Equipment**	**Tooling**
1	Right Hand Turning	Lathe	Cutting Tool
2	External Grooving	Lathe	Cutting Tool
3	Drilling	Lathe	Cutting Tool
4	Stack Removal	Lathe	Cutting Tool
5	Turning	Lathe	Cutting Tool
6	Drilling	Lathe	Cutting Tool
7	Stack Removal	Lathe	Cutting Tool
8	Cut-off	Lathe	Cutting Tool
9	Dimension Check	Lathe	Digital Caliper

Name of the part :	Outer Pipe		
Part Number:	2		
Quantity to be manufactured:	8		
Material used:	Aluminum 7075		
Operation No:	**Description of the operation**	**Equipment**	**Tooling**
1	Right Hand Turning	Lathe	Cutting Tool
2	Boring	Lathe	Cutting Tool
3	Boring	Lathe	Cutting Tool
4	Cut-off	Lathe	Cutting Tool
5	Dimension Check	Lathe	Digital Caliper

APPENDIX C – MATLAB CODES

Healthy Walking Model – Gait Cycle Analysis Using Fourier Series

fourier_series_analysis.m

```
function a = fourier_series_analysis(F,t,T,not)
    % Calculating Fourier series coefficients
    omega_0 = 2*pi/T;
    k = -1*floor(not/2):not-floor(not/2)-1;
    a = zeros(1,not);
    for i = 1:not
        a(i) = (1/T) * trapz(t,F.*exp(-1j*k(i)*omega_0.*t));
    end
end
```

fourier_series_synthesis.m

```
function Ff = fourier_series_synthesis(a,t,not)
    % Reassembling the function using Fourier series coefficients
    k = -1*floor(not/2):not-floor(not/2)-1;
    Ff = zeros(1,size(t,1));
    for ti = 1:size(t,1)
        for ki = 1:not
            % Ff(ti) = Ff(ti) + a(ki)*exp(1j*k(ki)*2*pi*t(ti)); % Complex
Form
            Ff(ti) = Ff(ti) + abs(a(ki))*cos(k(ki)*2*pi*t(ti) +
angle(a(ki)));
        end
    end
end
```

gait_cycle_fs.m

```
%% Gait Cycle Analysis using Fourier Series
% Mehmet Furkan Do?an
% 12 November 2022
clc;clear;close all;
%% IMPORT DATA
%%%
```

```
fibula_y = A_2(:,24)*1e3;    % mm
ankle_x = A_2(:,27)*1e3;     % mm
ankle_y = A_2(:,30)*1e3;     % mm
heel_x = A_2(:,33)*1e3;      % mm
heel_y = A_2(:,36)*1e3;      % mm
metat_x = A_2(:,39)*1e3;     % mm
metat_y = A_2(:,42)*1e3;     % mm
toe_x = A_2(:,45)*1e3;       % mm
toe_y = A_2(:,48)*1e3;       % mm
%%%
```

```
%%  ANGLES
foot_theta_f = fit_y(foot_theta,t,15,'foot_theta.txt');      % degree
leg_theta_f = fit_y(leg_theta,t,15,'leg_theta.txt');      % degree
thigh_theta_f = fit_y(thigh_theta,t,15,'thigh_theta.txt');    % degree
HAT_theta_f = fit_y(HAT_theta,t,15,'HAT_theta.txt');      % degree
% A4
hip_theta_f = fit_y(hip_theta,t,15,'hip_theta.txt');     % degree
knee_theta_f = fit_y(knee_theta,t,15,'knee_theta.txt'); % degree
ankle_theta_f = fit_y(ankle_theta,t,15,'ankle_theta.txt'); % degree
%% FORCES AND MOMENTS
F_foot_ground_x_f = fit_y(F_foot_ground_x,t,17,'F_foot_ground_x.txt');  % N
F_foot_ground_y_f = fit_y(F_foot_ground_y,t,17,'F_foot_ground_y.txt');  % N

%% PLOT
%% RIB X
f_rib_x = figure('name','Rib x coordinate','numbertitle','off');hold
on;grid on;
plot(t,rib_x,t,rib_x_f,'linewidth',1.5);
xlabel('t (s)');ylabel('rib x (mm)');
legend('filtered','Fourier series fit','location','best');
%% RIB Y
f_rib_y = figure('name','Rib y coordinate','numbertitle','off');hold
on;grid on;
plot(t,rib_y,t,rib_y_f,'linewidth',1.5);
xlabel('t (s)');ylabel('rib y (mm)');
legend('filtered','Fourier series fit','location','best');

%% HIP X
f_hip_x = figure('name','Hip x coordinate','numbertitle','off');hold
on;grid on;
plot(t,hip_x,t,hip_x_f,'linewidth',1.5);
xlabel('t (s)');ylabel('hip x (mm)');
legend('filtered','Fourier series fit','location','best');
%% HIP Y
f_hip_y = figure('name','Hip y coordinate','numbertitle','off');hold
on;grid on;
plot(t,hip_y,t,hip_y_f,'linewidth',1.5);
xlabel('t (s)');ylabel('hip y (mm)');
legend('filtered','Fourier series fit','location','best');

%% KNEE X
f_knee_x = figure('name','Knee x coordinate','numbertitle','off');hold
on;grid on;
plot(t,knee_xr/100,t,knee_x,t,knee_x_f,'linewidth',1.5);
xlabel('t (s)');ylabel('knee x (mm)');
legend('raw','filtered','Fourier series fit','location','best');
%% KNEE Y
f_knee_y = figure('name','Knee y coordinate','numbertitle','off');hold
on;grid on;
plot(t,knee_yr/100,t,knee_y,t,knee_y_f,'linewidth',1.5);
xlabel('t (s)');ylabel('knee y (mm)');
legend('raw','filtered','Fourier series fit','location','best');

%% FIBULA X
f_fibula_x = figure('name','Fibula x coordinate','numbertitle','off');hold
on;grid on;
plot(t,fibula_x,t,fibula_x_f,'linewidth',1.5);
xlabel('t (s)');ylabel('fibula x (mm)');
legend('filtered','Fourier series fit','location','best');
```

```
%% FIBULA Y
f_fibula_y = figure('name','Fibula y coordinate','numbertitle','off');hold
on;grid on;
plot(t,fibula_y,t,fibula_y_f,'linewidth',1.5);
xlabel('t (s)');ylabel('fibula y (mm)');
legend('filtered','Fourier series fit','location','best');

%% ANKLE X
f_ankle_x = figure('name','Ankle x coordinate','numbertitle','off');hold
on;grid on;
plot(t,ankle_x,t,ankle_x_f,'linewidth',1.5);
xlabel('t (s)');ylabel('ankle x (mm)');
legend('filtered','Fourier series fit','location','best');
%% ANKLE Y
f_ankle_y = figure('name','Ankle y coordinate','numbertitle','off');hold
on;grid on;
plot(t,ankle_y,t,ankle_y_f,'linewidth',1.5);
xlabel('t (s)');ylabel('ankle y (mm)');
legend('filtered','Fourier series fit','location','best');

%% HEEL X
f_heel_x = figure('name','Heel x coordinate','numbertitle','off');hold
on;grid on;
plot(t,heel_x,t,heel_x_f,'linewidth',1.5);
xlabel('t (s)');ylabel('heel x (mm)');
legend('filtered','Fourier series fit','location','best');
%% HEEL Y
f_heel_y = figure('name','Heel y coordinate','numbertitle','off');hold
on;grid on;
plot(t,heel_y,t,heel_y_f,'linewidth',1.5);
xlabel('t (s)');ylabel('heel y (mm)');
legend('filtered','Fourier series fit','location','best');

%% METATARSAL X
f_metat_x = figure('name','Metat x coordinate','numbertitle','off');hold
on;grid on;
plot(t,metat_x,t,metat_x_f,'linewidth',1.5);
xlabel('t (s)');ylabel('metat x (mm)');
legend('filtered','Fourier series fit','location','best');
%% METATARSAL Y
f_metat_y = figure('name','Metat y coordinate','numbertitle','off');hold
on;grid on;
plot(t,metat_y,t,metat_y_f,'linewidth',1.5);
xlabel('t (s)');ylabel('metat y (mm)');
legend('filtered','Fourier series fit','location','best');

%% TOE X
f_toe_x = figure('name','Toe x coordinate','numbertitle','off');hold
on;grid on;
plot(t,toe_x,t,toe_x_f,'linewidth',1.5);
xlabel('t (s)');ylabel('toe x (mm)');
legend('filtered','Fourier series fit','location','best');
%% TOE Y
f_toe_y = figure('name','Toe y coordinate','numbertitle','off');hold
on;grid on;
plot(t,toe_y,t,toe_y_f,'linewidth',1.5);
xlabel('t (s)');ylabel('toe y (mm)');
legend('filtered','Fourier series fit','location','best');

%% ANGLES
```

```
%% A3
f_foot_theta = figure('name','Foot Angle','numbertitle','off');hold on;grid
on;
plot(t,foot_theta,t,foot_theta_f,'linewidth',1.5);
xlabel('t (s)');ylabel('foot angle (degrees)');
legend('filtered','Fourier series fit','location','best');

f_leg_theta = figure('name','Leg Angle','numbertitle','off');hold on;grid
on;
plot(t,leg_theta,t,leg_theta_f,'linewidth',1.5);
xlabel('t (s)');ylabel('leg angle (degrees)');
legend('filtered','Fourier series fit','location','best');

f_thigh_theta = figure('name','Thigh Angle','numbertitle','off');hold
on;grid on;
plot(t,thigh_theta,t,thigh_theta_f,'linewidth',1.5);
xlabel('t (s)');ylabel('thigh angle (degrees)');
legend('filtered','Fourier series fit','location','best');

f_HAT_theta = figure('name','HAT 1/2 Angle','numbertitle','off');hold
on;grid on;
plot(t,HAT_theta,t,HAT_theta_f,'linewidth',1.5);
xlabel('t (s)');ylabel('HAT 1/2 angle (degrees)');
legend('filtered','Fourier series fit','location','best');
% A4
f_hip_theta = figure('name','Hip Angle','numbertitle','off');hold on;grid
on;
plot(t,hip_theta,t,hip_theta_f,'linewidth',1.5);
xlabel('t (s)');ylabel('Hip angle (degrees)');
legend('filtered','Fourier series fit','location','best');

f_knee_theta = figure('name','Knee Angle','numbertitle','off');hold on;grid
on;
plot(t,knee_theta,'k-',t,knee_theta_f,'r-','linewidth',1.5);
xlabel('Time (s)');ylabel('Knee angle (\circ)');
legend('filtered','Fourier series fit','location','best');

f_ankle_theta = figure('name','Ankle Angle','numbertitle','off');hold
on;grid on;
plot(t,ankle_theta,'k-',t,ankle_theta_f,'r-','linewidth',1.5);
xlabel('Time (s)');ylabel('Ankle angle (\circ)');
legend('filtered','Fourier series fit','location','best');

f_GRFx = figure('name','Ground Reaction Force x','numbertitle','off');hold
on;grid on;
plot(t,F_foot_ground_x,'k-','linewidth',1.5);
xlabel('Time (s)');ylabel('Ground Reaction Force in x direction (N)');
legend('filtered','location','best');

f_GRFy = figure('name','Ground Reaction Force y','numbertitle','off');hold
on;grid on;
plot(t,F_foot_ground_y,'k-','linewidth',1.5);
xlabel('Time (s)');ylabel('Ground Reaction Force in y direction (N)');
legend('filtered','location','best');

figure('name','Ankle Force x','numbertitle','off');hold on;grid on;
plot(t,F_foot_ankle_x,'linewidth',1.5);
xlabel('t (s)');ylabel('Ankle Force x (N)');
legend('filtered','location','best');
```

```
figure('name','Ankle Force y','numbertitle','off');hold on;grid on;
plot(t,F_foot_ankle_y,'linewidth',1.5);
xlabel('t (s)');ylabel('Ankle Force y (N)');
legend('filtered','location','best');

figure('name','Ankle Moment','numbertitle','off');hold on;grid on;
plot(t,M_foot_ankle,'linewidth',1.5);
xlabel('t (s)');ylabel('Ankle Moment (N*m)');
legend('filtered','location','best');
```

gait_cycle_animation.m

```
%% Gait Cycle Animation
% Mehmet Furkan Do?an
% 28 November 2022
clc;clear;close all;
%% IMPORT DATA
% A2
A_2 = readtable('A_2.csv','VariableNamingRule','preserve'); % Filtered
Marker Kinematics
T = 0.987;                          %s
% 1:f 2:t 3-8:rib 9-14:hip 15-20:knee 21-26:fibula 27-32:ankle 33-38:heel
% 39-44:metat 45-50:toe
% for every part: x(m) vx(m/s) ax(m/s^2) y(m) vy(m/s) ay(m/s^2)
A_2 = table2array(A_2);
t = A_2(:,2);
rib_xd = A_2(:,3)*1e3;        % mm
rib_yd = A_2(:,6)*1e3;        % mm
hip_xd = A_2(:,9)*1e3;        % mm
hip_yd = A_2(:,12)*1e3;       % mm
knee_xd = A_2(:,15)*1e3;      % mm
knee_yd = A_2(:,18)*1e3;      % mm
fibula_xd = A_2(:,21)*1e3;    % mm
fibula_yd = A_2(:,24)*1e3;    % mm
ankle_xd = A_2(:,27)*1e3;     % mm
ankle_yd = A_2(:,30)*1e3;     % mm
heel_xd = A_2(:,33)*1e3;      % mm
heel_yd = A_2(:,36)*1e3;      % mm
metat_xd = A_2(:,39)*1e3;     % mm
metat_yd = A_2(:,42)*1e3;     % mm
toe_xd = A_2(:,45)*1e3;       % mm
toe_yd = A_2(:,48)*1e3;       % mm
%% CALCULATIONS
tinc = 0.01; % time increment
N = 7;  % Number of steps
tr = 0:tinc:N*T;
tl = -T/2:tinc:N*T-T/2;
% Right Leg
rib_xr = rib_x(tr);
rib_yr = rib_y(tr);
hip_xr = hip_x(tr);
hip_yr = hip_y(tr);
knee_xr = knee_x(tr);
knee_yr = knee_y(tr);
fibula_xr = fibula_x(tr);
fibula_yr = fibula_y(tr);
ankle_xr = ankle_x(tr);
ankle_yr = ankle_y(tr);
heel_xr = heel_x(tr);
heel_yr = heel_y(tr);
```

```
metat_xr = metat_x(tr);
metat_yr = metat_y(tr);
toe_xr = toe_x(tr);
toe_yr = toe_y(tr);
% Left Leg
rib_xl = rib_x(tl);
rib_yl = rib_y(tl);
hip_xl = hip_x(tl);
hip_yl = hip_y(tl);
knee_xl = knee_x(tl);
knee_yl = knee_y(tl);
fibula_xl = fibula_x(tl);
fibula_yl = fibula_y(tl);
ankle_xl = ankle_x(tl);
ankle_yl = ankle_y(tl);
heel_xl = heel_x(tl);
heel_yl = heel_y(tl);
metat_xl = metat_x(tl);
metat_yl = metat_y(tl);
toe_xl = toe_x(tl);
toe_yl = toe_y(tl);
%% INITIALIZING THE FIGURE
f1 = figure('name','Gait Cycle','numberTitle','off');
hold on;
set(gca,'NextPlot','replacechildren','DataAspectRatio',[1 1 1]);
xlim([0 3000]);ylim([0 1200]);
f1.Position = [2         476        1361         208];

f2 = figure('name','Gait Cycle','numberTitle','off');
hold on;
set(gca,'NextPlot','replacechildren','DataAspectRatio',[1 1 1]);
xlim([0 10000]);ylim([0 1200]);
f2.Position = [ 2          32        1364         358];
%% ANIMATION
% INITIALIZING THE VIDEO
v1 = VideoWriter('walking_data.avi');
v1.FrameRate = 1/0.0145;
v2 = VideoWriter('walking_extended.avi');
v2.FrameRate = 1/tinc;
open(v1);
open(v2);
% DATA
figure(f1);
for i = 1:size(t,1)
    HAT1_2_xr = [rib_xd(i),hip_xd(i)];
    HAT1_2_yr = [rib_yd(i),hip_yd(i)];
    Thigh_xr = [hip_xd(i),knee_xd(i)];
    Thigh_yr = [hip_yd(i),knee_yd(i)];
    Leg_xr = [fibula_xd(i),ankle_xd(i)];
    Leg_yr = [fibula_yd(i),ankle_yd(i)];
    Foot_xr = [ankle_xd(i),heel_xd(i),metat_xd(i),ankle_xd(i)];
    Foot_yr = [ankle_yd(i),heel_yd(i),metat_yd(i),ankle_yd(i)];
    Foot2_xr = [metat_xd(i),toe_xd(i)];
    Foot2_yr = [metat_yd(i),toe_yd(i)];

plot(HAT1_2_xr,HAT1_2_yr,Thigh_xr,Thigh_yr,Leg_xr,Leg_yr,Foot_xr,Foot_yr,Fo
ot2_xr,Foot2_yr,'linewidth',1.5);
    F1(i) = getframe(gcf);
    writeVideo(v1,F1(i));
    clf(f1)
    set(gca,'NextPlot','replacechildren','DataAspectRatio',[1 1 1]);
```

```
    xlim([0 3000]);ylim([0 1200]);
end
figure(f2);
for i = 1:size(tr,2)
    % RIGHT
    HAT1_2_xr = [rib_xr(i),hip_xr(i)];
    HAT1_2_yr = [rib_yr(i),hip_yr(i)];
    Thigh_xr = [hip_xr(i),knee_xr(i)];
    Thigh_yr = [hip_yr(i),knee_yr(i)];
    Leg_xr = [fibula_xr(i),ankle_xr(i)];
    Leg_yr = [fibula_yr(i),ankle_yr(i)];
    Foot_xr = [ankle_xr(i),heel_xr(i),metat_xr(i),ankle_xr(i)];
    Foot_yr = [ankle_yr(i),heel_yr(i),metat_yr(i),ankle_yr(i)];
    Foot2_xr = [metat_xr(i),toe_xr(i)];
    Foot2_yr = [metat_yr(i),toe_yr(i)];
    % LEFT
    deltax = rib_xr(i) - rib_xl(i);
    HAT1_2_xl = [rib_xl(i)+deltax,hip_xl(i)+deltax];
    HAT1_2_yl = [rib_yl(i),hip_yl(i)];
    Thigh_xl = [hip_xl(i)+deltax,knee_xl(i)+deltax];
    Thigh_yl = [hip_yl(i),knee_yl(i)];
    Leg_xl = [fibula_xl(i)+deltax,ankle_xl(i)+deltax];
    Leg_yl = [fibula_yl(i),ankle_yl(i)];
    Foot_xl =
[ankle_xl(i)+deltax,heel_xl(i)+deltax,metat_xl(i)+deltax,ankle_xl(i)+deltax
];
    Foot_yl = [ankle_yl(i),heel_yl(i),metat_yl(i),ankle_yl(i)];
    Foot2_xl = [metat_xl(i)+deltax,toe_xl(i)+deltax];
    Foot2_yl = [metat_yl(i),toe_yl(i)];

plot(HAT1_2_xr,HAT1_2_yr,Thigh_xr,Thigh_yr,Leg_xr,Leg_yr,Foot_xr,Foot_yr,Fo
ot2_xr,Foot2_yr,'linewidth',1.5);
    hold on;

plot(HAT1_2_xl,HAT1_2_yl,Thigh_xl,Thigh_yl,Leg_xl,Leg_yl,Foot_xl,Foot_yl,Fo
ot2_xl,Foot2_yl,'linewidth',1.5);
    F2(i)  = getframe(gcf);
    writeVideo(v2,F2(i));
    clf(f2)
    set(gca,'NextPlot','replacechildren','DataAspectRatio',[1 1 1]);
    xlim([0 10000]);ylim([0 1200]);
end
figure(f1);
movie(F1,1,1/0.0145);
figure(f2);
movie(F2,1,1/tinc);
close(v1);
close(v2);
```

piston_movement.m

```
%% Piston Movement During Walking
% Mehmet Furkan Do?an
% 17.12.2022
clc;clear;close all;
%%
% A4
A_4 = readtable('A_4.csv','VariableNamingRule','preserve');
A_4a = table2array(A_4);
t = A_4a(:,2);
knee_theta = A_4a(:,6);
knee_omega = A_4a(:,7);
```

```
% Fourier Series
knee_theta_f = fit_y(knee_theta,t,15,'knee_theta.txt'); % degree
knee_omega_f = fit_y(knee_omega,t,15,'knee_omega.txt'); % degree

% Piston Lenght Calculation
alpha_e = 102.87;   % degree (full extension)
a = 23.529; % mm (From knee joint to upper piston joint)
b = 180.004; % mm (From knee joint to lower piston joint)
alpha = alpha_e - knee_theta_f;
L_piston = sqrt(a.^2 + b.^2 + 2.*a.*b.*cosd(alpha));    % mm
v_piston = 0.5.*L_piston.^(-1).*(-2).*a.*b.*sind(alpha).*(-knee_omega_f); %
mm/s
v_piston = v_piston * 1e-3; % m/s

v_walking = 1.6;    % m/s
cf = v_walking/1.411844;
fprintf('For a walking velocity of %.3f m/s : \n',v_walking);
fprintf('Max piston velocity in extension direction: %.3f
m/s\n',max(v_piston)*cf);
fprintf('Max piston velocity in flexion direction: %.3f m/s\n',(-
1)*min(v_piston)*cf);

figure('name','Piston Length','numbertitle','off');hold on;grid on;
plot(t./cf,L_piston,'k-','linewidth',1.5);
xlabel('t (s)');ylabel('Piston Lenght (mm)');
xlim([0,t(end)./cf]);xticks(0:0.1:t(end)/cf);
yticks(floor(min(L_piston)):2:ceil(max(L_piston)));
title(['Piston length for a walking speed of ',num2str(v_walking),' m/s']);

figure('name','Piston Velocity','numbertitle','off');hold on;grid on;
plot(t./cf,v_piston.*cf,'k-','linewidth',1.5);
xlabel('t (s)');ylabel('Piston Velocity (m/s)');
xlim([0,t(end)./cf]);xticks(0:0.1:t(end)/cf);
title(['Piston velocity for a walking speed of ',num2str(v_walking),'
m/s']);


% f_knee_theta = figure('name','Knee Angle','numbertitle','off');hold
on;grid on;
% plot(t,knee_theta,t,knee_theta_f,'linewidth',1.5);
% xlabel('t (s)');ylabel('Knee angle (degrees)');
% legend('filtered','Fourier series fit','location','best');
%
% f_knee_omega = figure('name','Knee Angular
Velocity','numbertitle','off');hold on;grid on;
% plot(t,knee_omega,t,knee_omega_f,'linewidth',1.5);
% xlabel('t (s)');ylabel('Knee angular velocity (rad/s)');
% legend('filtered','Fourier series fit','location','best');
```

Forces_on_strain_gauges.m

```
%  Forces on strain gauges
% 09.12.22
clc;clear;close all;
%% IMPORT DATA
%%%
```

```
t = A_3a(:,2);
leg_theta = A_3a(:,12);      % degree
%%%
```

```
    M_a = F(1,:).*L;
    M_sg = M_a.' + M;

    % PIPE
    R_i = 30e-3;     % m
    R_o = 34e-3;     % m
    b = 8e-3;        % m
    h = 2.1e-3;      % m
    A_sg = b*h;   % m^2
    A_tube = pi * (R_o^2 - R_i^2);
    A_total = A_sg + A_tube;

    sigma_a = F(2,:).'./A_total; % Pa

    % Moment of Area
    I_c = pi * (R_o^4 - R_i^4)/4;
    I_r = 2*b*h^3/12 + 2*b*h*(12.5e-3)^2;
    I = I_c + I_r;

    c = (13.1e-3);
    sigma_b = M_sg .* c / I;
    sigma_sg_1 = sigma_a + sigma_b;
    sigma_sg_2 = sigma_a - sigma_b;

    E = 72e9;        % Pa
    strain1 = sigma_sg_1 ./ E;    % m/m
    strain2 = sigma_sg_2 ./ E;    % m/m

    %% STRENGHT ANALYSIS
    sigma_b = M_sg .* R_o / I;
    sigma_sg_1 = sigma_a + sigma_b;
    sigma_sg_2 = sigma_a - sigma_b;

    cf = 135/56.7;
    sigma_sg_1 = sigma_sg_1.*cf;     % Pa
    sigma_sg_2 = sigma_sg_2.*cf;     % Pa
    % fprintf('Max stress = %.3f MPa\n',1e-
6*max([max(sigma_sg_1),max(sigma_sg_2)]));
    strain1 = strain1.*cf;    % m/m
    strain2 = strain2.*cf;    % m/m
    max_strain = max([max(abs(strain1)),max(abs(strain2))]);

    YS = 505e6;      % Pa

    SF1 = YS ./ abs(sigma_sg_1);
    SF2 = YS ./ abs(sigma_sg_2);

    scf = 7.1 / 20.862 ; % Stress Concentration Factor

    SF1 = SF1 * scf;
    SF2 = SF2 * scf;

    min_SF = min([min(SF1),min(SF2)]);

end
```

APPENDIX D – COST ANALYSIS

Part Number	Description	Quantity	Unit Cost	Cost
1	Rasperry Pi Pico W	3	₺155.15	₺465.45
2	Breadboard	3	₺20.61	₺61.83
3	10K Resistor Set	2	₺1.18	₺2.36
4	22K Resistor Set	2	₺1.18	₺2.36
5	Cable Set	1	₺63.44	₺63.44
6	Buzzer	3	₺4.43	₺13.29
7	Mini Vibration Motor	1	₺10.62	₺10.62
8	Micro Vibration Motor	1	₺14.75	₺14.75
9	Adjustable Voltage Regulator	2	₺59.59	₺119.18
10	LCD Display	2	₺37.17	₺74.34
11	Header	5	₺1.77	₺8.85
12	Battery Management System	1	₺23.05	₺23.05
13	Charging Circuit	1	₺9.97	₺9.97
14	Buck-Boost Converter	1	₺109.49	₺109.49
15	Motor Driver Module	1	₺22.16	₺22.16
16	Panasonic 18650 Battery	2	₺202.96	₺405.92
17	Full Bridge Strain Gages	6	₺130.00	₺780.00
18	Strain Gage Application Kit	1	₺450.00	₺450.00
19	7075 Aluminum	750 Gram	₺170.00	₺127.50
		Total Cost		₺2,764.56

APPENDIX E – SUSTANIBILITY ANALYSIS RESULTS

Middle East Technical University

SOLIDWORKS
Sustainability Report

Model Name:	Lower Leg
Weight:	145.65 g
Product Lifetime:	10 years

Production Area

Use Area

Assembly		Use	
Region:	Europe	Region:	Europe
Energy type:	None	Energy type:	None
Energy amount:	0.00 kWh	Energy Amount:	0.00 kWh
Built to last:	10 years	Duration of use:	10 years

Transportation		End of Life	
Truck distance:	1900 km	Recycled:	25 %
Train distance:	0.00 km	Incinerated:	24 %
Ship distance:	0.00 km	Landfill:	51 %
Airplane Distance:	0.00 km		

Environmental Impact (calculated using CML impact assessment methodology)

Carbon Footprint

Material:	20 kg CO_2e
Manufacturing:	0.350 kg CO_2e
Use:	0.00 kg CO_2e
Transportation:	0.146 kg CO_2e
End of Life:	0.098 kg CO_2e

21 kg CO_2e

Total Consumed Energy

Material:	250 MJ
Manufacturing:	6.7 MJ
Use:	0.00 MJ
Transportation:	2.2 MJ
End of Life:	0.073 MJ

260 MJ

Air Acidification

Material:	0.150 kg SO_2e
Manufacturing:	2.3E-3 kg SO_2e
Use:	0.00 kg SO_2e
Transportation:	6.8E-4 kg SO_2e
End of Life:	5.7E-5 kg SO_2e

0.153 kg SO_2e

Water Eutrophication

Material:	4.9E-3 kg PO_4e
Manufacturing:	8.5E-5 kg PO_4e
Use:	0.00 kg PO_4e
Transportation:	1.5E-4 kg PO_4e
End of Life:	9.9E-5 kg PO_4e

5.2E-3 kg PO_4e

Financial effect of material 3.40 USD

Environmental Impacts of the Parts
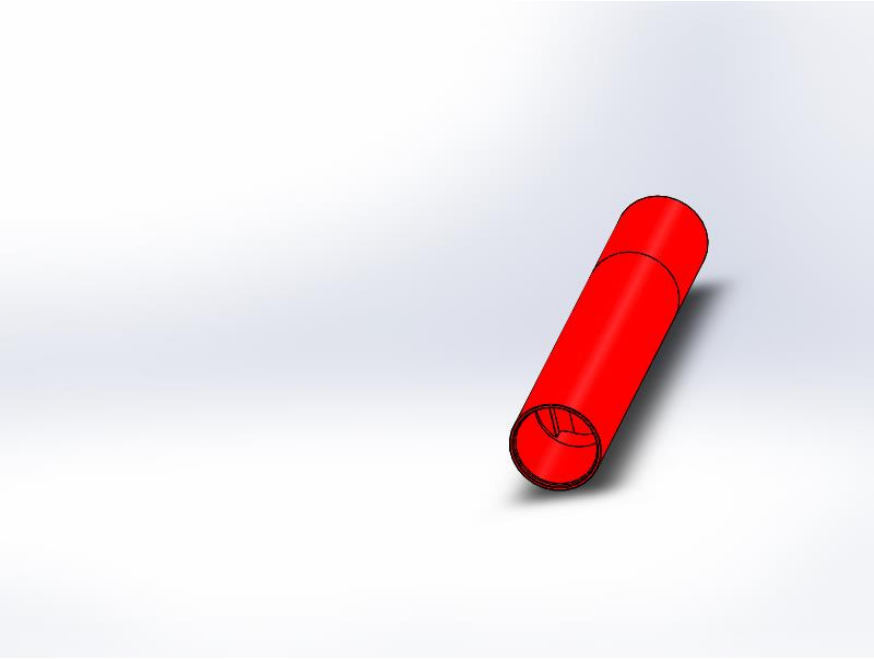
Part	Carbon	Water	Air	Energy
Tube	1.5	3.6E-4	0.011	18
Strain Gauge Holder	0.637	1.5E-4	4.6E-3	7.8